Software error compensation of machine tools

Software Error Compensation of Machine Tools

H.A.M. Spaan

Software Error Compensation of Machine Tools

H.A.M. Spaan

Software Error Compensation of Machine Tools

Proefschrift

ter verkrijging van de graad van doctor
aan de Technische Universiteit Eindhoven,
op gezag van de Rector Magnificus, prof.dr. J.H. van Lint,
voor een commissie aangewezen door het College van Dekanen
in het openbaar te verdedigen op
maandag 11 december 1995 om 16.00 uur

door

Henrikus Adrianus Maria Spaan

Geboren te Eindhoven

Dit proefschrift is goedgekeurd door de promotoren:

prof.dr.ir. P.H.J. Schellekens

en

prof.dr.ir. A.C.H. van der Wolf

en de copromotor:

dr.ir. H.M. de Ruiter

Summary

The objective of the research presented in this thesis is to develop different strategies to improve the dimensional accuracy of products manufactured on numerically controlled machine tools by software error compensation. This error compensation should be applicable to both existing and new machine tools and compensate the quasi static errors of a machine tool.

The investigated quasi static error sources are the geometric, finite stiffness and thermally induced errors of a machine tool. For each error source different measurement techniques have been applied to determine the model parameters. New indirect calibration techniques have been developed to access the model parameters more quickly than the conventional direct measuring methods. The model parameters describing the finite stiffness and thermally induced errors depend on the machine's status. Strain gauges and temperature sensors are attached to the machine tool to measure the actual load and the temperature distribution on the machine tool and adapt the compensation parameters during actual operation.

A software error compensation system has been designed with an open architecture. This allows the implementation of different error models without any major changes to the compensation strategy itself. By superposition of the different models the actual compensation functions are determined.

Two different compensation strategies have been developed: a real-time software error compensation and an NC-code software error compensation.

The real-time error compensation is implemented in the machine tool controller. Different compensation methods have been investigated to achieve an optimal compensation algorithm, which could be evaluated within the available interpolation time. Also the problems with the stability and virtual hysteresis have been investigated which occur with the discretization of the compensation functions.

An NC-code software error compensation enables software compensation on existing machine tools. This compensation strategy alters the programming code (NC-code). After a translation and interpolation of the programmed trajectory, this NC-code is compensated for the quasi static errors and sent to the machine tool during the actual milling process.

Both compensation methods have been validated with different measurement techniques and test workpieces. Evaluation of these validation experiments showed a significant accuracy improvement of the machine tool. The geometric errors have been reduced from 109 μm without compensation to 11 μm with compensation, resulting in an averaged modelling efficiency of 84%. The finite stiffness errors have been reduced from 78 μm to 14 μm and an efficiency of 75 %. The thermally induced errors have been reduced with 80%. Milling the test-workpieces with and without compensation showed an averaged accuracy improvement of 80%. The maximum remaining error of 131 μm present in the workpiece milled without compensation is reduced to 32 μm for the workpiece milled with compensation.

Samenvatting

Het doel van het onderzoek, beschreven in dit proefschrift, is de verbetering van de dimensionele nauwkeurigheid van produkten. Deze verbetering van de nauwkeurigheid wordt gerealiseerd met software compensatie door het corrigeren van de quasi statische afwijkingen in numeriek bestuurde machines. De compensatie is hierbij toepasbaar op zowel nieuwe als op bestaande machines.

Het onderzoek heeft zich toegespitst op de afwijkingen in de geometrie van de geleidingen van een machine, afwijkingen door een belasting en afwijkingen ten gevolge van temperatuurvariaties. Verschillende meettechnieken zijn toegepast voor elke afwijking. Speciale indirecte meettechnieken zijn ontworpen om deze metingen sneller en meer efficiënt te laten verlopen. Verschillende typen sensoren zijn aangebracht aan de machine. De belasting op de machine wordt gemeten met rekstroken. De variatie in de temperatuur wordt met een aantal temperatuursensoren gemeten. Deze sensor informatie wordt direct gebruikt om de model parameters aan te passen aan de actuele situatie.

Om de verschillende afwijkingen te compenseren is een software compensatie systeem ontwikkeld met een open architectuur. Deze architectuur laat de implementatie van verschillende modellen toe, zonder dat het compensatie-mechanisme zelf veranderd moet worden. De actuele compensatie waarde wordt verkregen door super-positie van de verschillende modellen.

Twee verschillende compensatie-mechanismen zijn ontwikkeld: een 'real-time' software compensatie en een 'NC-code' software compensatie.

De 'real-time' software compensatie is geïmplementeerd in de besturing van de machine. Deze implementatie vereist een optimaal compensatie algoritme wat geëvalueerd kan worden binnen de beschikbare interpolatie-tijd. Daarnaast is speciale aandacht besteed aan de problematiek met de

stabiliteit en een virtuele hysterese die optreedt bij de discretisatie van de compensatie functies.

De NC-code compensatie maakt een software compensatie mogelijk op bestaande machines, mits voorzien van een besturing. De compensatie wordt gerealiseerd door het aanpassen van de programma code (NC-code). Na een vertaling en interpolatie van de NC-code wordt de geprogrammeerde trajectory gecompenseerd voor de quasi statische afwijkingen in de machine. Deze gecompenseerde NC-code wordt gedurende het bewerkingsproces naar de machine verstuurd.

Beide compensatie methoden zijn gevalideerd met verschillende meetmethoden en test werkstukken. Uit deze verificatie experimenten kan een nauwkeurigheidsverbetering worden afgeleid voor de verschillende afwijkingen. De afwijkingen in de geometrie wordt van 109 μm teruggebracht tot 11 μm met een gemiddelde efficiëntie van 84%. De afwijkingen door een belasting worden gereduceerd van 78 tot 14 μm met een efficiëntie van 74%. De thermische afwijkingen worden gereduceerd met 80%. De verificatie met de test werkstukken laten een algehele nauwkeurigheidsverbetering zien van 80%. De afwijkingen in deze test werkstukken worden gereduceerd van 131 μm, voor het werkstuk wat is bewerkt zonder compensatie, tot een maximale afwijking van 32 μm voor het werkstuk wat bewerkt is met een volledige compensatie.

Table of contents

Chapter 1

Introduction

Dimensional accuracy is one of the most important factors in determining the quality of a machined component. With an increasing demand for higher accuracy of finished components to be achieved and maintained in an economically viable way, the accuracy of machine tools used in production is often the limiting factor. It is difficult to achieve the desired accuracy due to the complexity and interactions of the various error sources involved. Typical examples of these sources are programming errors, vibrations, temperature variations or errors attributable to the machine tool itself. In this chapter the error sources are discussed which affect the dimensional accuracy of the finished part. It is shown that the major contributors are the quasi static error sources. The accuracy enhancement will be realised by numerical error compensation strategies for errors from such sources. The compensation methodology will be introduced. Finally, the research objectives and the contents of this thesis will be presented in this chapter.

Error sources in the machining stage

Considering the errors in machining stage, the accuracy of the finished part is mainly determined by the sensitivity of the structural loop to various error sources. The structural loop comprises the components that realise the relative location between the tool and the workpiece. The structural loop of a machine tool consists of tool, workpiece, mechanical components and scales with controller (see Figure 1.1). The error sources affect the geometry of the structural loop components. This results in an actual trajectory of the tool with respect to the workpiece that differs from the nominal trajectory. The errors are considered as emanating from quasi static and dynamic error sources.

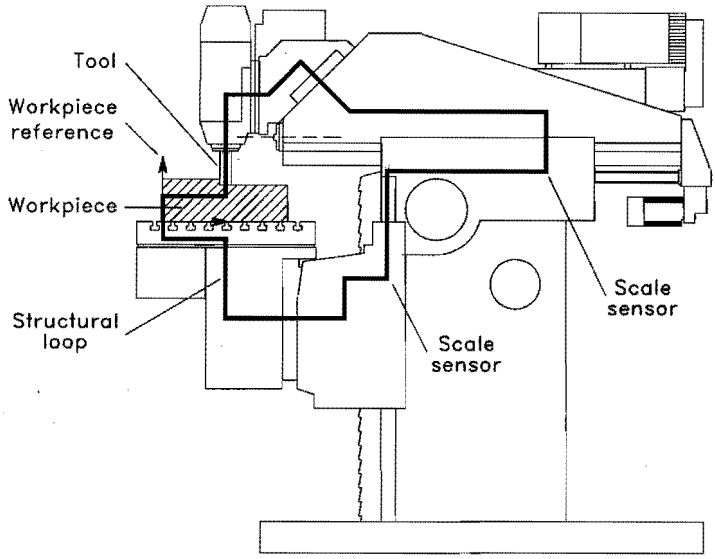

Figure 1.1 : Example of a structural loop during a milling operation.

Quasi static error sources are defined as the sources causing "Errors of relative location between the tool and the workpiece that are varying slowly in time and are related to the structure of the machine tool itself" [35]. These error sources include the geometric errors of the machine, the errors due to static and slowly varying forces and those due to the thermally induced strains in the structural loop.

- *Geometric errors;*

  The geometric errors are due to differences in the actual and nominal dimensions and geometry of the members of the machine's structural components and the joints between them. Typical examples of geometric errors are imperfect geometrical shape of the guides of a machine tool's axis, misalignment between the guides (e.g. squareness errors) or scale errors.

- *Errors due to static and slowly varying forces;*

  The components of the structural loop are subject to quasi static forces that affect the accuracy of the executed tasks due to the limited stiffness of these components. These quasi static force variations are introduced by the process, the weight of moving machine parts and the workpiece. In this thesis, the effect of process forces on the machine

accuracy is not considered, as process forces will be negligible with light finishing cuts. The force variations introduced by the weight of machine parts and the workpiece have a significant effect on the machine accuracy. The forces and moments exerted by the dead weight of the moved machine components will change by movements of the machine's axes. Also the position where these loads are introduced in the structure will change due to these movements. The result is that guideways will change their shapes and their relative locations. The workpiece weight has a similar effect on the deflection of the structural loop. Only in this case, the deformations are dependent on both position and weight of the workpiece as well as the position of the kinematic elements that support the workpiece.

- *Thermally induced errors.*

  A large number of internal and external heat sources affect the temperature distribution of the structural loop. Typical examples are the heat generated by friction in joints, gearboxes and spindle bearings, or the machine's environment. The resulting thermal distortions of the various components produce errors that dominate the achievable accuracy.

The quasi static errors account for the largest part (about 70%) of the errors attributable to the machine tool [34, 35, 46].

Besides by these quasi static errors, the realised trajectory is influenced by errors related to the dynamic behaviour of the structural loop. These dynamic errors are caused by sources such as the spindle error motion, self-induced and forced vibrations of the machine structure, chatter, controller errors and deflections under inertial forces. By their nature, the dynamic errors vary rapidly. Further, these errors predominantly affect the local characteristics of the workpiece (e.g. surface roughness or under-cutting of corners) rather than its dimensional accuracy. Therefore, the research presented in this thesis is focused on the reduction of the quasi static errors.

Accuracy enhancement by error compensation

The accuracy of the finished part is determined by the sensitivity of the structural loop to various error sources. Hence, the accuracy of the workpiece can be improved either by reducing the sensitivity of this structural loop, by removing the error source, or by compensation of the resulting error.

- *Reduction of the sensitivity of the structural loop*

  The hardware of the machine tool (e.g. the milling head or the guides) can be improved by a reduction of the sensitivity of the structural loop to the error sources. As an example, the influence of the workpiece weight on the accuracy of the workpiece can be reduced by a construction with an increased stiffness. The effect of temperature variations on the machine tool's structure can be reduced by making a temperature invariant construction.

- *Elimination of the error source*

  With a temperature control unit temperature variations can be eliminated by heating or cooling the machine's structure.

- *Error compensation methods.*

  Instead of reducing the sensitivity of the structural loop to the various error sources, it is also possible to compensate for these errors. This compensation can be achieved by additional components, or by small adaptations to the structural loop. A typical example of a mechanical compensation method is the leadscrew corrector cam. This compensation method was commonly applied on often manually operated high precision machines to improve its positioning accuracy.

In figure 1.2 an example is depicted for two different compensation methods to reduce the errors due to the weight of machine components. By a convex and a concave ground guide plate, the error is reduced of the horizontal axis which supports the workpiece table. Two tension rods are applied to reduce the bending of the ram when the ram is pulled out. The tension rods are manufactured of a material with a higher stiffness than the material of the ram, which is made of cast iron. In combination with a pre-load on the tension rods, the stiffness of the horizontal ram is increased.

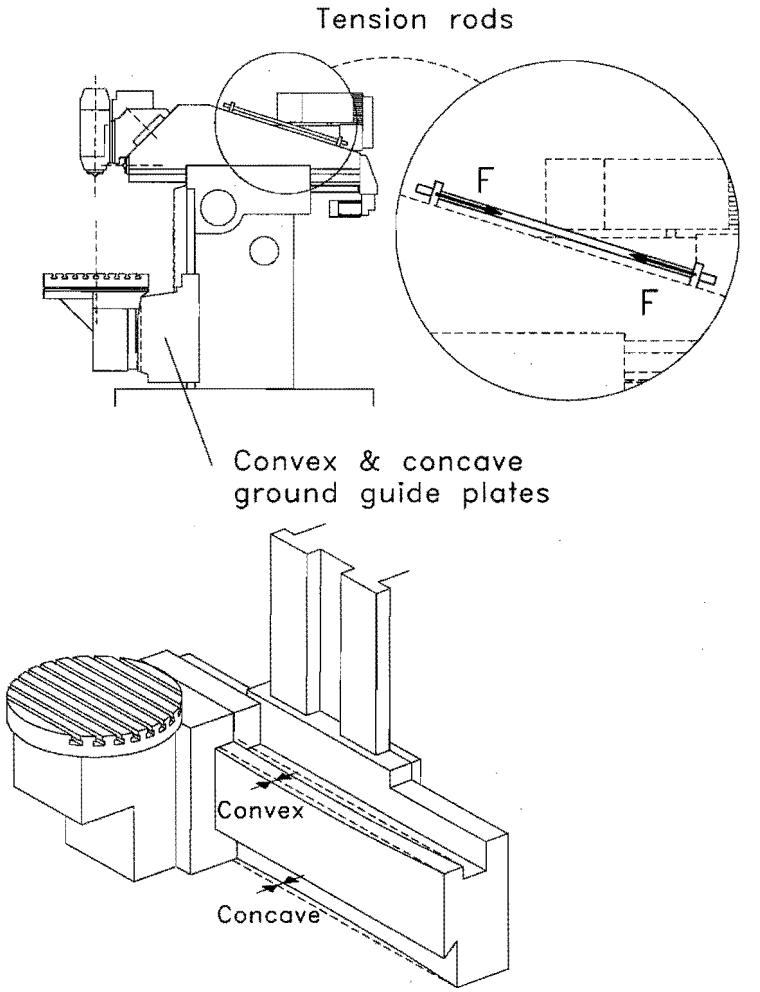

Figure 1.2 : Two compensation methods to reduce the errors due to the weight of machine components.

Although the presented compensation methods actually realise an accuracy enhancement, the efficiency of the compensations is rather limited:

- *The errors cannot completely be eliminated*

  In principle it is possible to remove the error source from the machine. As an example, some of the internal heat sources could be removed from

the machine: the main engine could be placed outside the machine. However, the internal heat sources cannot be totally avoided

- *Partial compensation*

  Convex and concave ground guide plates will only compensate for the errors due to the weight of the moving table, not for the additional weight of a workpiece positioned on this table.

- *Interaction between the error sources and the additional hardware*

  Temperature variations induced by the machine tool itself, for example, will change the pre-load in the tension rods (see figure 1.2) due to the different material expansion coefficients.

- *Wear*

  The errors in the machine tool will change due to wear. It is often very difficult to readjust the hardware compensation for these changes.

- *Achievable manufacturing accuracy;*

  The accuracy of the various parts utilised in machine tools is limited due to technical reasons (e.g. it is not possible to create a perfectly straight guide plate).

- *Economical reasons.*

  Apart from these technical limitations, most of the present compensation methods are very expensive, since they have to be manufactured with a very high accuracy.

For these reasons, new techniques to improve the accuracy of a machine tool are being developed. One of these new techniques is a numerical error compensation strategy.

Software error compensation

Most modern machine tools are supplied with a numerical controller, which controls all movements of the machine tool. Based on a special programming language or manual input, the machine is commanded to move along a specified trajectory. Due to the various error sources, the actual trajectory of the tool with respect to the workpiece will differ from the commanded trajectory. With the numerical error compensation strategy the commanded trajectory can be changed. These changes will result in a trajectory compensated for the effect of the various error

sources. This compensation strategy will be carried out by software. Therefore, it is called 'Software error compensation'.

Software error compensation can be much more flexible than the other compensation methods. The compensation parameters can be readjusted whenever it is necessary, e.g. when a workpiece is placed on the table or when the temperature changes. This readjustment can even be carried out during normal operation. However, software error compensation can only compensate for the errors which are controllable. E.g. when the machine is not equipped with a rotary axis, it is not possible to compensate for the error in the orientation of the tool.

Research objectives and contents thesis

In 1988 a research project has been initiated at Eindhoven University of Technology to develop different strategies to improve the dimensional accuracy of products manufactured on numerically controlled machine tools by software error compensation. Firstly, the various error sources have been investigated influencing the accuracy of the machine tool. The possibility to compensate these errors with software error compensation techniques has been investigated. This work which has also resulted in a simplified version of a software error compensation system has been published by Theuws in 1992 [95].

In January 1990 a European research project (BCR-project) has been started to develop methods for the numerical error compensation of machine tools. At the end of this project (December 1992) a software error compensation system was present, which can compensate the quasi static errors of a machine tool. This compensation system is embedded in the controller of the machine tool and therefore only applicable for new machines. The research project has been carried out under the responsibility of the author. Hence, some of the work presented in this thesis can also be found in the final project report [78], which has been written by the present author.

Parallel to these investigations a study has been carried out on different models to analyse the quasi static errors of machine tools. The results of this investigation has been published by Soons in 1993 [87]. During this study also a new calibration strategy has been developed to determine the

geometric errors of a machine using distance measurements. In Chapter 2 the work previously carried out by Theuws and Soons will be discussed together with the results of a literature study on available error compensation methods including different models and measurement techniques

In this thesis special attention will be paid to the development of a software error compensation system. It is assumed that adequate and accurate models are available to describe the quasi static errors. To enable software error compensation on different machine types these models were further refined to make them machine type independent. The software error compensation system has been designed with an open architecture. This architecture allows the implementation of different error models, without any major change to the compensation mechanism itself. In order to enable software compensation on both existing and new machine tools two different compensation strategies have been developed : the real-time software error compensation and the NC-code software error compensation. In Chapter 2 the global design of this software error compensation system will be described.

The quasi static errors sources (geometric errors, finite stiffness errors and thermally induced errors) are modelled separately. In order to determine the necessary parameters for each model, different calibration techniques have been applied. New indirect calibration techniques have been developed to access the model parameters more quickly than the existing direct measuring methods. In Chapters 3, 4 and 5 the modelling and the determination of the three quasi static errors is discussed.

The model parameters describing the finite stiffness and thermally induced errors depend on the machine's status (respectively load and temperature). Different sensors are attached to the machine tool to determine its status and adapt the compensation parameters during actual operation. In Chapter 4 the application of strain gauges is discussed to determine the actual load. In Chapter 5 the application of the temperature sensors is presented.

The real-time software error compensation has been developed for implementation in the controller of the machine tool. In Chapter 6 different compensation methods will be presented to achieve an optimal compensation algorithm which can be evaluated within the available interpolation time. Also the problems which occurred with the

discretization of the compensation functions, like instability and virtual hysteresis, will be discussed in this chapter.

In order to apply software error compensation on existing machine tools, a compensation strategy has been developed which acts on the programming code (NC-code). This NC-code compensation will be presented in Chapter 7.

Both software error compensation methods have been validated. Besides the application of direct measurement techniques, also artefacts experiments have been carried out. These artefacts are either measured with or milled on the machine tool. In Chapter 8 the results of these experiments will be presented, which will show the actual efficiency of the developed software error compensation systems.

Finally, the research is summarised in Chapter 9. In this chapter, conclusions are presented together with recommendations for future research.

Chapter 2

Design of a Software Error Compensation System

A software error compensation system will improve the product accuracy without any changes to the hardware of the machine. Using special designed compensation algorithms the actual trajectory of a machine tool can be compensated for the effect of various error sources involved. Therefore, for every error source an adequate model should be available to describe the effect of the error source on the accuracy of the programmed trajectory. Hence, an efficient software error compensation system can not be achieved by efficient compensation algorithms alone, but also depends on the applied error models and measurement techniques. In this chapter, first a literature study will be presented, covering all these items. This study will reveal the possibilities and limitations of existing methods and establish the research presented in this thesis. In the next two paragraphs the global design of the software error compensation system will be presented. The compensation system has been developed using a kinematic model as a basis for all error models. This kinematic model has been optimised to achieve a model with as few construction parameters as possible without losing its modelling capabilities. Inherently, different error models can be implemented in the software compensation system without interference with the compensation mechanism itself. This design has been called 'Open architecture design'.

Bibliographical study

'Machine Tool Accuracy' [35], the fifth volume of 'Technology of Machine Tools', reports on the state of the art of machine tool technology in the early 1980's. The editors and contributors of this valuable document have made a number of recommendations for future research, many of which are still valid directions for research. One such recommendation is to combine the individual machine deviations to form a total accuracy picture in three

dimensional space. This picture could be used for accuracy analysis of a machine tool. Many investigators have addressed this problem from different perspectives. Besides an accuracy analysis, this accuracy picture could also be used as a basis for error compensation techniques: when the error vector is known on every position in the workspace of the machine tool, a compensation for this error can be established. To establish an accuracy picture adequate models and different measuring methods to determine the model parameters should be available. Therefore a bibliographical study, concerning software error compensation should also include different modelling techniques and measuring methods. In this paragraph, a brief discussion will be presented concerning the available literature for all mentioned topics.

Geometric error models

Different modelling techniques are available for the geometric error modelling of machine tools. Firstly, volumetric approaches were investigated. In the 'error-matrix' method reported by Dufour and Groppetti [24], error vector components at different locations in the machine's work space are stored. Error predictions are obtained by interpolation between the stored values. Sata [73] describes a similar approach to model and compensate the geometric errors of a machining centre in a single plane. To calculate the error components at an arbitrary point in the plane, it is assumed that these components can be expressed by quadratic functions of the axis' coordinates.

Later on the parametric approaches were favourite to many investigators. With this approach, the errors in the actual location of an axis are described by 3 rotation and 3 translation errors, corresponding to the degrees of freedom of that body (see figure 2.1). Early approaches to this modelling technique presented by Leete [60], Wong [113], French [29] and Love [61] rely on trigonometric techniques to analyse the effect of each parametric error individually.

Later work is based on the use of coordinate frames which are attached to various components of the structural loop (see figure 2.2). The parametric errors are defined as the three angular and three linear errors in the relative location of two successive frames (see figure 2.2). The mathematics of rigid body kinematics is used to model the propagation of these parametric errors to the errors in the relative location of the tool with

respect to the workpiece. This systematic approach allows a complete analysis of any machine structure.

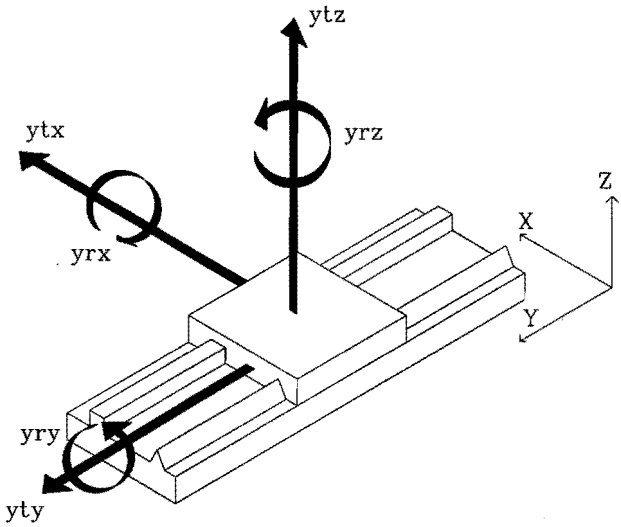

Figure 2.1 The errors in the location of an axis. The individual error components are described with a notation according to VDI 2617 [98]. The first character denotes the axis of movement; the second one the type of error; the third one the axis along which the error is acting.

Examples of models based on this approach can be found in the work of many investigators [5, 10, 19, 20, 22, 27, 36, 55, 68, 76, 78, 84, 85, 95, 115]. Only subtle differences between the various presentations can be identified, e.g. regarding the mathematical apparatus used to derive the models, the place where the errors are defined, and the treatment of machines with moving tables.

In this thesis, the kinematic modelling procedure will be applied to describe the geometric errors of the investigated machine tool. This modelling procedure has proven to be accurate and very flexible with respect to different machine constructions. Also a lot of experience was already available on kinematic models and its application for software error compensation [78, 87, 95].

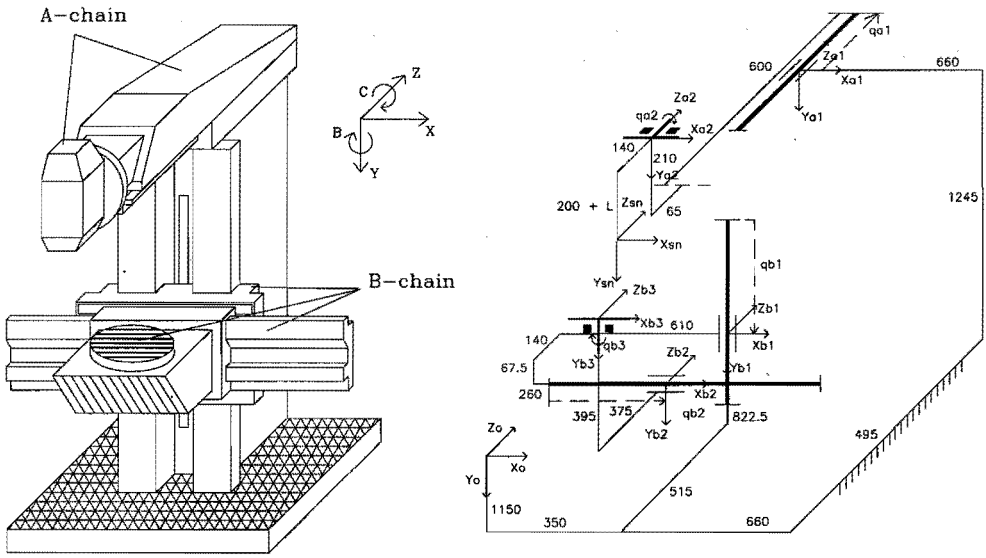

Figure 2.2 A schematic and a kinematic representation of a 5-axis milling machine. The coordinate frames are located in the centroid of each axis. Also a separation has been made between the chain supporting the tool (A-chain) and the chain supporting the workpiece (B-chain) [76, 78].

Errors due to static and slowly varying forces

Although many researchers report that the respective deflection of the structural loop may cause significant errors, their modelling has received little attention. Only the process forces and related structural loop deflections during machining operations have received much attention [57, 94, 108]. However, in order to achieve a very accurate product not only the geometry of the product should be very accurate, but also the roughness of the milled surface should be very small. Therefore, a workpiece should be milled in two steps.

- Most of the material is removed during milling the workpiece with large depths of cut and a large feed;
- To achieve the desired dimensions, the workpiece is finished by milling with small depths of cut and a small feed.

During the finishing process the static component of the cutting forces on the deflection of the structural loop is negligible due to the relatively high static stiffness of modern machine tools [93]. Therefore the effect of process forces on the machine accuracy is not considered in this thesis. The required analysis of the machining process and (dynamic) structural loop stiffness is beyond the scope of this research.

Contrary to the process forces, the effect of load variations introduced by the weight of moving machine components and workpiece is a significant part of the research presented in this thesis. In most cases these errors are largely determined by the properties of the nominal machine structure. This enables, at least in principle, an analytical approach to error modelling. The complex mechanics of multi-axis machines, however, puts restrictions on this approach. In addition, the major deformations will be found in the joints and not in the links of the machine tool. Therefore, the load variations will be described with empirical models (see chapter 4).

Thermally induced errors

To describe the thermally induced errors, both analytical and empirical approaches can be found in the literature. Considering the analytical approach, one, two or three models are required, dependent on the chosen input. The first model relates the heat flows into the structural loop to operating conditions like spindle speed. The second model describes how these heat flows affect the temperature distribution of the structural loop. The third model relates the errors in the location of the tool to this temperature distribution.

Yosida [114], for example, uses the assumption of stress-free thermal deformation to analytically model the thermal errors of a lathe and a milling machine as a function of the temperature distribution under steady state conditions. Approximately 50 temperature sensors are used. A method to reduce the number of sensors is presented, based on an assumed exponential form for the temperature field around the heat source. Similar analytical models are presented by Balsamo [4], Trapet [96] and Soons [87].

Finite difference or finite element techniques are used by many researchers to model the thermal errors. (see e.g. [2, 44, 74, 104, 105 108, 110]. In general these techniques are used to calculate both the temperature distribution and the resulting deformations. The input to these models are analytically or empirically determined heat flows. In some cases, the

measured temperature distribution is taken as input. The result of this modelling technique is a large system of relatively simple algebraic equations that can be solved by a computer. These models require a large effort both in their construction and evaluation. Venugopal [105] offers a solution to the latter problem by summarising the obtained model by relatively simple regression models estimated from the computed deformations.

In analytical models the relevant material constants introduce an uncertainty. For example, the thermal expansion coefficient of steel may vary from 10.5 to 13.5 [μm/°Cm] depending on the hardness and composition [9]. Also the uncertainty of the intensity and location of the heat sources or the uncertainty of the actual heat transfer introduce a major cause of uncertainty in analytical models. In spite of these restrictions, many researchers have successfully achieved to assess (part of) the thermally induced errors using an analytical approach.

A number of empirical models have been reported that relate the thermal errors to the temperature distribution (see e.g. [19, 27, 57, 77, 95, 105]). Here either the parametric errors or the resulting errors in the location of the tool are related to the readings of a number of characteristic temperature sensors by relatively simple regression models. The presented models are static, i.e. the thermal errors at a certain time are expressed as a function of the measured temperatures at that time. Both Soons and McClure [62, 87] use a dynamic approach by respectively including the history of the temperature distribution into the model or relate the error in the location of the tool to the change of environmental temperature and operating conditions in time. The parameters of both models are empirically estimated using step-response tests. Both modelling techniques require less sensors, but show an increased sensitivity to disturbances.

As both analytical and empirical models show reasonable results, the software error compensation should not be limited to the application of one particular model. Therefore, the software error compensation system will be designed to allow the implementation of different (thermal) error models.

Measurement techniques

Many different tests for assessing the machine errors have been developed. In 1932 Schlesinger established a systematic framework of measurements

for acceptance testing of machine tools [80]. Formulated from the viewpoint of machine tool building, these tests were focused on the straightness of guideways, their mutual squareness, and their parallelism or squareness with the spindle axis and workpiece table. Similar tests can be found in the early Standards (see e.g. [13, 15, 16, 37]). Both Schlesinger's classic tests and these Standards were intended for manually operated machines. Especially with the introduction of NC machine tools, the measurement and definition of parametric errors were refined further.

Direct measurement techniques were introduced to measure the parametric errors of NC machine tools separately. All six degrees of freedom of an axis are measured directly [14, 99]. Also the squareness between two guides is measured directly. These direct measurement techniques provide comprehensive information on the machine condition with a possible high sampling density, but require much time, skill, and expensive equipment. Therefore, machine performance tests were introduced to achieve a reasonable indication of the machine's performance within a short period of time. These tests comprise the milling of workpieces on the machine tool with hole-patterns or simple contouring operations [64, 99-103]. After the evaluation of the workpieces on a reference coordinate measuring machine, the errors incorporated during the milling process can be determined. However, it is not possible to extract parametric errors from the evaluation of these workpieces. Therefore, it has generally been accepted that a complete calibration should consist of a separate measurement of the errors introduced in the components of the machine.

In recent years a variety of measuring methods using artefacts have been suggested and applied. With the measurement results of these artefacts the parametric errors of the machine are determined. They comprise the measurement of suitable reference artefacts, such as hole plates [56, 58], space frames [5, 45, 49], and (laserinterferometric) step gauges [116]. These artefacts, which are mostly intended for coordinate measuring machines, are measured on various locations in the workspace.

Bryan [7, 8] developed the magnetic ball bar to obtain the position errors of machine tools at various points. The test, though not complete, is quick and easy to perform and gives a good estimate of some of the geometric error components. Knapp [52, 53], reports an interesting test that consists of probing along the edge of a pre-measured circular gauge in different planes. The geometric error components of the machine can be obtained by

analysing the error observations. Both the ball bar and the circular test are also capable of determining some dynamic errors of a machine tool (e.g. following errors).

The large interest in these methods is due to a number of important advantages over the conventional direct measurement of the parametric errors. Direct measurement techniques provide comprehensive information on the machine condition with a possible high sampling density, but require much time, skill, and expensive equipment. In contrast, the artefact can usually be applied by a local operator. Another and fundamental advantage of artefact based calibration methods is that the machine accuracy is estimated from observed deviations of tasks which resemble the intended operation of the machine. However, due to the lack of appropriate software, the subsequent estimation and analysis of the parametric errors still presents problems. In chapter 3 artefact based calibration techniques will be presented to obtain the geometric errors of a machine tool.

Software error compensation

Nowadays, software error compensation is commonly applied on coordinate measuring machines to improve their volumetric accuracy (see e.g. [10, 36, 55, 85, 87, 115]). Compared to software compensation of machine tools, software compensation of measurement tasks is relatively straightforward since it can be achieved by directly subtracting the predicted errors from the measured location after a point has been measured. In contrast, software compensation on machine tools requires the adaptation of the whole commanded trajectory of the tool. The error compensation should interfere before or during the actual movement of the machine. It is not possible to correct an error afterwards, as the material will then already be removed by the cutter. Also the error sources in a machine tool affecting the structural loop are of an order of magnitude higher than in measuring machines. Therefore, commonly available machine tools are not provided with a software error compensation system. Only relatively simple compensations, as lead-screw compensation, can be found in a commercially available machine tools. Also the amount of literature on software error compensation is limited:

- A software compensation system for machine tools is reported by Asao and Takeuchi [1, 92]. A post-processor is applied to generate a compensated NC program which can significantly improve the quality of

the parts machined in an NC lathe. This post-processor is fed with results from a finite element analysis and analytical solutions to predict the workpiece and cutting tool expansion.

- Ferreira [50] has developed different strategies for obtaining compensations when locating the cutting tool at a point in the work space or moving it along a straight line or circular trajectory. These strategies could be applied to generate a compensated NC program.

- French and Humphries [29] also show how compensation of quasi static errors can be achieved in the part programming stage.

- Dufour and Groppetti [24] suggest a number of schemes for incorporating the corrections in the machine's control circuit, once the error vector is known. Although these strategies seem to be very promising, an actual implementation of the developed technique and verification on the CNC machine has not been carried out. They also provided a vertical boring mill with a mechanical compensation system, which can be considered as a synthesis of both a hardware and a software compensation system. Based on a software model an actuator is applied to compensate the horizontal guideway for bending due to dead-weight of machine components.

- The actuators developed by Hatamura [32] which deform the machine's structure based on a software model seem to be a promising way to correct systematic errors in precision machining, but it has not been tested yet on a machine.

In these papers different concepts of software error compensation techniques are described. However, only partial compensations are possible with these concepts. Currently no method exists to compensate all mentioned quasi static errors.

Also an actual implementation and verification is not found in these articles. Only in the Quality in Automation project carried out at NIST (National Institute of Standards & Technology) and the already mentioned BCR-project an actual implementation of a software error compensation has been carried out:

- In the Quality in Automation project carried out at NIST [20, 21] a software error compensation system has been developed. This error compensation system alters the encoder-signals before they are sent to

the controller. Pulses are added or subtracted from the signals. This alters the counter in the controller and thus the trajectory. This system has been applied to a two-axes lathe to compensate for the geometric and thermally induced errors. With this system the possibilities of a software error compensation system are clearly shown. However, one major problem with this system is that is has difficulties with fastly moving axes: the system is too slow. As the system is applied between the position feed-back device and the controller it can also become unstable (see Chapter 6). Also some necessary process parameters like tool dimension and orientation or swivelhead positions are not directly accessible for the system.

- In January 1990 a European research project (BCR-project) has been started to develop methods for the numerical error compensation of machine tools. At the end of this project (December 1992) a software error compensation system was developed, which was able to compensate the quasi static errors of a machine tool. This compensation system is embedded in the controller of the machine tool and therefore only applicable for new machines.

In this thesis the development of two different compensation strategies will be presented. Firstly, a software error compensation strategy which can be implemented in the controller will be described. This error compensation strategy which is called 'Real-time software error compensation' will be a further refinement of the compensation system developed in the BCR-project. This project has been carried out under the responsibility of the present author. Hence, some of the work presented in this thesis can also be found in the final project report [78], which has been written by the present author.

Secondly, a post-processor compensation strategy will be described which will generate a compensated NC-program. This compensation strategy is called 'NC-code software error compensation'. Contrary to the compensation strategies found in the literature [1, 29, 50, 92], the developed NC-code compensation is only limited by the number of axes present in the machine tool (= degrees of free-motion), not by the underlying compensation model. Hence, when NC-code compensation is applied to a three axes machine tool, all errors in the position of the tool can be compensated; when the NC-code compensation is applied to a five-axes machine tool, also the error in the orientation of the tool can be compensated.

Error propagation model

A software error compensation system will be presented, using a kinematic model as a basis for all error models. This kinematic model relates the errors in the location of the tool to errors in the relative location of coordinate frames attached to successive elements of the structural loop (e.g. the various carriages). The latter parametric errors describe the combined effect of all error sources on the geometry of the element enclosed by two coordinate frames. With such a model both the position and the orientation errors of the tool can be modelled adequately.

In the previous paragraph, the kinematic modelling technique has already been introduced. In figure 2.1 the definition of the parametric errors is given; in figure 2.2 an example of a kinematic model for a five-axes milling machine is depicted. The main purpose of the the kinematic models found in the literature (including the model presented in figure 2.2) is to achieve the best possible model describing all errors involved. However, the main purpose of the kinematic model presented in this thesis is to achieve a basis for software error compensation in the most efficient way. Therefore, the following simplifications and modifications have been carried out:

- *Errors of the rotary axes;*

  A kinematic error model is able to describe both the rotation and translation errors of the tool, induced by translational and rotational elements. Hence, these errors can principally be compensated by a software error compensation system. However, full software compensation of the significant five degrees of freedom is only possible when the machine contains these rotary axes. Most machine tools are not equipped with these axes. Also a software error compensation for the errors in the rotary axes will result in complex and time-consuming calculations, as sine and cosine functions have to be evaluated. Especially for the software error compensation implemented in the controller the available calculation time will be limited. Therefore, the errors of the rotary axes will not be considered with this software error compensation system.

- *Compensation of rotation errors;*

  Rotary axes applied on a machine tool show a relatively low dynamic servo-stiffness, compared to the other machine components. Therefore,

rotary axes are most of the time clamped on a fixed position which increases the dynamic stiffness. When the rotation errors of the tool should be compensated continuously with the available rotary tables, this clamping would be too slow. Therefore, the software compensation system will only compensate the translation errors and not the rotation errors of the tool. This simplification will only be carried out in the compensation mechanism. This means that the evaluation of the different models will be carried out using all information available from the model, including the rotational terms.

- *Location of the coordinate frames.*

  Contrary to the applications of the kinematic model found in the literature the coordinate frames are not attached to the different elements of the structural loop, but are located in the workspace of the machine. With a coordinate frame attached to an element the potentiality of the model to analyse the individual errors increases. When a coordinate frame is chosen on the position of the scale, the translation error iti (xtx, yty, ztz) directly reflects the scale error (no Abbe-offset). Also finite stiffness errors can be modelled more adequately when the coordinate frames are chosen on the right place as the bending of an axis can directly be modelled by a rotation error.

  When the coordinate frames are attached to the elements of the structural loop of the machine tool, several construction parameters have to be included in the model. This would result in a different model for every machine type. Also, a model with the coordinate frames in the workspace requires less calculations for the software error compensation system as all these construction parameters has to be accounted for. Therefore, the coordinate frames are located in the workspace of the machine, resulting in a machine type independent model, which can be evaluated fastly.

  When the coordinate frames are located in the workspace of the machine, the modelled errors don't directly reflect the physical errors (e.g. the scale error). In figure 2.3 an example is depicted for the linearity error xtx. xtx_{scale} Directly reflects the scale error when the coordinate frame is located in the X-axis, at the location of the scale. xtx_{model} Represents the linearity error in the workspace of the machine tool. This error includes the scale error xtx and an additional term (δ_m) consisting of a rotation error xry multiplied with arm-length D. The arm-length D is the distance

in Z-direction between the coordinate frames in the workspace and the scale. This example clearly depicts that choosing the location of the coordinate frame in the workspace doesn't deteriorate the compensation model as both linearity error xtx_{scale} and xtx_{model} can be expressed as a function of each other, the rotation error xry and the distance D.

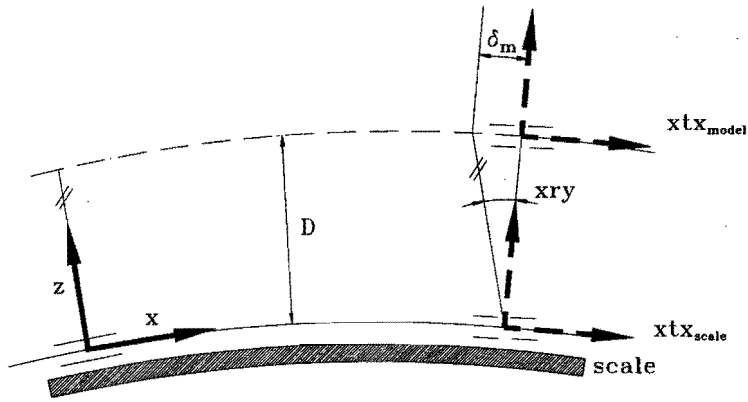

Figure 2.3 Linearity error xtx defined on two different locations.

- *One kinematic chain*

The kinematic modelling procedure found in the literature [78, 87, 95] distinguishes two different chains. An A-chain accounts for the errors incorporated in the chain from machine-base to the tool. A B-chain accounts for the errors from the base to the workpiece. The main reason for this separation is the applied measurement technique. With the parametric measurement method (see Chapter 3) the measurements are always related to the machine's base. Then, the position error of the tool with respect to the workpiece is calculated with:

$$\underline{E} = \underline{E}_{B-chain} - \underline{E}_{A-chain} \qquad [2.1]$$

The implementation of two different chains in the error propagation model would result in 4 different models, dependent on the number of axis present in a chain. Therefore, the error propagation model is based on only one chain, from the workpiece table to the tool. The measurement results obtained with the mentioned parametric method have to be translated to this model. Hence, the machine's construction has to be considered during the data-acquisition.

Using the presented simplifications and modifications the error propagation model can be described as follows:

$$\underline{E} = \begin{bmatrix} E_x \\ E_y \\ E_z \end{bmatrix} = \sum_i \underline{E}_i \qquad [2.2]$$

where $\underline{E}$ describes the position error of the tool.

$$\underline{E}_i = \underline{e}_i + \underline{\varepsilon}_i \times \underline{p}_i \qquad [2.3]$$

$$\underline{e}_i = \begin{bmatrix} itx \\ ity \\ itz \end{bmatrix} \qquad [2.4]$$

$$\underline{\varepsilon}_i = \begin{bmatrix} irx \\ iry \\ irz \end{bmatrix} \qquad [2.5]$$

$$\underline{p}_i = \begin{bmatrix} l_x \\ l_y \\ l_z \end{bmatrix} + \begin{bmatrix} b_{ix} \cdot X \\ b_{iy} \cdot Y \\ b_{iz} \cdot Z \end{bmatrix} \qquad [2.6]$$

$$i \in \{x, y, z\}$$

With:

$\underline{E}_i$: Effect of the errors in axis i on the position error of the tool.

$\underline{e}_i$: Translation errors of axis i.

$\underline{\varepsilon}_i$: Rotation errors of axis i.

$\underline{p}_i$: This vector describes the Abbe offset of the errors introduced in axis i (see figure 2.4).

l_i : Component i of the tool vector.

b_{ii} : Parameters which describe the machine configuration (0 or 1).

X, Y, Z : Actual axis' position (machine coordinate system).

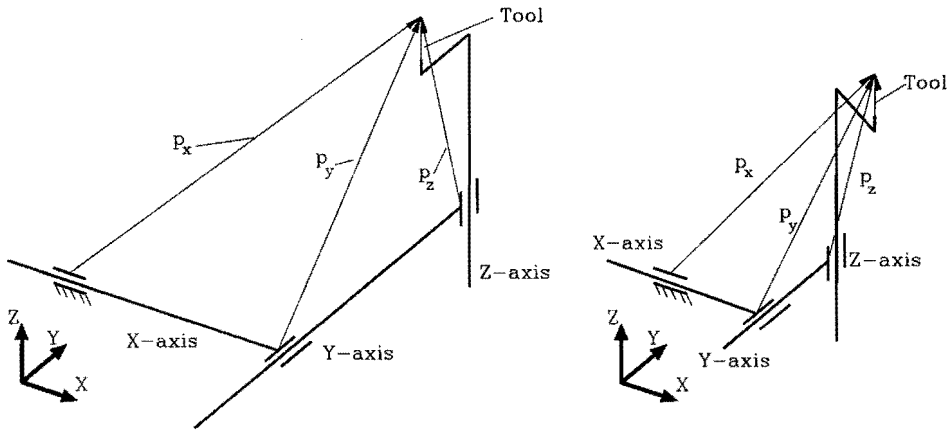

Figure 2.4 The vectors $\underline{p}_x$, $\underline{p}_y$, $\underline{p}_z$ describe the Abbe offsets of the errors introduced respectively in the X-, Y- and Z-axis. These vectors include the axis' position and the construction offsets introduced by the machine. In this figure two different positions are presented with the vectors $\underline{p}_i$.

During the milling process the machine tool can be equipped with different tools. The different lengths of the tool holder are represented by the tool vector (l_x, l_y, l_z). This vector represents the actual position of the tool-tip with respect to the spindle nose. Whenever a tool change occurs, this vector will be updated. Also when the machine tool is equipped with a rotating tool head (e.g. C-axis of the investigated milling machine) and/or with a swivelhead (which enables both horizontal and vertical milling) the change in the tool vector is taken into account. Therefore, some construction of the machine tool can be found in the vectors $\underline{p}_i$ (see figure 2.4).

Example

In figure 2.5 a schematic presentation is given of a three-axes machine tool. With the conventional modelling technique, the kinematic model would include a lot of construction parameters. In figure 2.6 the kinematic model of the machine presented in figure 2.5 is given.

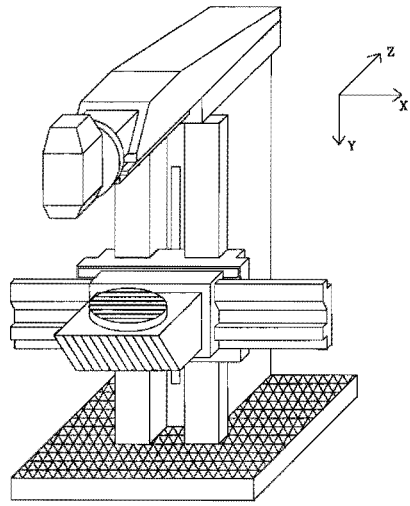

Figure 2.5 Schematic representation of a three-axes milling machine.

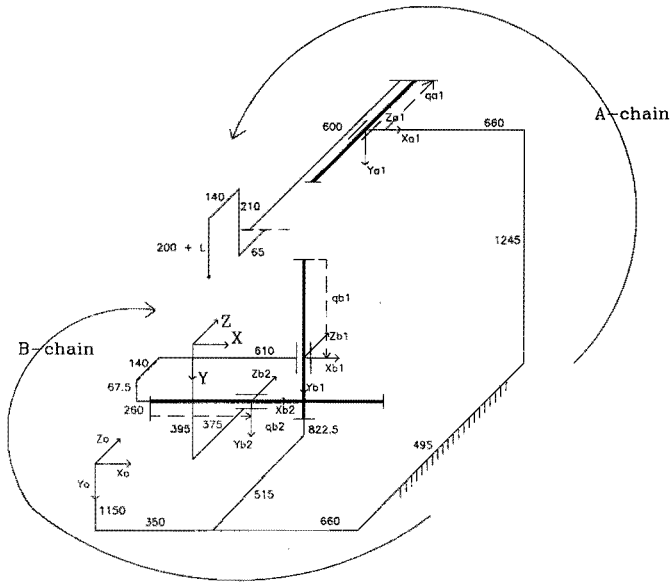

Figure 2.6 Conventional kinematic model of the milling machine presented in figure 2.5.

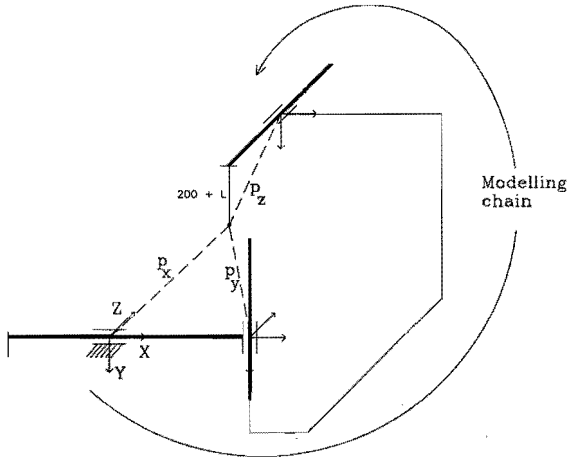

Figure 2.7 Kinematic presentation of the milling machine presented in figure 2.5, using the newly developed modelling strategy. The model has one chain; only one construction parameter (distance between tool holder and C-axis) has to be defined.

Using the newly developed technique the resulting model only includes one construction parameter (offset tool holder and Z-axis). In figure 2.7 this model is depicted. In this picture the Abbe offsets are presented with the following vectors:

$$\underline{p}_x = \begin{bmatrix} l_x \\ l_y \\ l_z \end{bmatrix} + \begin{bmatrix} X \\ Y \\ Z \end{bmatrix} \qquad [2.7]$$

$$\underline{p}_y = \begin{bmatrix} l_x \\ l_y \\ l_z \end{bmatrix} + \begin{bmatrix} 0 \\ Y \\ Z \end{bmatrix} \qquad [2.8]$$

$$\underline{p}_z = \begin{bmatrix} l_x \\ l_y \\ l_z \end{bmatrix} + \begin{bmatrix} 0 \\ 0 \\ Z \end{bmatrix} \qquad [2.9]$$

These vectors (equation 2.7, 2.8 and 2.9) should be substituted in equation 2.2 to get the complete error propagation model.

Open architecture design

The software error compensation system will be based on the error propagation model as described in the previous paragraph. With this model the parametric errors of each axis can directly be related to the resulting error of the tool. The parametric errors will be described with error functions, which are obtained by superposition of contributions of the parametric errors resulting from individual error models. Each individual model describes the effect of one single error source (geometry, static forces and temperature). This design will enable direct implementation of the different models in the software error compensation system without effecting the compensation mechanism itself. This, so called 'Open Architecture Design' will allow the investigation of different error models during the actual operating conditions.

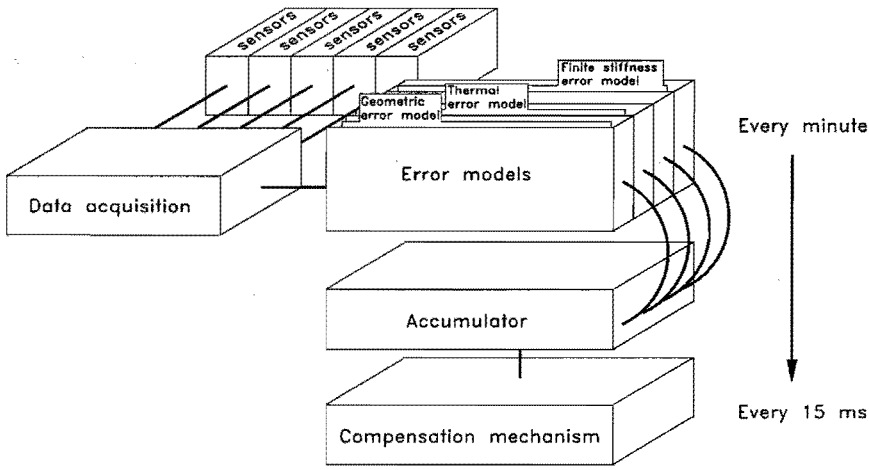

Figure 2.8 Open architecture software error compensation system.

The developed open architecture software error compensation system consists of the following parts (see figure 2.8):

- *Data acquisition;*

  Data acquisition is necessary to determine the machine's status (e.g. the temperature on different locations). The data acquisition is carried out at time-discrete points (every minute).

- *Error models;*

  The software error compensation system can operate with different error models. The individual error models should be independent to enable an optimal exchangeability for different models. For each axis a total of 6 error functions are available which enables the modelling of all degrees of freedom for that element (itj and irj). Each error function may be a function of the axis' position (X, Y, Z) and the sensor readings.

- *Accumulator;*

  The accumulator builds the compensation model by superposition of the individual error models (itj and irj). The resulting model consists of 18 compensation functions, all dependent on the position of one axis. A correlation between the various compensation functions is not allowed. This restriction is necessary to limit the amount of memory and especially the calculation time, needed for the evaluation of the full model. Each compensation function may be a discrete or a continuous description of the compensation value as a function of the axis' position.

- *Compensation mechanism.*

  The compensation mechanism calculates the actual compensation value, using the compensation model received from the accumulator. This compensation model is a functional description of each individual error as a function of the actual position of the machine's axis. This implies that whenever the position of one of the machine tools axes changes, the compensation model has to be evaluated. Two different compensation strategies have been developed to accomplish this task: The 'Real-time software error compensation' and the 'NC-code software error compensation'. In Chapters 6 and 7 these compensation strategies will be discussed extensively.

In the next three chapters the different error models will be presented, which are applied in the software compensation system. These models will generate the individual parametric errors before they are sent to the accumulator.

Chapter 3

Determination of Model Parameters for the Geometric Errors

In this chapter the determination of the model parameters for the geometric errors is discussed. The models for the geometric parametric errors are based on least squares fitted piecewise polynomials. In the first paragraph the application of piecewise polynomials will be discussed. Three different measurement techniques have been applied on the Maho 700S milling machine to determine these geometric errors. After a presentation of the experimental setup, firstly, the results of the direct measurement techniques will be discussed. Secondly, the application of an artefact, a hole plate, will be presented. Thirdly, a new indirect measurement technique is introduced to determine all geometric errors with a ball bar. Each individual measurement technique will be presented and its performance will be evaluated considering its capability to determine the parameters for software error compensation purposes. In the last paragraph a comparison of the three measurement methods will be presented.

Modelling the parametric errors with piecewise polynomials

A kinematic model has been applied as a basis for all error models. This kinematic model relates the errors in the location of the tool with respect to the workpiece to errors in the relative location of coordinate frames. The latter parametric errors describe the combined effect of all error sources on the geometry of the element enclosed by two coordinate frames (see Chapter 2).

Although most mathematical functions can be used to describe the parametric errors, their application is limited to model the frequently disjointed or disassociated nature of the residual. That is to say that the behaviour of an error in one region of the domain may be totally unrelated

to the behaviour in another region. Polynomials, along with most other mathematical functions, have just the opposite property. Namely their behaviour in a small region determines their behaviour everywhere [76, 87]. Thus, the irregular nature of many geometric errors requires the use of special functions that possess this property to a lesser extend. A suitable approach to this problem is to divide the range of the joint position into segments and fit an appropriate function in each segment. This can be achieved by so-called piecewise polynomials [55, 56, 78, 85, 87, 95].

With piecewise polynomials the parametric errors can be estimated efficiently in the presence of noisy calibration data. The resulting model of the machine accuracy is mathematically easy to handle (e.g. regarding the number of coefficients) and has good properties for software error compensation (e.g. regarding its smoothness). Finally, in addition to using the functions as an approximation tool (i.e. a curve fitting tool), also statistical testing procedures can be readily applied to investigate the accuracy of the estimated error model, error trends, points of structural change, or the significance of certain errors or error components.

Piecewise polynomials can be described as a set of polynomials defined on limited continuous parts of the domain. The various pieces join in the so-called knots, obeying continuity restrictions with respect to the function value and an arbitrary number of derivatives. The number and degrees of the polynomial pieces, the nature of the continuity restrictions, and the number and positions of the knots may vary in different situations, which gives piecewise polynomials the desired flexibility. A straightforward mathematical implementation of the continuity restrictions can be obtained by the use of truncated polynomials or '+'-functions as basic elements in the piecewise polynomial models. The '+'-function is defined as:

$$u_+ = u \quad \text{if } u > 0 \qquad [3.1]$$

$$u_+ = 0 \quad \text{if } u \le 0 \qquad [3.2]$$

In general, with k knots $t_1, \ldots t_k$ and k+1 polynomial pieces each of degree n, the truncated power representation of a piecewise polynomial p(x) with no continuity restrictions can be written as:

$$p(x) = \sum_{j=0}^{n} \beta_{0j} \cdot x^j + \sum_{i=1}^{k} \sum_{j=0}^{n} \beta_{ij} \cdot (x - t_i)_+^j \qquad [3.3]$$

Note that the presence of a term $\beta_{ij} \cdot (x - t_i)_+^j$ allows a discontinuity at t_i in the j-th derivative of p(x). Thus different continuity restrictions can be imposed at different knots by deleting the appropriate terms. Normally, it is sufficient to ensure that each model is continuous with respect to the function value and its first derivative.

An inherent problem in constructing the individual model is the unknown nature of the errors to be described. The model's potential to accommodate irregular errors, is to an extensive degree determined by the number and position of the knots. If the position of these knots are considered variable, that is, parameters to be estimated, they enter into the regression problem in a non-linear fashion, and all the problems arising in non-linear regression are present [87]. The use of variable knot positions also carries the practical danger of overfitting the data, and makes testing of hypotheses, considering areas of structural change, virtually impossible. Unless prior information is available, we use a basic model which contains enough polynomial pieces with a fixed length and a maximum allowable degree of two, to accommodate the most complex error expected. In the parameter estimation process, a stepwise regression procedure is implemented to remove statistically insignificant parameters from the model [87]. The reason for this removal is twofold:

- Including insignificant parameters hardly improves the model's quality of fit, but increases the variance of the estimated parameters and response;
- Identification of structural parameters enhances the diagnostic properties of the individual model.

All the parametric errors are described with piecewise polynomials. In the paragraph describing the direct measurement technique, an example is given of a piecewise polynomial fitted on the measured error zry (see figure 3.4).

Experimental setup

Several methods exist to measure the geometric errors of a machine tool. These methods can be separated into three different classes: direct measurement techniques, artefacts and indirect measurement techniques:

- *Direct measurement technique;*

  The individual parametric errors are measured directly using measurement instruments like laserinterferometer or electronic levelmeters.

- *Artefacts.*

  The third method to determine the geometric errors of a machine is by the application of artefacts. By evaluation of the measurement data, gathered with an artefact, the parametric errors can be determined.

- *Indirect measurement technique;*

  Contrary to the direct measurement techniques, the indirect measurement technique does not directly reflect the individual parametric errors. From a large data set of measurements (e.g. length measurements), the parametric errors are estimated using linear least square estimation techniques. This method has been introduced by Soons [86, 87].

These different measurement techniques have been applied on the Maho 700S milling machine.

Before the actual measurements of the geometric errors can be carried out, first a thermal reference state has to be defined. This thermal reference state has been defined as the state in which all components of the structural loop have a uniform temperature distribution of 20°C. This definition is motivated by a strict separation of geometric and thermal errors. Secondly, most measurement equipment used to assess the geometric and finite stiffness errors require a stable thermal environment of 20°C. Unfortunately, such a reference state cannot be achieved. 'Every' machine has heat sources that are not related to operational parameters such as spindle speed and joint movements. However, these local heat sources cause a relatively small deviation in the reference state, which will be be compensated (e.g. expansion of the scales). The movements are

carried out relatively slow and the main spindle is not rotated during the geometric measurements to avoid quick changes in the machine temperature.

As the number of measurements required for the determination of the geometric errors is very large dedicated software has been developed. This software has basically two main tasks:

- *Control of the position of the machine tool*

  The Grundig Numeric controller, which is attached to the Maho 700S milling machine, can be connected to a PC using the RS232 serial port. The software on this PC has been designed to communicate with the controller of the milling machine using the DNC message protocol and the LSV/2-datalink protocol. The use of the DNC message protocol [30,31] allows advanced control of the controller by the external PC.

- *Collecting and storing of the measurement results*

  In order to realise a fully automated experimental set-up, the applied measurement instruments also have to be connected to the PC. Therefore both RS232 and the IEEE-488 interface have been implemented in the software. Most instruments have been connected to the IEEE-488 interface, which is a well supported industry standard.

In figure 3.1 a schematic overview is presented of the applied interfaces and used measurement instruments. All the experiments described below are carried out by application of the software package.

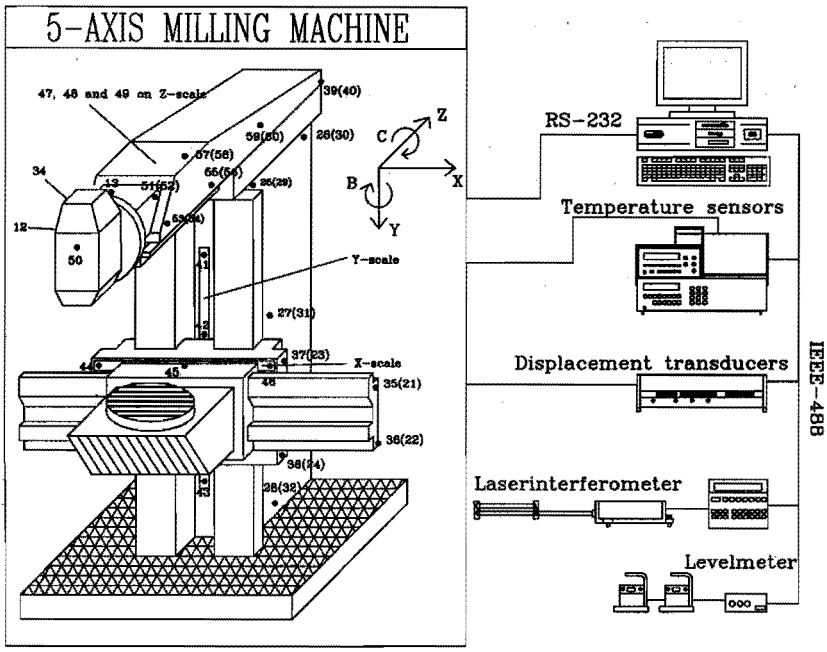

Figure 3.1 Scheme of the applied experimental set-up. The numbered dots indicate the position of the applied temperature sensors (see Chapter 5).

Direct measurement technique

One of the most commonly applied methods to determine the geometric errors of a machine tool is the direct measurement method. This measurement technique has been introduced to measure the parametric errors of NC machine tools separately. All six degrees of freedom of an axis are measured directly [14, 99]. Also the squareness between two guides is measured directly, resulting in a total of 21 measurements for a orthogonal three axis machine.

Using the above described experimental setup, all 21 geometric errors present in the system of the three linear axes have been determined. The measurement sequence of these experiments is defined over the entire range of the respective axis of movement with a measurement step of 10 mm. For the measurement of the translation errors and the rotation errors

irj (with i ≠ j and i,j = X, Y or Z) a Hewlett Packard 5528 laserinterferometer has been applied with accompanying optics. In figure 3.2 a photograph of the measurement setup is presented applied to determine the translation error ztz. For the rotation errors iri (i = X, Y or Z) electronic levelmeters are applied. The squareness errors between the three linear guides (i.e. xsy, xsz and ysz) have been measured using a ceramic square in combination with displacement transducers.

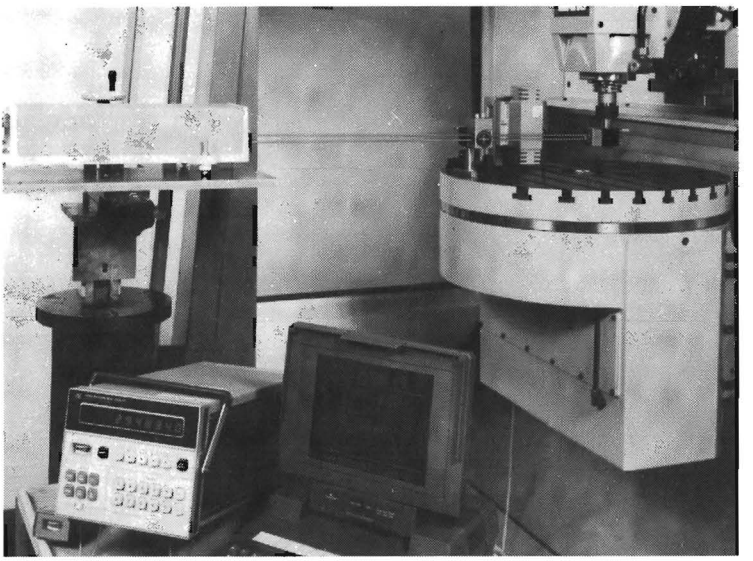

Figure 3.2 Measurement setup for ztz.

A problem when estimating the various parametric errors is that it is usually not possible to measure these errors at the location where they are defined (i.e. in the origin of the respective coordinate frames). Thus measurements of translational parametric errors are 'contaminated' with the effect of several angular parametric errors through their respective Abbe offsets. One approach to this problem calls for the sequential estimation of the various parametric errors after compensating the measurement data for the effect of parametric errors already estimated. Here the angular parametric errors are estimated before the translation parametric errors. By compensating displacement measurement data for the effect of (angular) errors already included in the model (using this

model), the residual data for the respective translation parametric error 'automatically' describes this error at the location where it is defined. We use this approach when the various parametric errors are individually measured.

As a typical example of the estimation procedure we consider the modelling procedure for the angular error around the Y-axis when moving the Z-axis of the milling machine, denoted as zry. The error is measured with a laserinterferometer using the setup depicted in figure 3.3. The measurement is carried out back and forth over the total range of the Z-axis (600 mm), using a sampling distance of 10 mm. At each measurement point, the axis motion is halted. After a short delay to eliminate dynamic effects induced by the axis motion, five samples of the angular error are taken. The complete measurement procedure is executed automatically using the described experimental setup.

Before estimating the model, the measurements are corrected for the drift of both measurement equipment and machine. Here the measurement data are divided into several cycles, each containing one back and forth run. The observed errors of each cycle are plotted as a function of the elapsed time at their measurement since the start of the cycle. As every measurement position is reached with an equidistant time interval a linear temporal drift can be estimated. The residuals of the observed errors with respect to a least-square line represent the drift corrected error data. This approach is only allowed and applied, when the respective error shows no (significant) backlash.

The proposed model for this error is a second order piecewise polynomial, continuous with respect to the function value and its first derivative, having 11 knots placed at 50 mm intervals. After the stepwise regression procedure, 5 knots were retained (at a significance level of 99.99% for adding or removing a regressor). The estimated model is presented in figure 3.4 together with a validation dataset of also five back and forth measurements executed directly after those used to estimate the model.

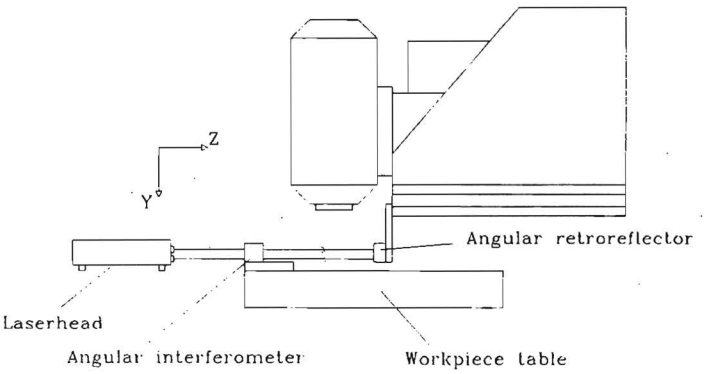

Figure 3.3 Schematic representation of measurement setup for zry.

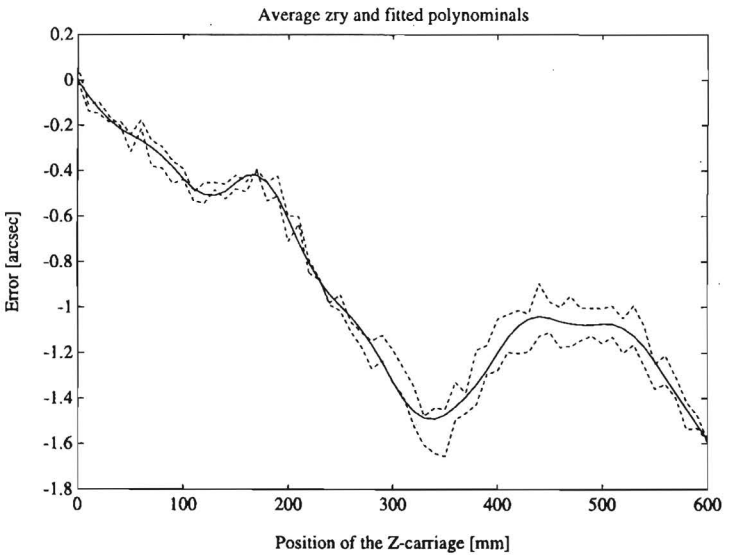

Figure 3.4 Example of fitting with piecewise polynomials on the measured geometric error zry. The continous line represents the estimated model. Both dotted lines represent the result of a verification measurement.

Hole plate

A hole plate is an artefact specially designed for calibration of coordinate measuring machines [58]. A hole plate consists of an equally spaced grid of high-precision holes. Each hole should be measured by a mechanical probe. Before a hole plate can be applied to calibrate a machine, the plate itself has to be calibrated. Special calibration routines have been developed at PTB (Physikalisch Technische Bundesanstalt, Braunschweig Germany) to accomplish this task with a very high accuracy [58]. The hole plate available for the experiments has been calibrated with a remaining uncertainty of 0.1 μm. Hence, the location of each hole is known within 0.1 μm.

The exact location of each hole being known the hole plate can be applied for geometric calibration purposes. After a compensation of the linear expansion of the scales and the hole plate, by measuring the actual temperature of the machine and the hole plate, the geometric errors remain. The errors due to a load are neglectable as the errors due to the load of the mass of a hole plate is very small compared to the weight of the workpieces which are normally placed on the machine.

A hole plate is a two-dimensional artefact. This implies that one experiment includes the geometric errors in two dimensions. To determine the geometric errors in three dimensions the hole plate has to positioned on different locations. In order to achieve a complete accuracy picture of the machine tool the hole plate has to be positioned on three different locations in the workspace of the machine (see figure 3.5) and the hole plate has to be measured with two different probe configurations [56, 58].

A hole plate has fixed dimensions. Thus, in principle, the dimensions of a hole plate should be designed to fit in the workspace of a machine. When a machine, for example, has an X-axis with a range of 2000 mm, this would result in a hole plate with at least a length of 2000 mm. Such a hole plate would be very difficult to handle. Therefore, the hole plate has to be placed on different locations across the diagonal of the machine's workspace. When each individual location of the hole plate has at least two holes coincident with holes of the previous location of the plate, the new location of the hole plate can be calculated (see figure 3.6).

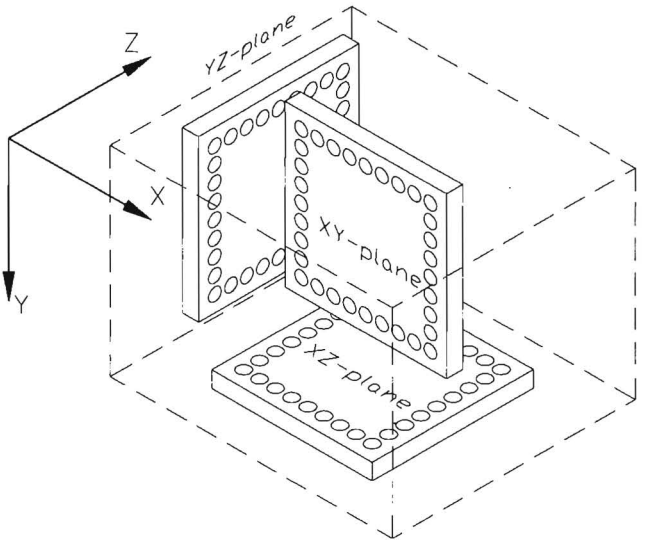

Figure 3.5 A hole plate located in three different planes.The hole plate has to be measured with two different probe configurations to achieve a complete calibration.

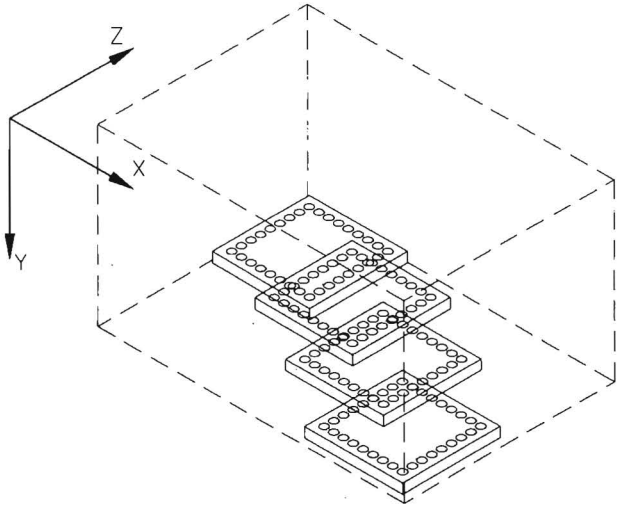

Figure 3.6 A hole plate has to be positioned across the diagonal of a workplane to cover the whole range of the machine.

A total of 11 hole plate measurements have been carried out on the investigated milling machine. Six hole plate measurements are used for the estimation of the geometric error model. Two hole plate measurements have been carried out in the XZ-plane, two in the XY-plane and two in the YZ-plane. The other five measurements are applied for verification. These verification measurements are carried out on locations different from the first measurements or with different probes. The verification measurements are also applied for the verification of the other measurement techniques (see the last paragraph of this chapter).

In figure 3.7 a photograph is depicted of a hole plate measurement carried out in the XZ-plane.

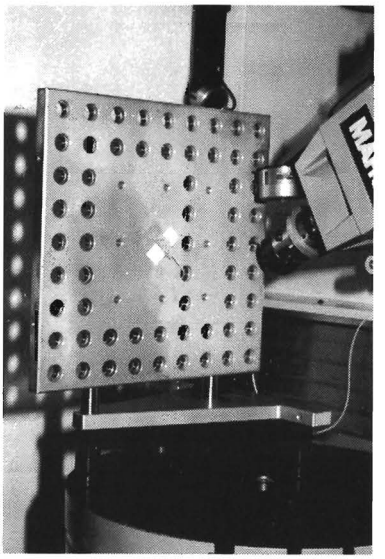

Figure 3.7 A hole plate measurement carried out in the XZ-plane on the milling machine.

The error in the location of each hole is calculated with respect to the first hole of the plate. As the hole plate cannot be perfectly aligned to an axis of the investigated machine, this alignment is carried out mathematically. The measurement results of the hole plate are rotated so that the straightness errors of the first row of the hole plate are minimised in a

least square sense. This implies that the first row of holes of a hole plate measured in the XY-plane is aligned to the X-axis of the machine; a hole plate measured in the YZ-plane is aligned to the Y-axis of the machine.

The applied kinematic model describes the errors in the location of the tool as a function of the errors in the relative location of the coordinate frames (see first paragraph). This relationship is linear as all second order terms are neglected (i.e. cosine errors). Therefore, implementation of the machine's error model, obtained by an appropriate combination of the models for the parametric errors with the machine's kinematic model, yields a linear relation between the determined error and the parameters of the piecewise polynomials. Thus the measurement results determined from the hole plate measurements can be presented mathematically as:

$$\underline{\Delta P} = X\underline{\beta} + \underline{\gamma} \qquad [3.4]$$

With:

$\underline{\Delta P}$: A vector $(\Delta x, \Delta y, \Delta z)$ which contains the difference between the measured and the nominal position of a hole.

X : A matrix with row i describing the effect of coefficient β_i on the measured error for every hole.

$\underline{\beta}$: A vector which contains all coefficients of the piecewise polynomials.

$\underline{\gamma}$: A vector of random errors (residuals), assumed to be independent and identically distributed with mean zero and variance σ^2.

Since the above model is linear in the unknown coefficients $\underline{\beta}$ they can be estimated using linear least-squares analysis [87]:

$$\underline{\hat{\beta}} = (X^T X)^{-1} X^T \underline{\Delta P} \qquad [3.5]$$

Both the matrix X and the vector $\underline{\Delta P}$ are filled with the measurement results obtained from the mentioned six hole plate experiments. The parameters $\underline{\beta}$ are calculated in one estimation procedure, using all measurement data together.

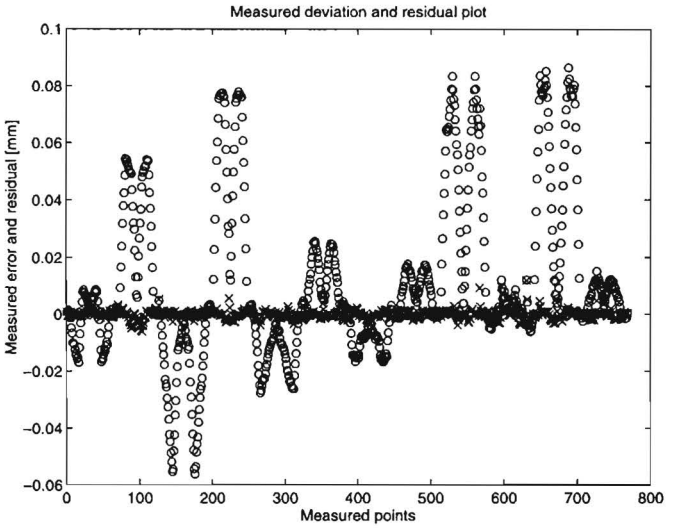

Figure 3.8 The measured error in every location of a hole (indicated with 'o') and the accompanying residual (indicated with 'x').

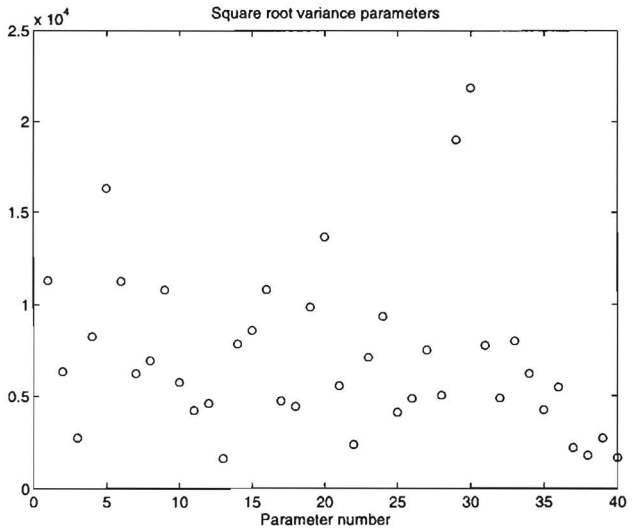

Figure 3.9 Analysis of variance carried out for every parameter included in the model.

In figure 3.8 the residuals of such an estimation procedure are given together with the measured error. In order to analyse the significance of a particular parameter included in the model, an analysis of variance is carried out (see figure 3.9). As explained in the first paragraph, a stepwise regression procedure is implemented to remove the statistically insignificant parameters.

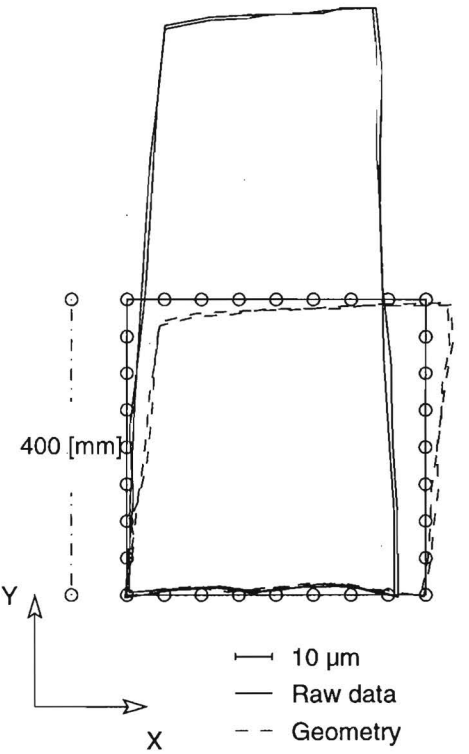

X-direction	
Max.dev	0,014 [mm]
Max.res.	0,009 [mm]
Efficiency	38%
Y-direction	
Max. dev.	0,079 [mm]
Max.res	0,007 [mm]
Efficiency	94%

Figure 3.10a: Simulation results of a hole plate experiment carried out in the XY-plane of the milling machine. The measurement results are indicated with the continuous lines; the difference between the measured error and the simulated error is calculated for every hole and represented by the dashed lines.

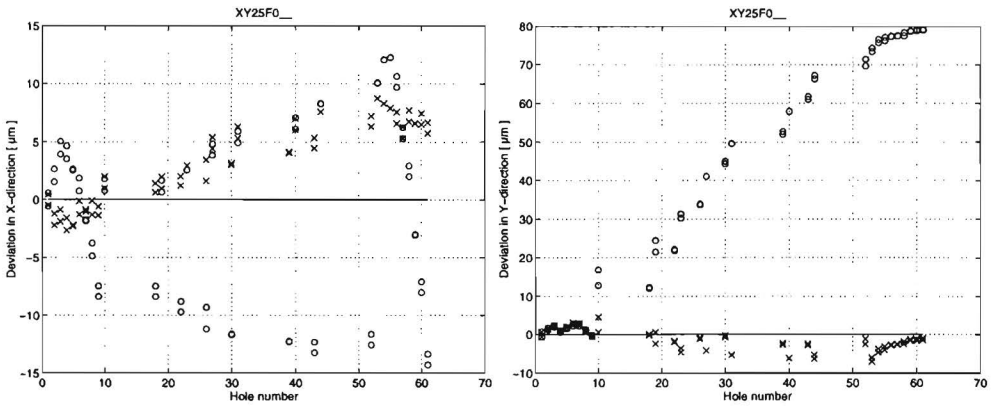

Figure 3.10b: Simulation results of a hole plate experiment carried out in the XY-plane of the milling machine. The measurement results are indicated with the 'o'; the difference between the measured error and the simulated error is calculated for every hole and represented by the '+'-symbols.

In figures 3.10a and 3.10b the measured error and the calculated residual is depicted for a hole plate measured in the XY-plane. This figure clearly depicts the high efficiency of the model in Y-direction, where the measured errors are relatively large. In X-direction the measured error is somewhat smaller, resulting in a lower efficiency of the model. However, the maximum residual found in both directions is almost equal (9 µm in X- and 7 µm in Y-direction).

Ball bar

A ball bar is a measuring device specially designed for dynamic measurements on machine tools. The device consists of two balls and a linear displacement transducer which measures the variation in the distance of both balls. During an actual measurement the machine is commanded to move along a circular path. This path has a radius which equals the nominal distance between the two balls. During the movement the measuring device is triggered continuously, resulting in a circular plot which includes the back-lash error of the machine, the servo-errors of the machine (i.e. following error) and the geometric errors of the machine. In

figure 3.11 the ball bar is schematically depicted together with a typical measurement result. In figure 3.12 a photograph of the applied ball bar is presented (Heidenhain DBB110).

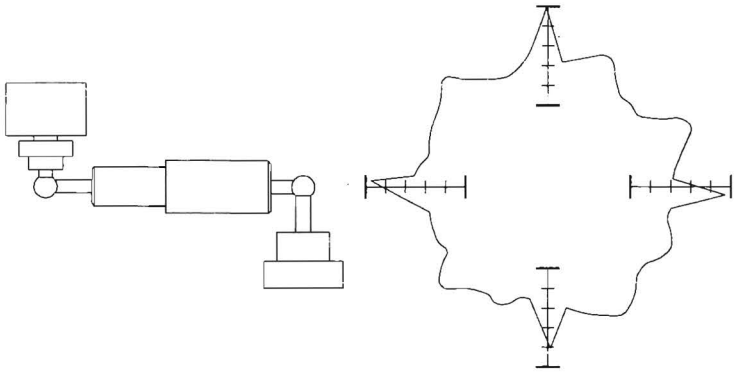

Figure 3.11 A schematic presentation of a ball bar together with a typical measurement result of a dynamic measurement. The result is obtained during a circular movement of the machine and a continuous read-out of the measuring device. Each division in the graph indicates 20 μm. The measurement results show a large error on a quadrant change. This measurement procedure is also referred to as 'circular test' [53].

The measurement results contain both dynamic and static errors. However, when the ball bar is applied as a static measuring device, by positioning the machine at discrete positions along the circle only the geometric errors remain in the measurement results. When this procedure is extended by movements along a sphere, a 3-dimensional test sequence is obtained from which the geometric errors of a machine tool can be determined. The gathered measurement results are similar to the length measurements carried out with a laserinterferometer by Soons [87] on a coordinate measuring machine. However, the major advantages of this method are:

- It is more robust and therefore more suitable for machine tools than the application of a laserinterferometer;
- The investigated machine has a moving table which makes it very difficult to position the laser and the turning mirrors on the table

without losing a significant part of the workspace caused by a possible collision;

- A laserinterferometer is a very expensive measuring device compared to the relative simple ball bar;
- A ball bar is a commonly applied device to determine the dynamic behaviour of a machine tool.

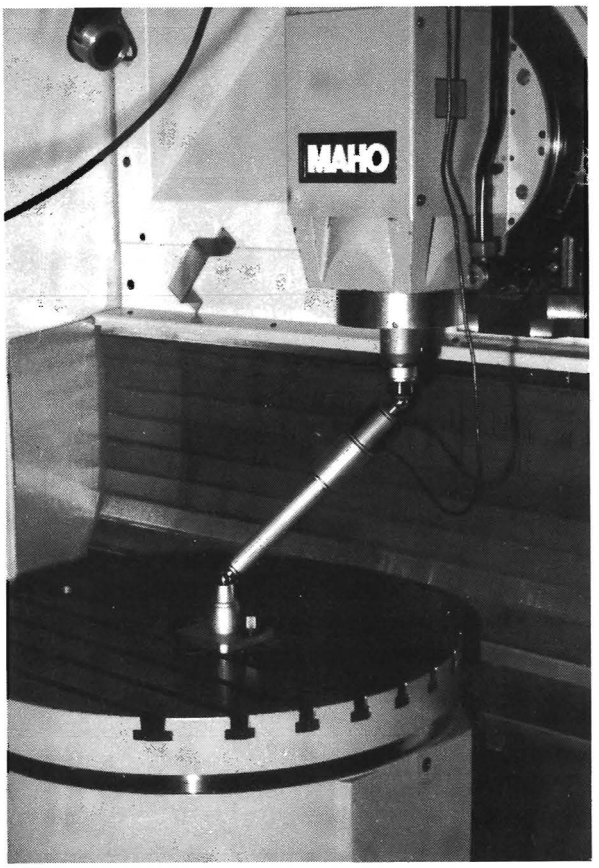

Figure 3.12 A photograph of the applied ball bar.

The major disadvantage of a ball bar is its limited range. Therefore, like the hole plate, several experiments have to be carried out to cover the whole workspace of the machine tool (see figure 3.13).

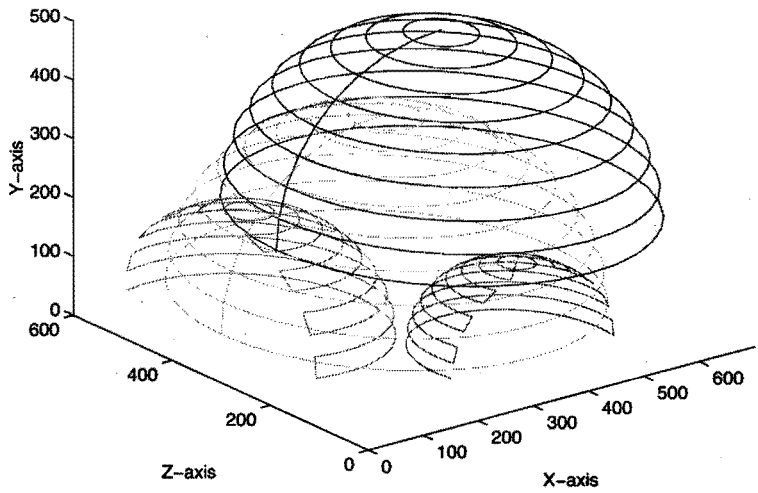

Figure 3.13 An example of some ball bar measurements carried out on different locations and with different radii to cover the whole workspace of a machine tool.

In order to overcome the problem of its limited range, the ball bar is supplied with several extension rods allowing the measurement with different radii (R=150, 200, 250 and 300 mm).

The six positions of the hole plate inherently introduce the application of different tool vectors (otherwise the plate cannot be measured in both the XY-, XZ- and YZ-plane). The ball bar experiments have to be carried out in a similar way to introduce all error components in the model. For example, the rotation error zrz of the investigated milling machine (see figure 2.5) can only be determined from the measurement data when different tool vectors are applied.

In table 3.1 an overview is given of the experiments included in the estimation procedure, together with the radius of the applied ball bar, the centre point of the sphere and the tool length.

Experiment	*Radius*	*Position centre*	*Tool*
4	300	300, 80, 300	110
14	150	300, 80, 300	110
27	300	400, 190, 300	110
29	250	400, 190, 300	110
89	300	50, 80, 300	110
99	150	350, 210, 300	245
105	300	350, 210, 300	245
137	300	350, 210, 0	245

Table 3.1 An overview of the experiments included in the estimation procedure.

As the actual location of the centre of the sphere is not exactly known, the centre point has to be estimated from the measurement results. All measurement data are recalculated for this new centre point. By measuring the temperature of the ball bar and the investigated milling machine the linear expansion of the ball bar and the scales are compensated.

The actual estimation procedure is similar to the hole plate. The vector $\underline{\Delta P}$ is filled with the measurement results obtained from the mentioned 8 ball bar experiments. The parameters $\underline{\beta}$ are calculated in one estimation procedure, using all measurement data together. In figure 3.14 the residual-plot and in figure 3.15 the analysis of variance are graphically depicted.

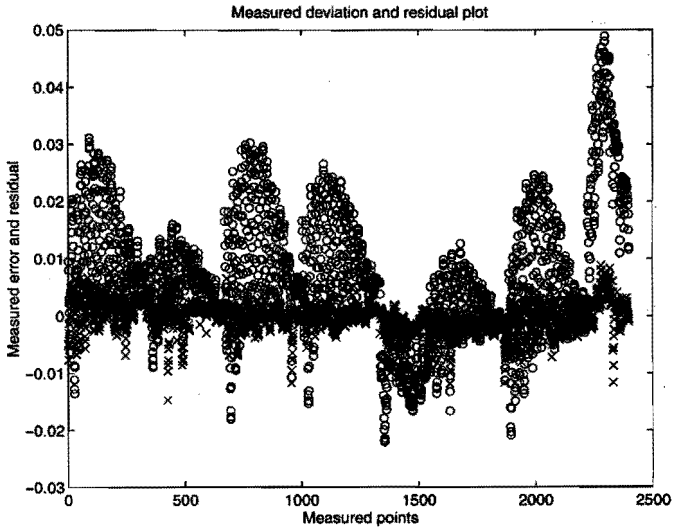

Figure 3.14 The measured error of the tool with respect to the calculated centre point represented as an error in the radius of the sphere (indicated with 'o') and the accompanying residual (indicated with 'x').

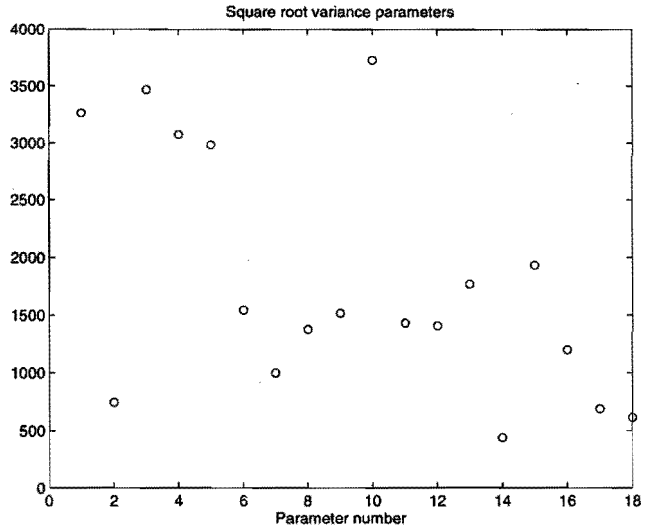

Figure 3.15 Analysis of variance for every parameter included in the model.

In figure 3.16 the measured error and the residual is depicted for experiment no. 4.

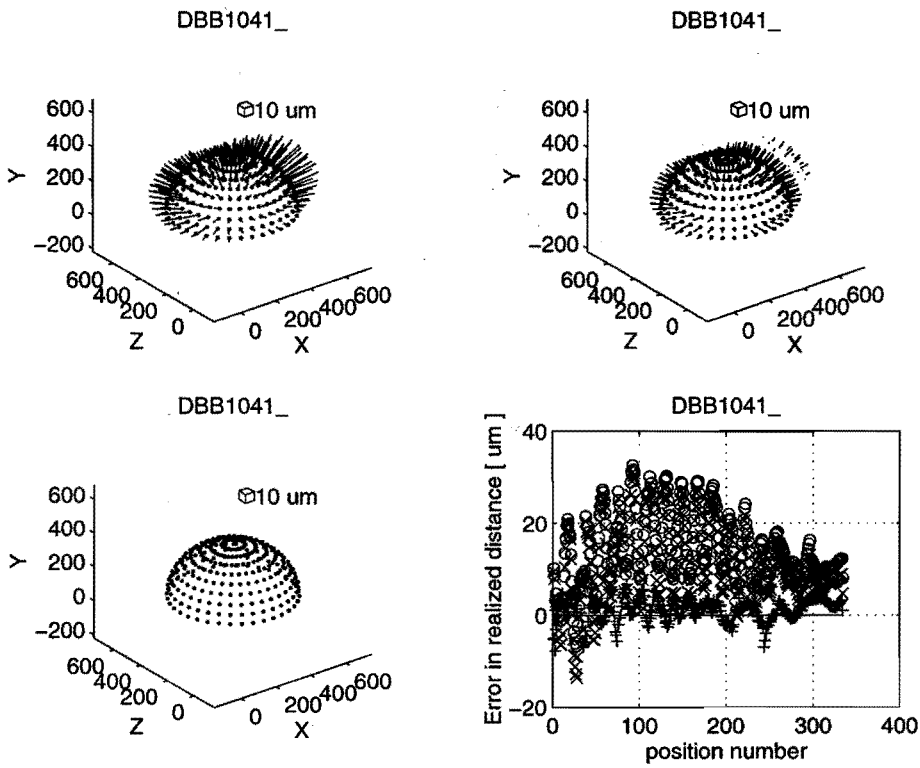

Figure 3.16 The measurement and simulation results of ball bar experiment no. 4. The upper-left graph presents the measured distance; the upper-right graph presents the measurement data after compensation of the thermal expansion; the lower left graph presents the calculated residual. In the lower-right graph all three errors are depicted.

Comparison measurement techniques

In this paragraph a comparison of all three measuring techniques is presented. A comparison between the three different measuring methods has been carried out considering the following items:

- Time necessary to carry out the experiments;
- Equipment and expertise needed to use the equipment in a correct way;
- Modelling efficiency.

The modelling efficiency is determined by a simulation of five hole plate measurements. Therefore, simulation software has been developed. A comparison is carried out of each simulation with the actual measurement using the five locations coincident with the locations in the simulation. The simulation is carried out for each measurement techique as defined in the previous paragraphs.

The five hole plate experiments are different from the six hole plate experiments used for the error identificantio using the hole plate technique. The next characteristics are calculated for every hole plate experiment:

- Maximum measured deviation;
- Maximum calculated residual;
- Variance in the residual;
- Modelling efficiency.

Direct measurement techniques

With the direct measurement techniques the investigated milling machine can be measured within two days. Only a skilled operator is capable of a correct measurement suitable for the estimation process. Especially the definition of the signs of the measured errors appears to be very difficult for an unexperienced operator and likely to introduce mistakes. The measuring method requires expensive equipment like laserinterferometers, electronic levelmeters etc.

The direct measurement technique provides comprehensive information on the machine's condition with a possible high sampling density. Therefore the individual parameters can be estimated very accurately. The method is not limited to the size of the machine; both large and very small machine tools can be measured with this technique. The highest possible accuracy of the method is limited as the total accuracy picture is constructed of individual measurements. Especially the uncertainty accompanied with the squareness measurement introduces a large uncertainty in the complete model.

The results of the verification of the model with the 5 hole plate measurements are depicted in table 3.2. In this table the maximum measured error in the location of the holes is presented. For each hole, the error in the location is calculated using the determined model. The maximum found difference between this simulation and the actual measurement is given together with the standard deviation of this residual. Finally, the efficiency of the model is given by:

$$\delta = \left[1 - \frac{\sum_{i=1}^{n} \left| \Delta_i^m - \Delta_i^s \right|}{\sum_{i=1}^{n} \left| \Delta_i^m \right|} \right] \cdot 100 \quad [\%] \qquad [3.6]$$

With :

Δ_i^m : Measured error [µm]

Δ_i^s : Simulated error [µm]

δ : Efficiency [%]

Table 3.2 clearly depicts the high modelling capacity of the kinematic model in combination with the direct measurement technique. The verification results show a relatively large residual of 15 µm in the YZ-plane and 13 µm in the XZ-plane. These residuals can be considered as outliers, as the residuals are only found in the measurement result of one hole. As every hole is measured twice the outliers could easily be detected. The outliers are probably caused by lubrication pulses.

Hole plate experiment		Measured [µm]	Residual [µm]	σ residual [µm]	Efficiency [%]
XY-plane	X-dir.	22	4	1	81
	Y-dir.	74	8	2	91
XZ-plane	X-dir.	25	10	4	69
(short)	Z-dir.	17	7	1	89
XZ-plane	X-dir.	42	13	3	73
(long)	Z-dir.	33	5	1	96
YZ-plane	Y-dir.	81	10	2	94
(left)	Z-dir.	17	15	2	43
YZ-plane	Y-dir.	85	9	2	93
(right)	Z-dir.	12	4	1	76

Table 3.2 An overview of the efficiency of the kinematic model using direct measurement techniques.

Hole plate

With six hole plate measurements the investigated milling machine can be measured within 4 - 6 hours. This can only be achieved when the dimensions of the hole plate fit the workspace of the machine tool. When the hole plate has to be moved across the diagonal of the workspace, the total measurement time increases significantly. The presented time includes the time needed for the measurement setup. The measuring time of a single plate is about 20 minutes.

The measuring method requires a calibrated hole plate and a probe on the investigated machine tool. This equipment is far less expensive than the equipment needed for the direct measurements.

Also a local operator can be instructed to carry out a correct measurement suitable for the estimation process. The evaluation of the data has to be carried out by a skilled engineer.

The hole plate is a very robust measurement technique which provides 2-dimensional information on the machine's condition. Therefore the individual parameters can be estimated very accurately. The sampling density is limited to the grid size of the plate. The method is limited by the size of the plate; only when the dimensions of the plate suit the workspace of the machine, the measuring method can be carried out in an efficient way. In principle, the possible accuracy of the method can be very high as the measurement data is obtained in the workspace of the machine with a very high accuracy (the uncertainty of the available plate was less than 0.1 µm).

The verification results of the model are depicted in table 3.3. As stated before, the verification is carried out with measurements not included in the estimation procedure. This table clearly depicts the high modelling capacity of the kinematic model in combination with the hole plate measurement technique. Similar to the direct measuring technique a large residual is found in the measurement results in the XZ- and the YZ-plane. Both residuals are caused by outliers. Considering these verification results the modelling capacity of the hole plate calibration method proves to be somewhat better than the direct measuring method.

Hole plate experiment		Measured [µm]	Residual [µm]	σ residual [µm]	Efficiency [%]
XY-plane	X-dir.	22	9	3	55
	Y-dir.	74	7	2	93
XZ-plane	X-dir.	25	5	1	91
(short)	Z-dir.	17	6	1	88
XZ-plane	X-dir.	42	13	3	84
(long)	Z-dir.	33	5	1	93
YZ-plane	Y-dir.	81	7	1	97
(left)	Z-dir.	17	17	3	52
YZ-plane	Y-dir.	85	6	1	97
(right)	Z-dir.	12	5	1	88

Table 3.3 An overview of the efficiency of the kinematic model using hole plate measurement data.

Ball bar

With eight ball bar measurements the investigated milling machine can be measured within 2 hours. Similar to the hole plate this can only be achieved when the radius of the ball bar suits the workspace of the machine tool.

The measuring method requires a ball bar and a computer for the interface. This equipment is the cheapest of all presented measuring methods.

The ball bar measurements can be carried out by a local operator. The evaluation of the data has to be carried out by a skilled engineer.

The ball bar is a very robust measurement technique but limited to its range; only spheres with a constant radius can be created in the workspace of the machine. A different radius is realised by the application of extension rods with a constant length. Caused by these discrete radii the individual parameters can be estimated with only a limited accuracy and sampling density. Also an efficient calibration procedure is only possible when the

applied radii suit the range of the machine. In principle, the possible accuracy of the method can be very high as the measurement data is obtained in the workspace of the machine with a very high accuracy (the uncertainty of the ball bar was less than 0.2 μm). However, it appeared that switching between the different extension rods introduced a systematic error in the measurement results up to 3 μm.

The verification results with the five hole plate measurements are depicted in table 3.4. This table clearly depicts that the ball bar has the least efficient modelling capacity. This is mainly due to experimental setup which could be improved significantly. Firstly, the centre point of the spheres had to be estimated as these centre points were not exactly known with respect to the machine zero point. When a special adapter would be applied to determine this centre position prior to the actual measurements, this estimation would not be needed anymore. Secondly, only two tool vectors were applied in the measurement setup, resulting in a bad modelling efficiency of the rotation errors present in the Z-axis. In table 3.4, the results of the hole plate simulations in the YZ-plane are deteriorated significantly by this effect. These measurements were carried out with long tool offsets in X-direction. Finally, when the ball bar would be equipped with a linear transducer with a longer range, the measurement sequence could be optimised further as fewer extension rods would be needed. The measuring time which can be gained by this modification, could be used to introduce new measurement setups with different tool vectors.

Hole plate experiment		Measured [µm]	Residual [µm]	σ residual [µm]	Efficiency [%]
XY-plane	X-dir.	22	11	3	50
	Y-dir.	74	7	2	94
XZ-plane	X-dir.	25	10	2	81
(short)	Z-dir.	17	8	3	31
XZ-plane	X-dir.	42	21	5	49
(long)	Z-dir.	33	14	5	58
YZ-plane	Y-dir.	81	27	6	77
(left)	Z-dir.	17	10	2	0
YZ-plane	Y-dir.	85	39	11	71
(right)	Z-dir.	12	13	5	0

Table 3.4 An overview of the efficiency of the kinematic model in combination with ball bar experiments.

All three methods are very well capable of modelling the geometric errors of a machine tool. Both the hole plate and ball bar can be applied by a local operator, but are limited with respect to their working range. The direct measurement technique has no limitation with respect to the range of the machine tool. However, expensive equipment and a skilled operator are needed. Both the direct measurement technique and the hole plate method showed a very high modelling efficiency. The ball bar method showed the smallest modelling efficiency, but can be optimised further with respect to the measuring device and the experimental setup.

Chapter 4

Machine Tool Errors due to the Weight of Machine Components and Workpiece

Machine tools are subject to errors due to static and slowly varying forces. The resulting deformation of the machine can alter the relative position of the tool and workpiece and thus degrade the machine accuracy. In this chapter a method is described to assess and model the errors due to the weight of machine elements and workpiece. As explained in Chapter 2, the process forces are not considered as with light finishing cuts the effect of the static component is negligible. Firstly, the effect of the weight of moving machine components is discussed. Secondly, the influence of a workpiece load positioned on the table is determined. An adequate model has been developed which is capable of describing the effect of different workpiece loads on the parametric errors used in the kinematic model. Finally, the application of strain gauges are discussed which are applied to estimate the effective workpiece load. The method has been published [88] and has succesfully been applied in the software error compensation system (see Chapters 6 and 8).

Errors due to the weight of moving machine components

A movement of a machine axis alters the forces and moments exerted by the deadweight of the moved machine components on the supporting machine structure. Also the position where these loads are introduced in this structure depends on the axis position. The result is that guideways change their shapes and their relative positions and orientations. The latter can be described by the parametric errors as introduced in Chapter 2. Then, the error in the location of the tool can be related to these parametric errors by application of the kinematic model.

Although the kinematic model is based on rigid-body kinematics, the deformation of machine elements does not limit its application. As far as first-order effects are concerned, the difference between the nominal and actual geometry of machine elements does not affect significantly the Abbe offsets (described in the vectors $\underline{p}_i$), nor the direction in which the various errors act.

The geometric parametric errors as introduced in Chapter 2 can also contain the finite stiffness errors of the various machine elements. However, it is not required to separate the respective independent terms from geometric or finite stiffness parametric errors dependent on the same axis position. A typical example is the error zrx (rotation around X during movement of Z) of the investigated Maho 700S milling machine. This error is mainly due to the finite stiffness of the Z-axis that results in a rotation of the Z-axis when the Z-carriage is moved outside the column. Although this method deteriorates the possibility of a physical interpretation of the modelled errors, the combined finite stiffness and geometric errors can directly be applied for software error compensation purposes. For the parametric error zrx a software error compensation would correct both the geometric and finite stiffness component measured in this error, without the need of any additional sensors. Such an error correction could simplify the construction of the machine tool as the applied tension rods (see figure 1.1) would not be needed any more.

Due to the finite stiffness of the structural loop, the movement of one carriage may also affect the errors in another carriage (cross-coupling). Several possible cross-coupling errors have been investigated on the milling machine. The only cross-coupling found is the error yrx. This error is both dependent on the position of the X- and Y-axis. In figure 4.1 the measurement results of yrx are depicted with the X-axis positioned on three different positions. In this figure a relatively small maximum difference of 10 μrad is found for the three different X-axis positions.

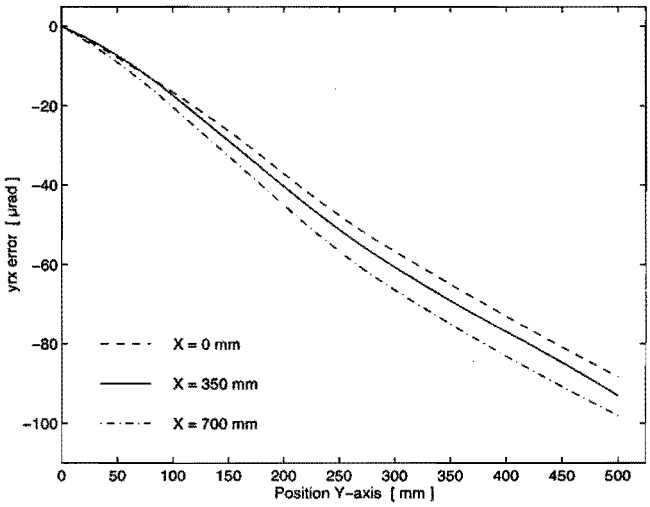

Figure 4.1 : Dependency of the error yrx on the position of the X-carriage.

The simulation software as applied in Chapter 2 for the comparison of the three different measuring methods has been extended to determine the influence of the cross-coupling effect on the machine accuracy. Using this module hole plate simulations have been carried out and verified with the actual measurements. In figure 4.2 the residuals between the actual measured error in the location of a hole and the simulated error is depicted for two different situations. Firstly, a simulation has been carried out without the mentioned cross-coupling effect. The presented continuously drawn line indicates the residual between the measured error in the hole plate and the simulated error using the geometric error model based on the direct measurement technique. Secondly, the cross-coupling effect has been included in the model. The dashed line represents the situation where the measured cross-coupling is included in the model. The modelling efficiency slightly improves. The effect shown only occurs in the YZ-plane of the milling machine, which is a worst-case situation. In the other two planes hardly a significant effect could be found. Considering the limited model improvement and the hazardous job to include two-dimensional parametric errors in the real-time software error compensation system, the cross-coupling effect is neglected in this thesis.

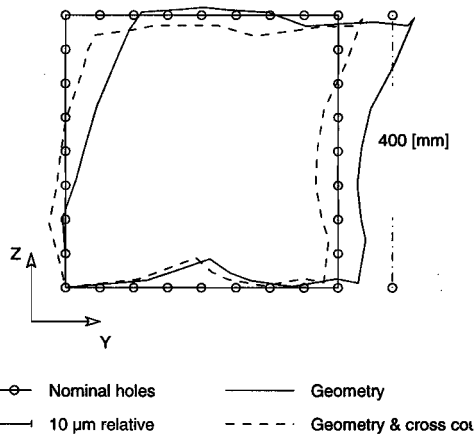

Figure 4.2 A hole plate simulation carried out with two different models. The continuously drawn line represents the residual when cross-coupling is neglected; the dashed line represents the simulation including the cross-coupling.

Errors due to workpiece weight

The finite stiffness errors introduced by the weight of a workpiece are generally confined to the elements of the structural loop that support the workpiece relatively to the foundation. However, for the investigated milling machine, only the effect on the parametric errors of the X-axis have to be considered. This is caused by the construction of the machine. Both the Y-axis and the Z-axis are mounted to the column of the machine. When the Y-axis would bend due to a heavy workpiece, the deflection is introduced in the part below the Y-axis carriage. Thus the upper part of the Y-axis, which constitutes the link to the Z-axis, is not influenced. Hence, the structural loop of the machine is not influenced by a deflection of the Y-axis.

As an example of the analysis carried out on the X-axis of the investigated machine tool, the rotation error xrx is considered as function of the different workpiece load situations.

First an experiment is performed to assess whether the dependency between workpiece load and angular error is linear. A laserinterferometer and two electronic levelmeters are used simultaneously to measure the variation in the orientation of the workpiece table relative to the tool at a fixed position of the machine axes with different workpiece loads (see figure 4.3). The maximum applied weight equals approximately that allowed by the manufacturer (5000 N). The loads are applied to the centre of the workpiece table through a relatively small support. The experiment was executed at the right edge of the machine workspace (X = 650 mm).

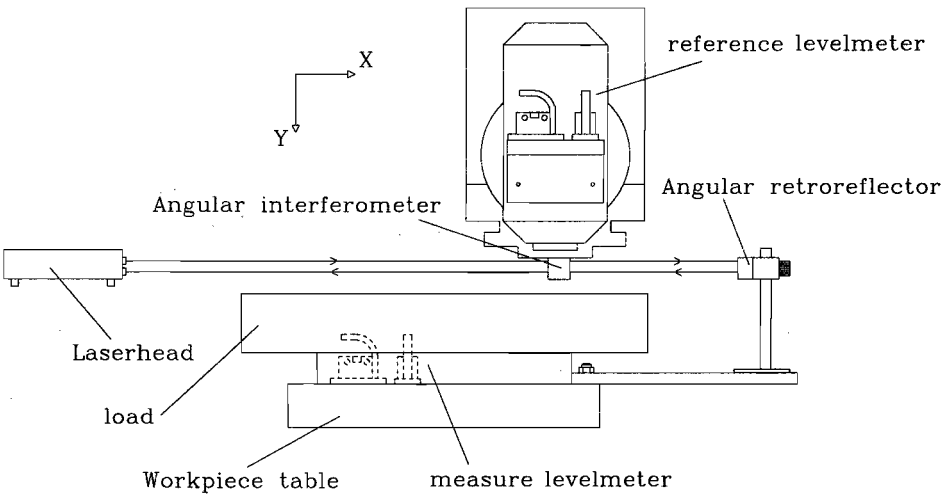

Figure 4.3 : Experimental setup applied for the measurement of the rotation errors due to a workpiece weight.

The measurement results are depicted in figure 4.4. They indicate a highly linear relation between workpiece load and angular error that simplifies the succeeding analysis.

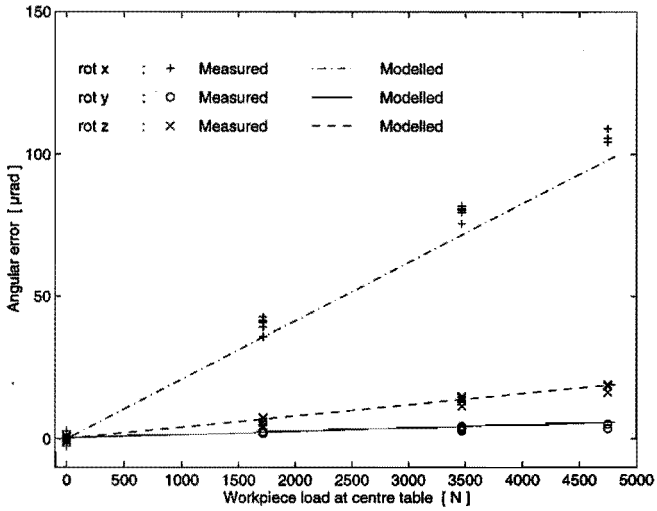

Figure 4.4 : Measured rotation of the workpiece table as a function of different workpiece loads. The experiment is carried out at X=650 mm.

This experiment addressed the combined deflection of all structural loop segments in response to the workpiece weight. To assess the dependency of this deflection on the position of the machine axes, further experiments are required.

Different workpiece weights have been placed on different positions on the machine's table. The moment exerted by the workpiece weight causes torsion of the X-axis guideway which results in an xrx roll error as the X-axis carriage is moved. Since the guideway is supported at its centre, the error increases as the carriage is moved from its centre position (X = 350 mm). A uniform guideway cross-section would result in a linear dependency. The observed, somewhat parabolic, curve is due to the contribution of the Y-axis carriage to the guideway stiffness (see figure 4.5 and 4.6).

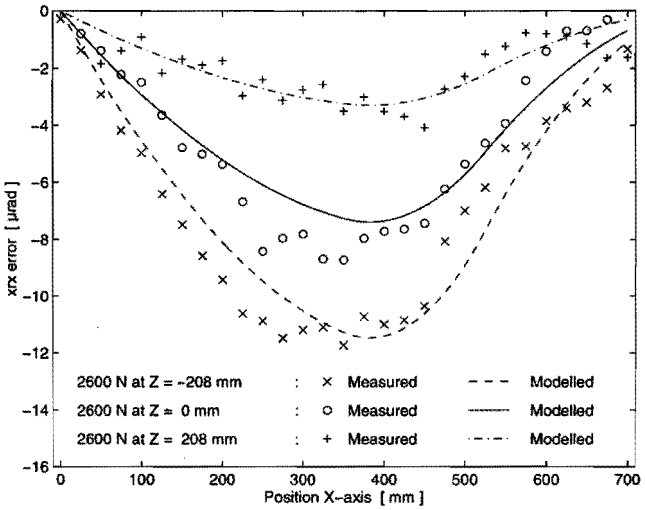

Figure 4.5 : Change in the xrx error due to a workpiece load of 2600 N at various positions, relative to the table centre. The lines represent the model; the symbols represent the measured error.

In order to describe this effect a relatively simple model has been applied. The error model is based on an estimated piecewise polynomial description for the observed xrx error due to a workpiece weight of 4900 N at the table centre. The xrx error due to an arbitrary load equals a fraction of this curve, calculated from the respective difference in the exerted moment around X:

$$xrx = xrx(X,4800) \cdot \frac{F_w}{4800} \cdot \frac{375 - p_l}{375} \qquad [4.1]$$

Here $xrx(X,4800)$ represents the fitted piecewise polynomial model for the measured error due to a workpiece weight of 4800 N located at the table centre. The used constant of 375 equals the distance between the weight and the centroid of the X-axis guideway in Z-direction. F_w is the applied workpiece load; p_l the position of the load on the table in Z-direction.

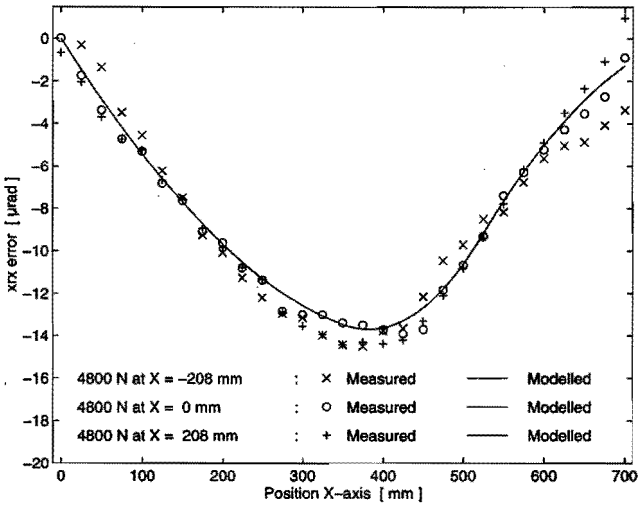

Figure 4.6 : Change in the xrx error due to a workpiece load of 4800 N at various positions, relative to the table centre. The lines represent the model; the symbols represent the measured error.

In figures 4.5 and 4.6 the modeled error xrx is compared with the actual measured error for different loads placed on different positions on the table. In figure 4.5 it is shown that the position of the load on the workpiece table in Z-direction has clearly a significant effect on the error xrx. In figure 4.6 the results of a verification experiment are shown with the load on different X-positions on the table. Clearly, the error xrx is not dependent on the X-position of the load on the workpiece table.

The measurement results depicted in figure 4.7 show the deflection of the structural loop segment between Y-axis and B-axis that is not dependent on the X- and Y-position of the machine axis. They affect the parallelism error between the B-axis and Y-axis. The linear dependence of the error on the position of the workpiece load in Z-direction suggests that the compliance of the X-axis and Y-axis bearings are the main factors. Bending would result in a non-linear dependency. The model to describe this error is based on a fitted straight line through the errors of the maximum weight. Since the angular deflection is linear in the workpiece load, the deflection under an arbitrary load is calculated as an appropriate fraction. Using the sequential modelling procedure, the estimated error is implemented as an offset at the tested position in the kinematic model.

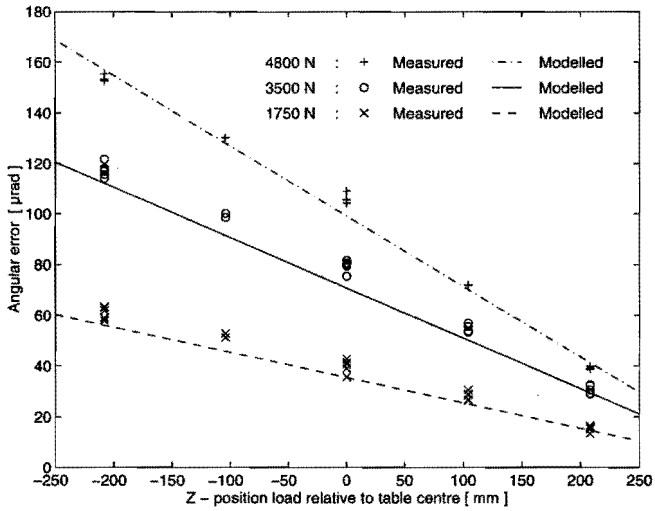

Figure 4.7 : Rotation error around X of the workpiece table relative to the tool as a function of the workpiece weight and - position. The symbols represent the measured error; the lines the modelled errors.

To complete the model, the deflection of the workpiece table relative to the B-axis has to be determined, as well as the table deformation. In contrast to the parallelism error between B-axis and Y-axis, the relevant angular error has an axis of rotation that changes when the B-axis is moved. Note that the experiment described in the preceding paragraph assesses the combined value of both these errors. Regarding the deformation of the workpiece table, the distribution of the workpiece load on the table needs to be known. Unless the workpiece is supported by well-defined fixtures, this load distribution is affected by form deviations of both workpiece and table and therefore difficult to predict. The same argument applies to the effect of the table deformation on the location of the bearings. When the workpiece load is applied to the table centre, a deformation was observed which resembles that of a membrane pushed in the centre. This causes the mismatch between the observed and predicted errors of figure 4.7 when the load is at the table centre.

Estimation of the effective workpiece load using strain gauges

Application of the error model, especially for the software error compensation, requires the estimation of the effective workpiece load. As a first approach the use of strain gauges has been studied. A major problem is that the load induced strains are very small. Various measurements showed that the deformation of the links is small compared to the load induced errors in the joints. A further complication is the temperature rise of the machine during machining that affects significantly the measured strain. Therefore the load is estimated from the change in the measured strain as the machine axes are moved. This also has the advantage that more information can be obtained from a strain gauge. A set of four strain gauges is placed at the top of the X-axis guideway at the middle X-position (see figure 4.8). Gauges are used whose reading is compensated for a thermal expansion coefficient close to that of the guideway. The gauges are placed in a full Wheatstone bridge configuration and the Z-minus X-strain is measured.

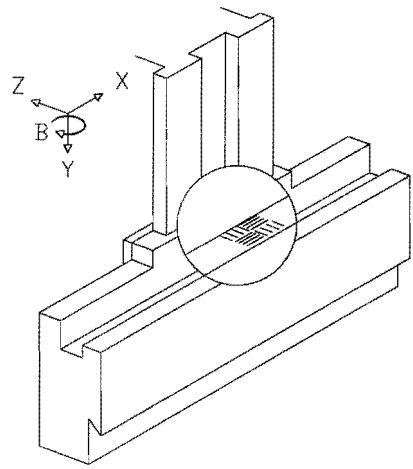

Figure 4.8 : A set of four strain gauges has been placed in the middle X-position of the X-axis to indicate the actual load placed on the table.

The position of the workpiece load relative to the table centre can be determined effectively from the strain variation during movement of the B-axis. Unfortunately, heavy workpieces tend to be large, which limits the range of B-axis rotation where no collision occurs. Therefore, the load is estimated from the measured strain variation as the X-axis is moved. In the figures 4.9 and 4.10 this signal is depicted for various workpiece loads. The offset of the workpiece load in X-direction can be assessed from the asymmetry in the strain gauge signals left and right from X=350. Identification of the Z-offset is difficult because the workpiece weight affects the strain in a similar manner. There is a subtle difference due to the bending of the X-axis guideway around Z that is not affected by the Z-position of the workpiece. A regression model is used to calculate the workpiece weight and position from the strain gauge signals at five X-axis positions (0, 150, 350, 550, and 700). Since the measured strain is significantly affected by the occasional lubrication pulse, a duplicate measurement is required.

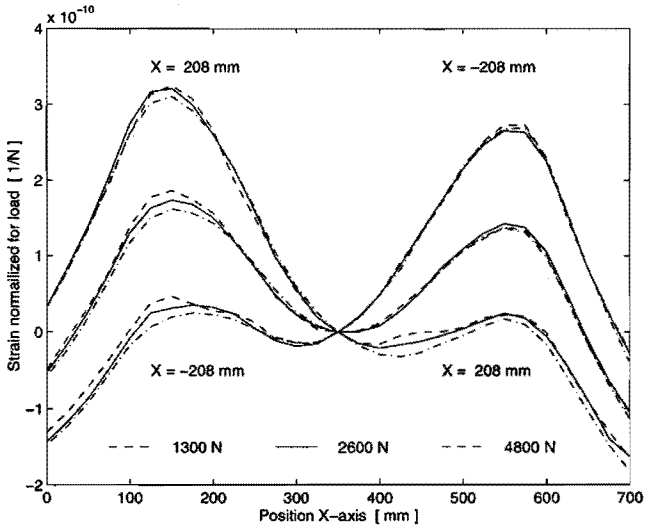

Figure 4.9 : Measured strain variation as the X-axis is moved. The middle curve corresponds to a load applied to the table centre. The two other curves describe a load eccentric in X-direction.

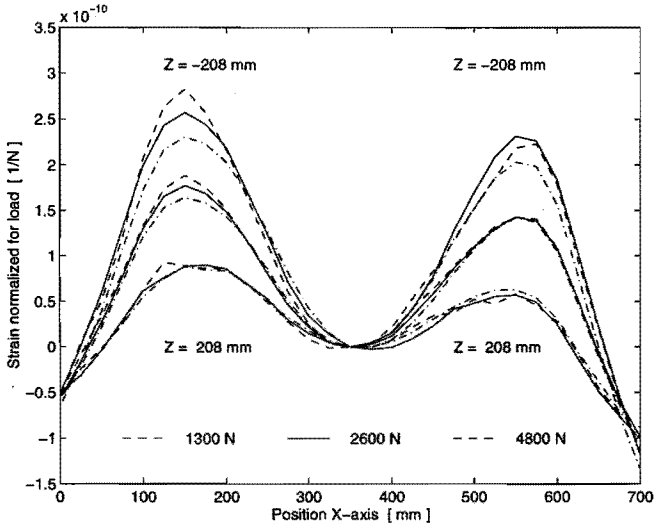

Figure 4.10 : Measured strain variation as the X-axis is moved. The middle curve corresponds to a load applied to the table centre. The two other curves describe a load eccentric in Z-direction.

With this setup the actual workpiece load and its position can be determined. Using this information, the additional error xrx, due to the workpiece load, is calculated and accounted for by the software error compensation system. In Chapter 8 some results will be presented to show the efficiency of the software error compensation system to correct the finite stiffness errors due to a workpiece load.

Chapter 5

Modelling the Thermal Drift of Machine Tools

The largest thermally induced error found in machine tools is the zero-point drift [19, 78, 87, 95, 104, 105]. The research presented in this chapter is focused on this error. To describe the thermal drift two different types of models are presented : a statistical model and an analytical model. The statistical model will be developed on the empirical relationship between the zero-point drift and the temperature distribution on the machine tool. Therefore, firstly an experimental set-up will be described which is capable of a simultaneous measurement of the zero-point drift and the thermal distribution in the machine tool. Both models have succesfully been applied for software error compensation purposes. A comparison of them has been carried out based on the test results extracted from test workpieces. These test workpiece have specially been designed to show the influence of the thermally induced errors. This test workpiece method and the results of the comparison are presented in the last two paragraphs of this chapter. Both the modelling techniques and the test workpiece method have been developed in the European research project "Development of Methods for the Numerical Error Correction of Machine Tools" [77, 78, 79].

Experimental set-up

In order to determine the thermal drift of machine tools a measurement set-up is built which is based on a commonly applied principle [3, 110]. A cylinder is mounted in the tool holder of the machine; on the workpiece table a base is mounted with six contactless eddy current displacement transducers. These transducers allow the simultaneous measurement of the displacement of the tool holder with respect to the workpiece in three directions, and of two rotations of the tool holder. The displacement transducers are calibrated which results in an uncertainty of less than 1 μm over the full range after application of a correction formula for

systematic errors. Also the influence of temperature changes on the measurement accuracy has been investigated [77]. The results show that temperature does not affect significantly the reading of the displacement transducers.

The transducers are linked to an amplifier (Hottinger Baldwin DMC9012A) that is capable of reading all signals simultaneously. The signals obtained from the amplifier are sent to a PC by means of an IEEE-488 interface. In figure 5.1 the measurement set-up is depicted as it is applied in the XZ-plane.

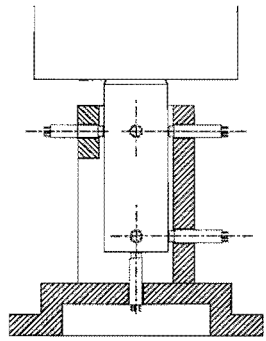

Figure 5.1 : Zero-point drift measurement set-up.

Distributed over the machine's structure a number of Pt-100 temperature sensors is mounted. Each temperature sensor is calibrated with an uncertainty of less than 0.1 °C, in a range from 15 to 60 °C, which is sufficient for this purpose [77].

The position of each sensor is depicted in figure 5.2. The choice of these positions has been determined by careful consideration of the location of the internal heat sources, using the results of infrared measurements [77]. Also the requirements of the analytical model have been considered. This model requires that the thermal gradients are measured in all directions. This is achieved by placing the sensors at the corner of each beam segment. Finally, the linear scales are provided with three temperature sensors each.

During an experiment the machine tool is loaded with a spindle speed over a specified time. The displacement of the tool holder and the temperature

distribution on the machine tool are measured with a sampling period of 60 seconds.

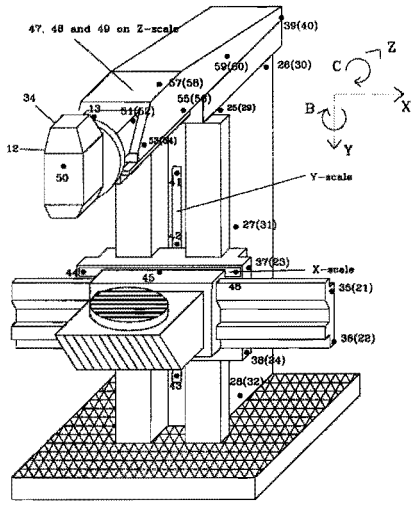

Figure 5.2 : Position of the temperature sensors on the machine tool.

The machine tool has been loaded with different duty cycles. In DIN 8602 [14] a spindle speed spectrum is defined which simulates the milling process where the machine tool is loaded with various spindle speeds. This spectrum consists of spindle speeds varying from zero to maximum spindle speed (n_{max}), with steps of 25% of n_{max}. For the investigated machine tool n_{max} is 6300 rpm. Each load situation is maintained for 15 minutes. A graphical presentation of this spectrum is depicted in figure 5.3 together with the measured displacement of the tool plotted against the elapsed time.

The DIN 8602 spectrum has been defined to simulate the practical milling process. However, for the determination of the transient states the spectrum should include more randomly distributed spindle speeds (e.g. like 'White Noise'). In order to create such a spectrum, the machine is loaded with randomly chosen spindle speeds for randomly chosen time intervals, during a time period of 24 hours.

To achieve a practically applicable spectrum for a milling machine during normal operation, the following restrictions have been chosen:

- The time interval is chosen between 5 and 45 min;
- The spindle speed is chosen between 800 and 6300 rpm or spindle stop.

The resulting spindle speed spectrum is depicted in figure 5.4.

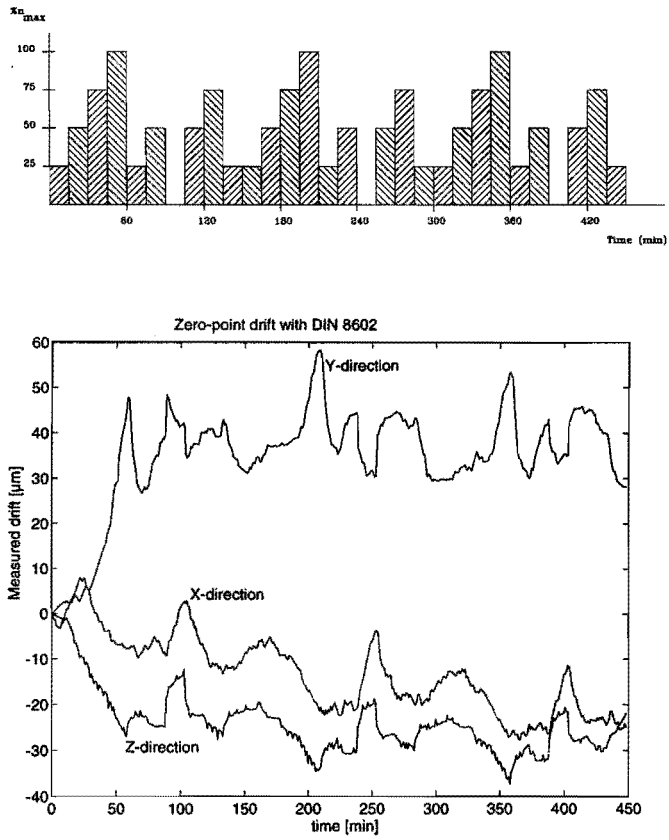

Figure 5.3 : The spindle speed spectrum as defined DIN 8602 is depicted in the upper part of this graph. The lower part presents the measured drift of the tool holder with this DIN 8602 spectrum applied.

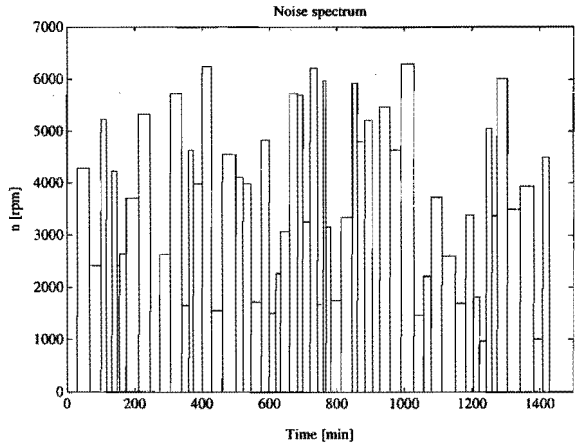

Figure 5.4 : Random spindle speed spectrum.

In order to complete the experimental set-up a measurement sequence is added which represents the machine tool in a thermally stabilised situation (steady state). Therefore, the milling machine is loaded with a spindle speed of 6000 rpm during 24 hours, followed with a cooling down period of 24 hours. The results of such a 'Steady State' experiment are depicted in figure 5.5.

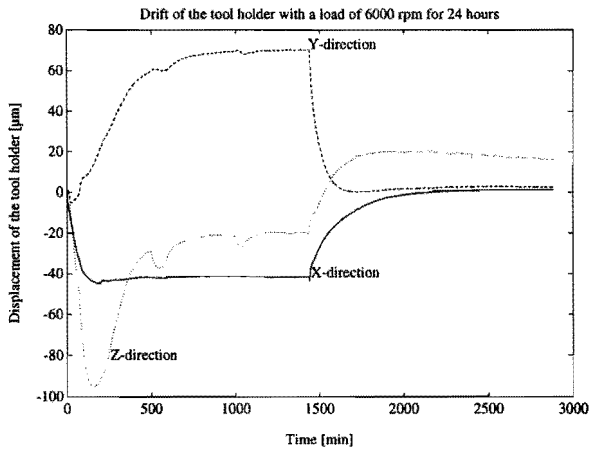

Figure 5.5 : Steady state experiment, with a load of 6000 rpm

The statistical modelling methodology

A statistical model has been developed which directly relates the error of the tool to the measured temperature distribution on the machine tool. The relationship between the relevant temperature sensors and the measured displacement of the tool holder is based on empirically obtained measurement results.

Several approaches are carried out in order to obtain a relation between the temperature of relevant sensors and the actual measured displacement of the tool holder [9, 19, 57, 76, 77, 95]. Firstly, preliminary calculations using least squares fitting procedures are performed. With an intuitive selection of the temperature sensors this method displayed fairly good results. However, as the theoretical importance of a particular temperature sensor is unknown, a methodology for relevance detection is desired. A possible approach is the use of statistical criteria for elimination and calculation of the optimal model. Therefore the measurement data are examined with the use of a software package for statistical analysis of data (SAS). This software package offers a wide range of utilities for regression analysis [72].

The task of this analysis was to determine:

- The temperature sensors relevant for the description of the displacement;
- An estimate of the coefficients of the regressors (temperature sensors);
- A statement on the confidence interval for future predictions on new data.

As there is more than one regressor, this is a multiple regression problem. A general notation of this problem is:

$$\underline{\Delta P} = X\underline{\beta} + \underline{\gamma} \qquad [5.1]$$

With:

$\underline{\Delta P}$: A vector (ntx, nty, ntz) which contains the measured zero point drift. The zero-point drift measured in X-direction is indicated with ntx, in Y-direction with nty and in Z-direction with ntz.

X : A matrix with the regressors in the total model (in this case the measured temperatures on various locations of the machine tool).

$\underline{\beta}$: A vector which contains all coefficients of the model.

$\underline{\gamma}$: A vector of random errors (residuals), assumed to be independent and identically distributed with mean zero and variance σ^2.

Since the above model is linear in the unknown parameters $\underline{\beta}$, these can be estimated using linear least-squares analysis [87].

Based on all available temperature sensors that are attached to the machine tool the best suitable model should be determined. Because evaluating all possible regression models - i.e. the models with one sensor, the models with all sets of two sensors, etc. - is computationally very extensive, various methods have been developed for evaluating only a small number of subset regression models by either adding or deleting regressors one at a time [63]. These methods are generally referred to as stepwise-type procedures. They can be classified into three categories: forward selection, backward elimination and stepwise regression, which is a combination of the first two.

Although the mentioned selection techniques gave good results [95], the presented forward, backward and stepwise regression techniques highly depend on the chosen cut-off values, SLE and SLS. These values are changed when the predictive capacity of the model is not good enough or when the number of sensors in the model is too high. As this is done rather intuitively, another technique has been applied to determine the temperature sensors relevant for the description of the displacement.

As already stated, it is computationally very extensive to evaluate all possible regression models. However, taken the restriction that the number of sensors should be very small, the number of possible regression models

can be reduced enormously when the maximum number of sensors is limited.

Using SAS software it is possible to determine the best regression model, given a fixed number of regressors. The regressors will be chosen such that the predictive capacity of the model is optimal for the modelling data set. This will be judged by the value of C_p, which has been introduced by Mallows [72]:

$$C_p = \frac{SSE_p}{MSE} + 2p - n \qquad [5.1]$$

With :

SSE_p : Sum of squares of the error for a model with p parameters (temperature sensors);

MSE : Mean square of the error for the full model which includes all temperature sensors;

p : Number of parameters (temperature sensors);

n : Number of observations.

The described technique can determine the best regression model for the given data set. However, the residual between actual results and regression model will always be smaller with a larger number of regressors [63, 95]. Therefore, including more sensors will always give a better C_p-value. Unfortunately, this will not always result in a better statistical model. When the number of sensors is increased, the predictive capacity of the statistical model will decrease, caused by nonsense relations (called 'Over-fitting').

In order to avoid this 'Over-fitting' the efficiency of the model is calculated for an independent verification data set. The efficiency of the model is given by:

$$\delta = \left[1 - \frac{\sum_{i=1}^{n} \left| \Delta_i^m - \Delta_i^s \right|}{\sum_{i=1}^{n} \left| \Delta_i^m \right|} \right] \cdot 100 \quad [\%] \qquad [5.2]$$

With :

Δ_i^m : Measured drift [μm]

Δ_i^s : Simulated drift [μm]

δ : Efficiency [%]

The independent data set can be created by other measurements. When it is impossible to carry out verification measurements, the measurement data can also be split randomly into equally sized parts. One part can be used for the estimation process and the other part for the verification.

The developed modelling procedure has been applied to the investigated milling machine. The machine was loaded with two different spindle speed spectra: the 'Noise'-spectrum and the 'Steady-state'-spectrum. During these spectra the temperature distribution is measured simultaneous with the zero-point drift. The machine tool was equipped with two main spindles to enable milling in both the XY- and XZ-plane. For each spindle a different thermo-mechanical behaviour is expected. Therefore, the experiment is carried out for each spindle. As the thermo-mechanical behaviour of the machine tool was found to be dependent on the position of the Z-axis the experiments have been carried out on three different Z-axis positions. This results in 18 sets of parameters linked to 18 sets of temperature sensors (2 planes with 3 times a set in respectively the X-, Y- and Z-direction).

The calculated efficiency of the model is depicted in figure 5.6 as a function of the number of sensors applied in the model. The three figures on the left side represent the efficiency of the model for the modelling data set respectively in X-, Y- and Z-direction. It clearly shows a better efficiency when the number of sensors is increased. On the right side the efficiency of the model is depicted for the verification data set. This data set is obtained by different measurements, however under the same operating conditions. One can clearly observe that when the number of sensors included in the model is increased above 9, the efficiency of the model in Y-direction suddenly decreases. As the zero-point drift in X-direction can be described very accurately with one temperature sensor, an 'over-fitting' is not found in X-direction.

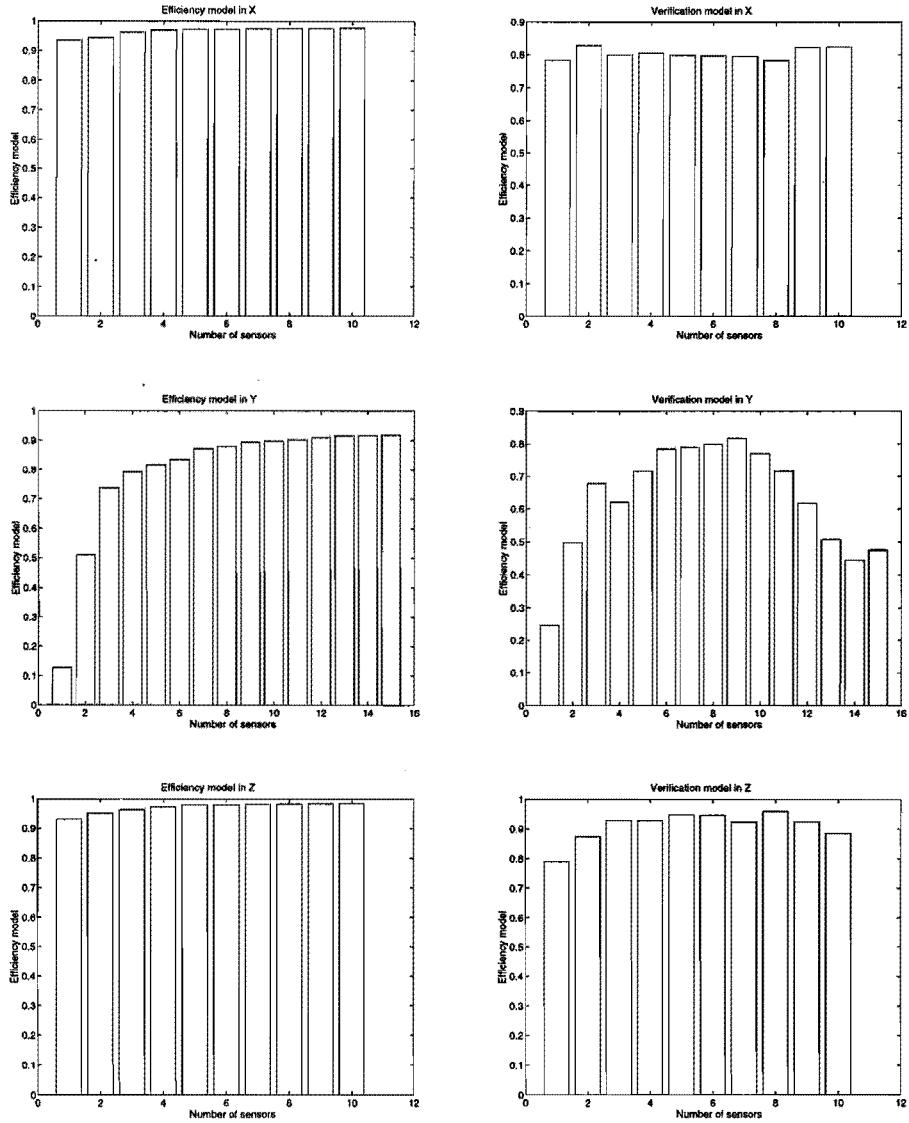

Figure 5.6 : Efficiency analysis of a zero-point drift model. The left three figures show the efficiency of the modelling data set; the right three figures show the efficiency using the verification data set. The verification of the model in Y-direction clearly shows the 'over-fitting'.

Based on the above described analysis, the following model for the thermally induced errors has been determined:

XZ-plane:	XY-plane:
• X-axis: 1 sensor;	• X-axis: 2 sensors;
• Y-axis: 9 sensors;	• Y-axis: 2 sensors;
• Z-axis: 8 sensors;	• Z-axis: 4 sensors.

Together, only 16 different temperature sensors are needed to achieve an optimal model for the zero-point drift of the milling machine.

This model has been applied in the software error compensation system. In Chapter 8 the results of several verification experiments can be found.

Analytical model

The analytical model has mainly been developed by PTB, one of the project partners in the mentioned BCR-project [78]. The underlying principles of this analytical model are described in this paragraph. Further information can be found in the literature [77, 78, 96].

The analytical model is based on three relations between the temperature distribution of a body and its deformation [78] (see figures 5.7 and 5.8):

- The expansion of a body is a linear function of the temperature change;
- A temperature gradient causes a spherical bending of a body;
- A differential gradient causes a torsion.

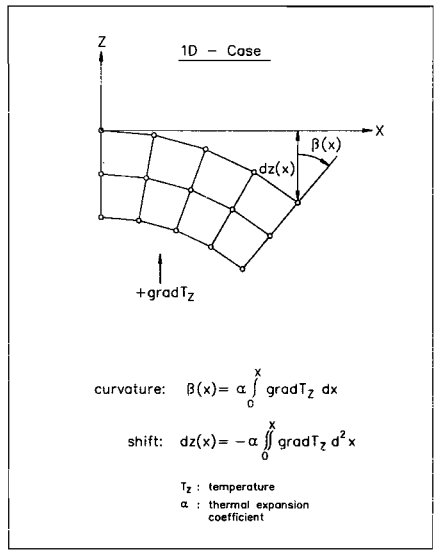

Figure 5.7 : Deformation of a segment with a temperature gradient in Z-direction.

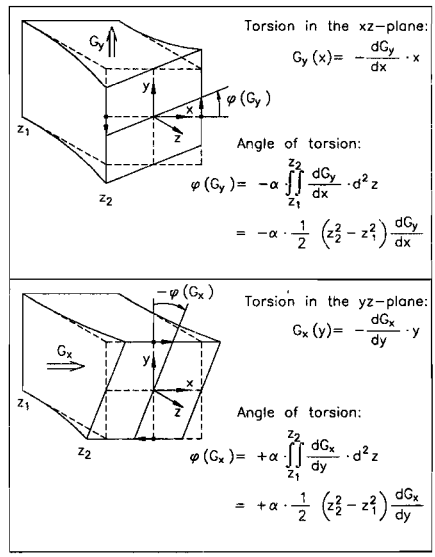

Figure 5.8 : Deformation of a segment due to differential gradients.

To apply these basic relations to a machine tool, its structure is divided into large segments (see figure 5.9). For each of the segments the deformations (expansion, bending and torsion) are determined based on the measured temperature distribution. The temperature distribution of the machine tool is measured with a total number of 39 sensors on the machine tool surface. The displacement of the tool relative to the workpiece is calculated from the superimposed deformations of each segment.

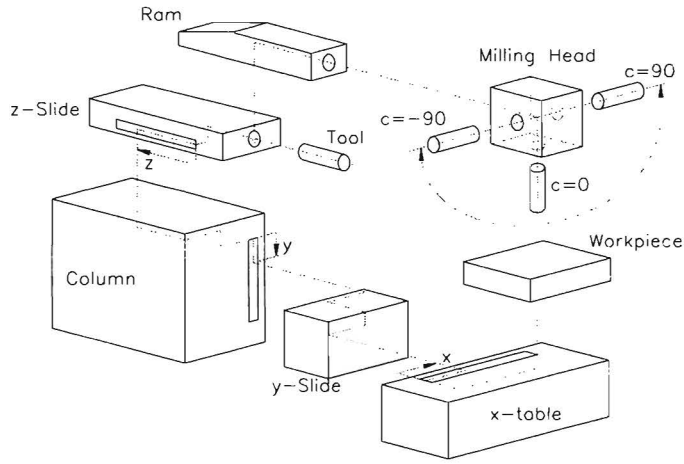

Figure 5.9 : Path of integration to calculate thermal expansions.

In order to complete the analytical model a fine-adjustment was necessary, due to the uncertainty of the actual value of the expansion coefficients included in the model and the complicated machine structure.

Using a simulation program the zero point drift has been calculated as a function of the measured temperature. The calculated drift components have been compared with the actual errors ntx, nty, ntz which were extracted from the test workpieces (see the next paragraph). The determined residual has been minimised by a small change in the value of the expansion coefficients included in the model [78].

Similar to the statistical model, the analytical model has been applied in the software error compensation system. In Chapter 8 the results of several verification experiments can be found.

Test workpieces

In order to achieve a verification method for both thermal error models the test-workpiece method has been chosen [78]. The test-workpieces combine the following features:

- Separation of all important error parameters as they are present in a real manufacturing process;
- Determination of the thermally induced errors during several hours of operation;
- High degree of reliability of the test results (real operating conditions);
- Low costs.

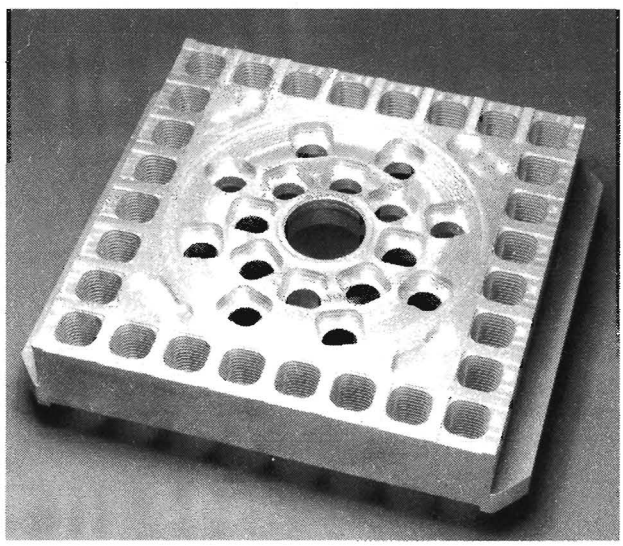

Figure 5.10 : A photograph of a test-workpiece. This test-workpiece also includes tracks for the verification of rotary tables.

Similar to a hole plate a test-workpiece consists of a rectangular grid of holes. In each hole 12 different levels are present. On each level four small planes are milled, from which the actual centre-point of the hole can be extracted. In between two holes, a small 'stair' is present. These stairs are also milled during the experiment which allows to extract information on errors perpendicular to the workpiece. Hence, a test-workpiece is a real three-dimensional test. In figure 5.10 a photograph of a test-workpiece is presented; in figure 5.11 a schematic representation is depicted. In figure 5.12 a detailed view of one hole is given.

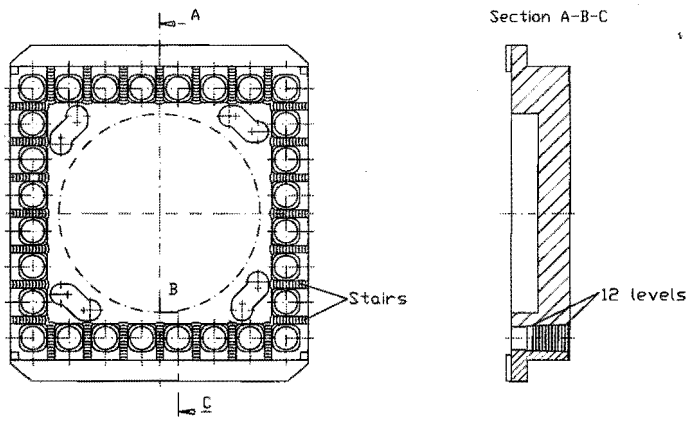

Figure 5.11 : A schematic representation of a test-workpiece.

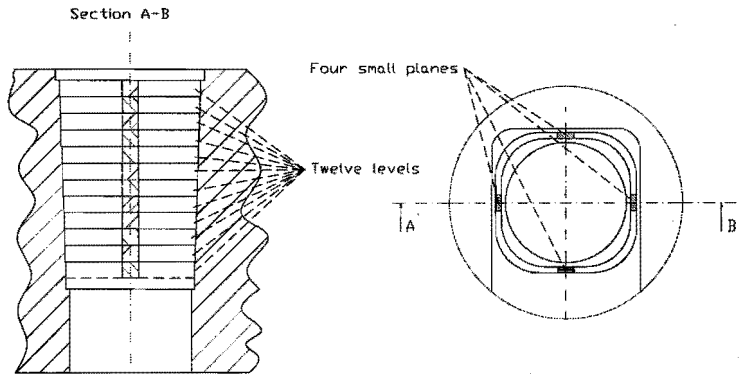

Figure 5.12 : Detailed view of one hole, milled in the test workpiece.

Two different spindle speed spectra have been defined for the test-

Two different spindle speed spectra have been defined for the test-workpieces. Firstly, a constant spindle speed has been chosen which equals the maximum spindle speed for the investigated machine (= 6300 rpm for the Maho 700S). Secondly, the spectrum defined in DIN 8602 has been applied. This spectrum has slightly been adapted. After 135 minutes, the machine should be loaded with 25 % of the maximum spindle speed for 30 minutes. This has been changed to 15 minutes to enable that the twelfth plane will be milled with the maximum spindle speed. This adapted spindle speed spectrum will be refered to as pseudo-DIN 8602 spectrum. In figure 5.13, both spectra are depicted. The test workpieces were made of a special aluminium alloy which allowed the large variation in spindle speeds without any significant problems during the cutting process.

A set of four test-workpieces have been milled on the investigated Maho 700 S milling machine. Two workpieces have been milled in the XZ-plane with respectively the constant spindle speed and the Pseudo-DIN spectrum. Also two workpieces have been milled in the XY-plane under similar operation conditions. In the next paragraph the results of these experiments will be used for a comparison of both models.

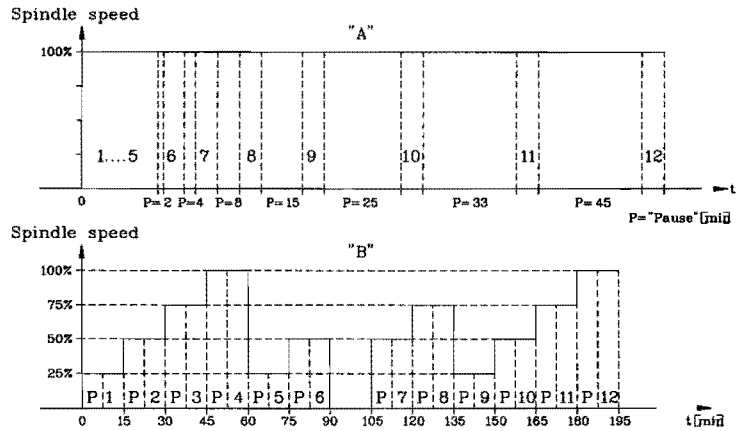

Figure 5.13 : Operation conditions applied for finishing of the test-workpieces. Operation condition 'A' represents the finishing process with a constant spindle speed; condition 'B' with the Pseudo-DIN 8602 spectrum. The numbers indicate the different levels in the test workpiece.

Comparison of the statistical and analytical model

Two totally different strategies have been applied to model the thermally induced errors of machine tools. A statistical model has been developed which directly relates the error of the tool to the measured temperature distribution on the machine tool. Contrary to this empirical approach the analytical model is based on the physical relationship between the measured temperature and the expansion of the succeeding elements.

In this paragraph a comparison of both models will be presented, considering its application for software error compensation purposes. The discussion will be presented as follows:

1. *Effort to create a model;*
2. *Utilisation;*
3. *Preconditions;*
4. *Sensitivity for disturbances;*
5. *Efficiency.*

Effort to create a model

- *Analytical model:*

  Comprehensive experience is required to create the analytical model. A large number of model parameters which are specific for the modelled machine type have to be determined and implemented in the model. An optimum position of the sensors can only be achieved after a thorough study on the temperature distribution on the machine tool. Hence, a large effort is required to realise an analytical model.

  A clear advantage of the analytical model is that both construction parameters and sensor positions have to be determined only once for a specific machine type. However, sensor reduction is not possible as the number of sensors is directly related to the number of segments.

- *Statistical model:*

  The model can be achieved with a relatively small effort, as it is fully based on experimental data. The modelling procedure does not take more than a few days. Also the amount of necessary experiments is limited to three days per position.

  The number of sensors can be optimised with respect to the desirable accuracy. Good results can already be achieved with a small number of sensors. However, special precautions have to be taken into account to reduce the chance of incorrect models for not verified machine states (by 'Over-fitting'). The statistical model has to be determined for every individual machine. Only the optimised position of the sensors can be used for another machine of the same type.

Utilisation

- *Analytical model*

  The analytical method can determine the thermal deformation of the machine tool with the axes located on any position within the range of the machine tool. Also the intermittent application of both the horizontal and the vertical spindle can be modelled efficiently. The model is based on a large number of deformations in the machine structure which have to be calculated. These calculations have to be carried out within every cycle time in which the software error compensation parameters are updated (see Chapters 6 and 7). With the current status of computing power, this is not a limitation for the application of the model. The number of temperature sensors for the analytical method is presently 39. This number is very large and limits the utilisation as 39 sensors introduce large costs during installation and maintenance of the machine tool.

- *Statistical model*

  Verification measurements have shown that the thermal behaviour highly depends on the positions of the Z-axis. The other axes have no significant influence [78]. As the Z-axis has been modelled on three positions, the model is very well capable of describing the thermal behaviour on all positions in the working volume by interpolating between the deformations in the three Z positions and neglecting the influence of the X- and Y-positions. The model has limited capabilities

in describing the thermal drift when both the horizontal and vertical spindle are applied intermittently. This is mainly due to the applied experimental set-up; not to the model. The amount of sensors can be reduced enormously by the developed sensor reduction method. Only 16 temperature sensors are needed for a very efficient model.

Preconditions

- *Analytical model*

  The analytical model describes the thermally induced errors relative to a modelled reference situation. This reference situation should be stable, as the geometric errors have to be determined in this reference situation. However, when the temperature is monitored during the determination of the geometric errors, these errors can be compensated for the effect of slowly varying temperatures. Better results are achieved when the investigated machine is placed in a temperature controlled environment.

  A good knowledge of the expansion coefficient of the large elements included in the model is essential for an analytical model.

  As the actual temperature is measured on the machine's structure, the use of cooling liquid does not influence the modelling capacity of the model. The same holds for the heat generated by the cutting process.

- *Statistical model*

  Like for the analytical model all experiments are carried out relatively to one specific thermal reference situation. This implies that the milling machine must be placed in a temperature stabilised environment in order to get repeatable results. It is also possible to compensate for the effect of slowly varying temperatures, when the temperature is measured during the geometric measurements.

  Unlike the analytical model, the statistical model is not very good in describing the effect of situations not included in the modelling stage. This implies that when the modelling data do not include the use of cooling liquid or the heat generated by the cutting process, the statistical model might give very poor results when these situations occur during verification or normal operation.

However, workpieces have been milled with and without cooling liquid. The results of these experiments show that the temperature distribution on the machine tool does not significantly change when cooling liquid is applied. Therefore it is concluded that the cooling liquid has no large influence on the thermo-mechanical behaviour of the machine tool.

Also temperature measurements have been carried out to investigate the heat generated by the cutting process. Fortunately, the heat generated during the finishing process is transferred to the chips and not the tool and workpiece. When these chips are insulated from the machine's structure, the influence of the cutting process is negligible. Also, during the finishing of a workpiece the amount of heat generated by the cutting process is rather limited. The modelling efficiency will be deteriorated when the chips heat the machine's structure. For example when these chips fall against the column of the machine, a thermal gradient can easily be introduced in this column. When the temperature of the column is not measured or included in the model, the statistical model will not account for this effect.

Sensitivity for disturbances

- *Analytical model*

  The analytical model is based on the physical relationship between temperature variations and the actual expansion. Although it has not been verified, it is expected that there is no change in the thermo-mechanical behaviour of the machine tool over a long period of time. Though, a change in the thermal behaviour due to ageing for example of the bearings may shift the optimum positions of the temperature sensors. Thus, the temperature distributions in the machine structure should be checked periodically under equal operating conditions.

  Also, due to the large number of temperature sensors the probability for a failure due to an error in temperature reading is high for the analytical model.

- *Statistical model*

  Due to ageing the heat-flow in the machine can significantly change, for example by the increased heat produced by worn main spindle bearings. Then the location of the temperature sensors and the model parameters will be less optimal resulting in a decreased modelling efficiency. In order to analyse this effect, verification measurements have been carried out over a period of one year [78]. The results show that the model has lost some of its predictive power. The averaged efficiency of the model decreases from 75% to 60%. Although this influence of ageing is relatively small, it is recommended to carry out periodic tests every half year to ensure an optimal thermo-mechanical model.

  The model will be influenced by a failure in the temperature readings. The magnitude of this disturbance depends on the indicated temperature and on the absolute value of the coefficients in the model. Therefore, 'Principle Components Analysis' has been applied to lower the absolute values of the coefficients. With 'Principle Components Analysis' the absolute values of the coefficient are lower without a structural loss of predictive power. This will improve the prediction power of the model if during actual operation a temperature is measured wrongly or a situation occurs that has not been included in the model.

Efficiency of both models with test-workpieces

The modelling capacity of both models has been verified by the application of test-workpieces. As stated in the previous paragraph, four test-workpieces are milled on the same machine tool. During the milling process, the temperature distribution is measured every minute. Based on the measured temperatures both models can estimate the drift of the tool holder. The calculated results are compared with the actual drift extracted from the workpieces.

In the figures 5.14a and 5.14b the results of a comparison in X-direction is depicted. The test-workpiece has been milled with a spindle speed of 6000 rpm. A very good similarity between modelled and actual drift is shown for both models.

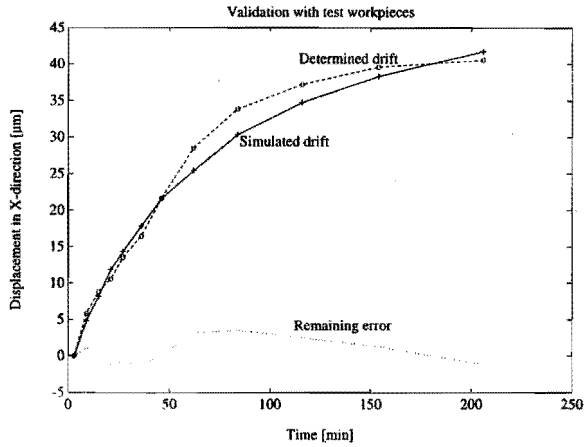

Figure 5.14a : Statistical model verified with a workpiece milled in the XY-plane (load: 6000 rpm).

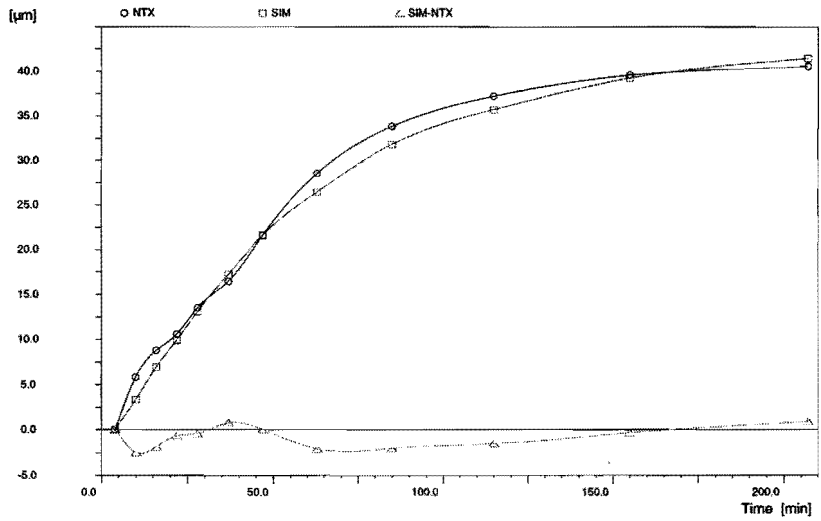

Figure 5.14b : Analytical model verified with a test workpiece milled in the XY-plane (load: 6000 rpm). 'ntx' indicates the determined zero-point drift in X-direction; 'SIM' the simulated drift in X; 'SIM-ntx' the difference between the simulated and the actual drift.

A complete overview of the modelling capacity of both models is given in tables 5.1 and 5.2. The efficiency of both models is calculated in three directions for every experiment. As the efficiency depends highly on the absolute values of the measured drift, also the maximum residual is given in these tables.

	Statistical model				Analytical model			
	N = 6000		Pseudo-DIN 8602		N = 6000		Pseudo-DIN 8602	
Axis	Res. [µm]	Eff. [%]	Res. [µm]	Eff. [%]	Res. [µm]	Eff. [%]	Res. [µm]	Eff. [%]
X	4	93	5	77	5	88	8	63
Y	25	86	13	85	14	87	19	85
Z	3	78	7	-16	11	51	9	31

Table 5.1 : Efficiency of both the statistical and analytical model verified with test workpieces. The workpieces have been milled in the XY-plane with the horizontal spindle using the indicated spindle speed spectrum.

	Statistical model				Analytical model			
	N = 6000		Pseudo-DIN 8602		N = 6000		Pseudo-DIN 8602	
Axis	Res. [µm]	Eff. [%]	Res. [µm]	Eff. [%]	Res. [µm]	Eff. [%]	Res. [µm]	Eff. [%]
X	10	74	8	77	8	64	9	59
Y	6	76	6	51	12	73	13	-39
Z	6	82	13	76	23	63	6	77

Table 5.2 : Efficiency of both the statistical and analytical model verified with test workpieces. The workpieces have been milled in the XZ-plane with the vertical spindle, using the indicated spindle speed spectrum.

Both models show a very good efficiency in describing the error in Y-direction when milling with the horizontal spindle in the XY-plane. However, the maximum remaining error is still 25 µm for the statistical model and 19 µm for the analytical model. The good efficiency is caused by the large actual drift (129 µm). Both models are capable of reducing this zero point drift with more than 100 µm!

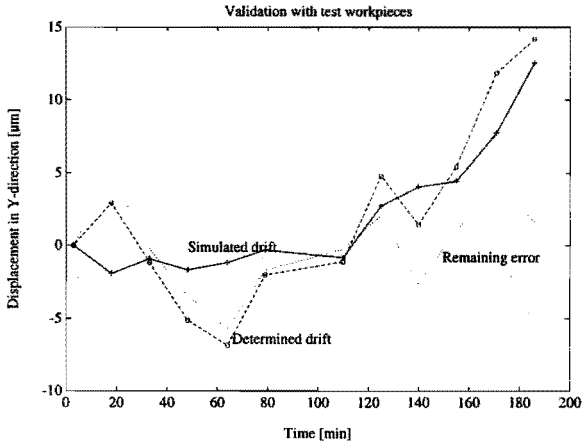

Figure 5.15a : Statistical model verified with a test workpiece milled in the XZ-plane (load: Pseudo-DIN 8602).

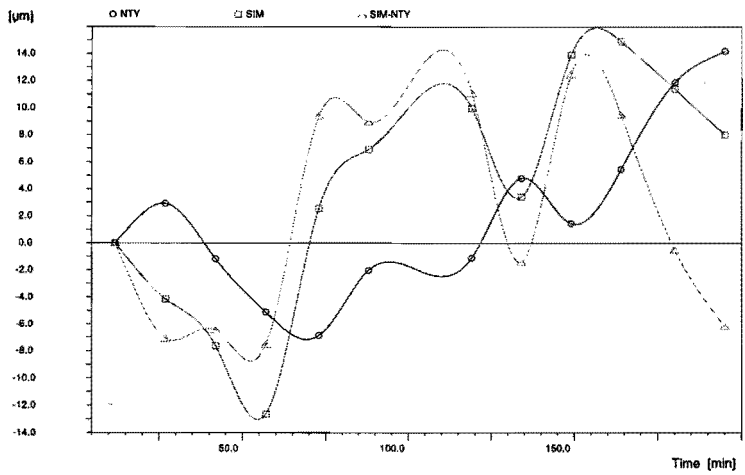

Figure 5.15b : Analytical model verified with a test workpiece milled in the XZ-plane (load: Pseudo-DIN 8602). 'nty' indicates the determined zero-point drift in Y-direction; 'SIM' the simulated drift in Y; 'SIM-nty' the difference between the simulated and the actual drift.

The opposite is found in Z-direction. Although both models show a bad efficiency for the Pseudo-DIN-workpiece, the remaining error is still very small. When milling in the XZ-plane with the vertical spindle a similar effect can be determined. In figures 5.15a and 5.15b the verification of both models is depicted in Y-direction for the Pseudo-DIN workpiece milled in the XZ-plane. A small zero point drift is found in this workpiece. So, the modelling efficiency might be small, the absolute value of the residual is also limited.

Both models show very good results for the workpieces milled with a constant spindle speed (N = 6000 rpm). The zero point drift can be described very accurately. The statistical model realises an averaged efficiency of 77% with the vertical spindle and 86% with the horzontal spindle. The analytical model realises a similar averaged efficiency of 67% with the vertical spindle and 75% with the horizontal spindle.

For the workpieces milled with the Pseudo-DIN 8602 spectrum, both models show a smaller efficiency. This is mainly caused by the quick temperature changes. As the temperature sensors are not attached close to the actual heat sources, these quick changes are detected relatively slow. This results in a smaller modelling efficiency for quick changes in the actual temperature distribution.

In order to achieve a more accurate model for these transient states further investigation is necessary. The statistical model can be extended by including history in the model; the analytical model can be extended with an empirical part (hybrid model). Also the dynamic model introduced by Soons [87] is a very promising technique and should be investigated on its modelling capacity for these transient states.

The statistical model can achieve an averaged efficiency of 71%, the analytical model 59%; whereas the averaged efficiency of the analytical model is deteriorated by the bad efficiency in Y-direction for the Pseudo-DIN 8602 workpiece milled with the vertical spindle.

With both models it is possible to describe the thermo-mechanical behaviour of the milling machine. Application of both models will result in a significant improvement of the accuracy of the milling machine. Both models are applied in the real-time software error compensation system. In Chapter 8, the results of a number of verification experiments will be presented.

Chapter 6

Real-time Software Error Compensation

In this chapter a software error compensation system will be described which has been implemented in a machine tool controller environment. A functional partition of the real-time software error compensation system is presented indicating the different processes that operate inside the NC-controller. The data-acquisition unit has been implemented on an external PC, as a direct communication between the NC-controller and the measurement instrumentation was not possible. The implementation of the different error models has also been realised on this PC. Based on these models compensation functions are created and sent to the controller. The implementation of the error models and the compensation functions will be discussed. The different kinematic configurations needed for a correct implementation of the compensation model, can be programmed in the controller. The definitions of the different configurations will be given. Finally, it is described how the individual compensation values are handled by the NC-controller. For the developed software error compensation system a patent has been applied [89].

Functional partition of the real-time compensation system

The real-time software error compensation system is implemented in the controller environment of a machine tool. The controller operates in a real-time environment with a multi-tasking operating system. This system allows the definition of different tasks which can be carried out mutually independently. Each task has its own priority and cycle-time.

The machine's axes can be moved very quickly (with the investigated machine movements up to 12 m/min are possible; with the latest machine tools movements up to 24 m/min are possible). This implies that the compensation values should be calculated and fed to the controller within a short period of time. Therefore, it is decided to implement the real-time

error compensation in the interpolation task. This task has a cycle-time of 15 ms which results in a maximum step-size of 3 mm for a machine tool moving with 12 m/min. Application of the real-time error compensation in this task means that the compensation values should be determined within this 15 ms. This fast cycle-time has already been considered with the design of the error compensation model as a minimum of calculations are necessary for the NC-controller to determine the actual compensation value.

This compensation value is calculated by addition of the linear compensation terms and a multiplication of the rotational terms with actual arm-lengths (see the error propagation model presented in Chapter 2). These arm-lengths are : the present axis positions of the machine and the applied tool vector. The tool vector is determined by the tool length and orientation. The investigated machine tool is equipped with a horizontal and vertical main spindle which enables milling in the XY- and XZ-plane respectively. A swivelling head is applied to switch between the vertical and the horizontal spindle head. The vertical spindle is equipped with a C-axis. With the C-axis the tool can be rotated around the Z-axis. A correct implementation of the developed compensation model can only be achieved when this tool vector is also considered. Therefore, the compensation system needs direct access to the actual status of these components.

In figure 6.1 the real-time software error compensation system is depicted in relation to its environment, with the input and output data.

The inputs are:

- Compensation functions;
- Machine parameters;
- The axes positions and actual tool.

The outputs are:

- The compensation values for the X, Y and Z axis;

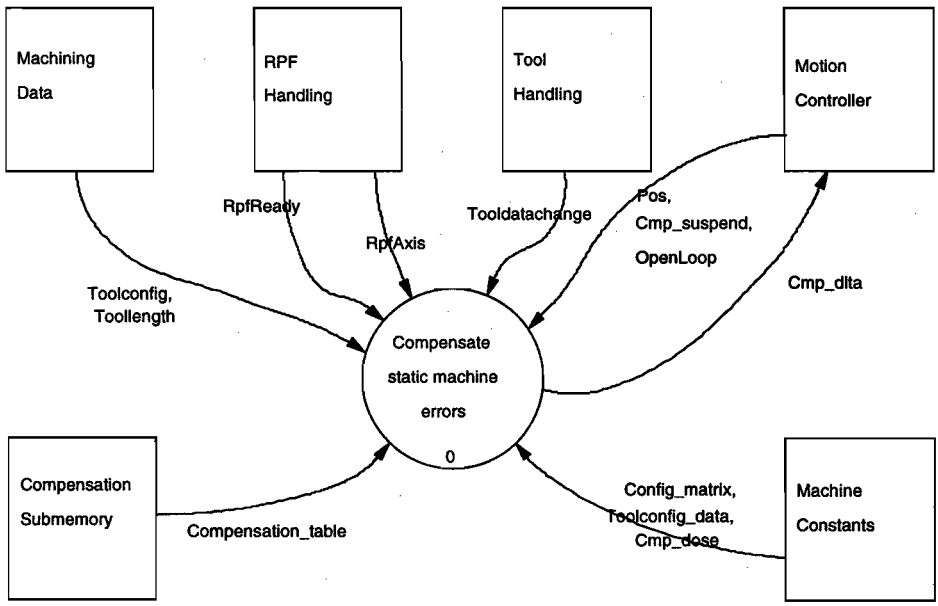

Figure 6.1: Data and control context diagram of the real-time software error compensation system [69, 70].

Figure 6.2 shows the functionality of the real-time software error compensation system. The compensation functions are received from an external PC. It reads the geometric errors and the sensor data, computes the error terms (see next paragraph) and sends the error tables to the NC-controller. The tables are the interface between the external PC and the controller. These table are read by process 1, interpolated to a fixed grid size and stored in the NC-controller. Process 2 computes the values of the tool vector components. Using this tool vector, process 3 calculates the compensations. Process 4 outputs the calculated compensations to the motion controller. Finally, process 5 resets the actual compensation when an axis is at its reference point.

Process 1 is activated every 60 s, processes 3 and 4 every 15 ms. Process 2 is activated when the tool-length and/or orientation changes (indicated with the parameter 'Tooldatachange'); process 5 when one of the machine's axis is at its reference point (indicated with the parameter 'RpfReady').

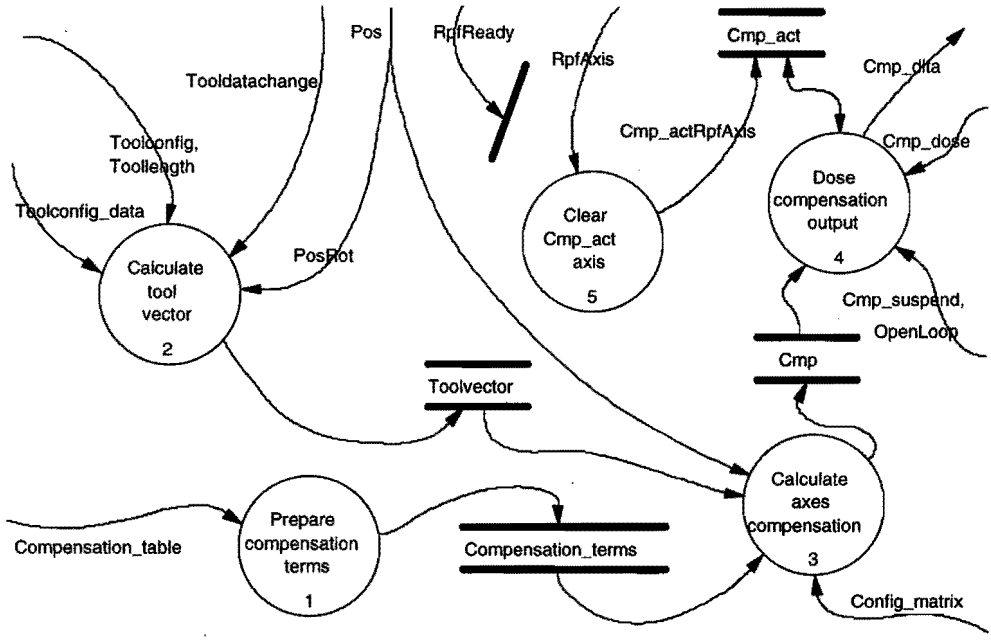

Figure 6.2 : Highest level data and control flow diagram of the real-time software error compensation system [69, 70].

In the next paragraphs the different elements will be presented of the real-time software error compensation system as depicted in figure 6.2. Firstly, the implementation on the external PC will be presented.

Implementation of the different error models

The applied error models, as described in the previous chapters, are implemented on the external PC with a cycle-time of 60 seconds. Within this period of time the data-acquisition is performed and the different error models are evaluated. Hence, each model is evaluated every 60 seconds.

Geometric error model

The geometric error model constitutes the basis for the software error compensation. This error model enables the implementation of 18 error functions to describe all degrees of freedom of a Cartesian three-axis machine. The software error compensation system is based on this model

(see Chapter 2). This allows the independent implementation of each model in the real-time software error compensation system.

The geometric errors will not change rapidly. However due to wear the geometric errors will change in time. Several calibrations over a long period of time have shown that a calibration period of one year is advisable [78]. Within this period, it is allowed to use the parameters of the geometric error model.

Errors due to static and slowly varying forces

The developed error model presented in Chapter 4 is capable of modelling the errors due to static and slowly varying forces. In this chapter it is clearly shown that a workpiece load results in a significant change in the geometric errors. This change is dependent on the actual load and the position of the workpiece. A set of strain-gauges is applied to determine the actual load and calculate the change in the error component. The calculated error components are added to the matching geometric errors by the accumulator (see Chapter 2).

Thermally induced errors : Analytical model

An analytical model has been developed to describe the most significant thermo-mechanical errors of the Maho 700S milling machine. The thermally induced errors are calculated with respect to the reference situation in which the geometric errors are defined. The analytical model describes the zero point drift (on one position), the thermally induced changes of the error components of the linear axes (scale expansion and squareness errors) and the thermal expansion of the workpiece. These parts have also been included in the software error compensation module.

The compensation module is divided into an initialisation sequence and a compensation sequence:

- *Initialisation*

  During the initialisation sequence the current temperature distribution is measured. Also the model parameters are defined (e.g. tool length and orientation or the position of the workpiece and the actual expansion coefficient). The thermo-mechanical errors are reset to zero in the reference situation.

- *Compensation sequence*

  In the compensation sequence the actual temperature distribution is measured and the mentioned errors are calculated. The following parameters are sent to the accumulator where they are added to the matching error components:

  - Zero point drift (ntx, nty and ntz);

    The zero point drift results in an offset, independent on the actual axes position and will be added to the X-axis compensation table.

  - Scale and workpiece expansion (xtx, yty and ztz);

    The scale and workpiece expansion are combined resulting in three error functions which are a linear function dependent on the axis position and added to the compensation functions iti (with i = x, y or z).

  - Squareness errors (xsy, xsz and ysz).

    The squareness errors will be added to the matching rotation compensation functions. The actual compensation strategy depends on the kinematic configuration of the machine tool. E.g. the squareness error xsy will be considered by the rotation compensation function yrz, when the machine has the following kinematic configuration X-Y-Z.

Thermally induced errors : Statistical model

Contrary to the analytical model, the statistical model is based on a model of the zero-point drift. The zero-point drift of the tool holder turned out to be dependent on the position of the Z-axis. Therefore, the statistical model is evaluated for three different Z-positions. The compensation values between these grid-points are obtained by linear interpolation.

Similar to the analytical thermo-mechanical correction module, the correction sequence for the statistical model is divided into an initialisation sequence and a compensation sequence:

- *Initialisation sequence*

  The initialisation is started with the machining process. During the initialisation sequence the current temperature distribution is measured. Also the model parameters are defined (e.g. tool length and orientation or the position of the workpiece and the actual expansion coefficient). The thermo-mechanical errors are reset to zero in the reference situation.

- *Compensation sequence*

  During the compensation sequence the actual temperature distribution is measured and the drift of the tool holder is calculated for three different Z-positions. Besides the zero-point drift, also the scale and workpiece expansions are calculated. These expansions are described as additional translation errors xtx, yty and ztz. Using the statistical model the following parameters are sent to the accumulator:

  - Zero point drift as a function of Z (ntx, nty, ntz);

    The zero point drift is modeled as a function dependent on the Z-axis position and added to the compensation functions zti (with i = x, y, z).

  - Workpiece and scale expansion (xtx, yty and ztz).

    The scale and workpiece expansion are combined resulting in three error functions which are a linear function dependent on the axis position and added to the compensation functions iti (with i = x, y or z).

Compensation functions

The individual error functions are received from the different error models and evaluated by the accumulator resulting in compensation tables which are sent to the controller. The compensation functions are stored in tables as it is very difficult to combine the piecewise polynomials received from the different error models. The compensation values are also stored in tables for compatibility reasons. The scale compensations which were already available in the previous versions of the Grundig NC-controller were also defined in compensation tables.

The compensation tables for the linear axes are stored in the NC-controller in three different parts for each linear axis. The parts are distinguished by their first address, the S address. S1 designates the compensation terms for the X-axis; S2 for the Y-axis and S3 for the Z-axis. The S address is followed by the position P of the grid point with respect to the machine reference point. For each position P three translation and three rotation components can be defined. In table 6.1 the defined table format is graphically depicted.

Every 60 seconds these compensation tables are evaluated and stored into an internal memory in the NC-controller to which the user has no access. This internal table is applied for the actual compensation calculations. In order to access and evaluate the compensation functions within the interpolation cycle-time (= 15 ms), the compensation functions are also stored in tables. Contrary to the user-accessible tables, the internal tables have a fixed grid of 200 intervals per axis. This results in a lookup table for each axis, which contains the grid points and the compensation values on the corresponding grid interval. Hence, the calculation of the individual compensation values is now limited to a search operation through a table. The 200 intervals are located between the negative and positive software end switch. In figure 6.3 the internal representation of the compensation functions is depicted graphically.

S1	P-100	T1=10	T2=6	T3=-6	R1=-1	R2=0	R3=3
S1	P-90	T1=9	T2=7	T3=-8	R1=3	R2=4	R3=1
S1	P-80	T1=8	T2=8	T3=-10	R1=5	R2=6	R3=0
..	..	..	..	..	..	..	..
S2	P-500	T1=3	T2=3	T3=5	R1=2	R2=4	R3=-1
S2	P-480	T1=3	T2=5	T3=4	R1=1	R2=2	R3=1
S2	P-460	T1=1	T2=7	T3=4	R1=0	R2=1	R2=1
..	..	..	..	..	..	..	..
S3	P-700	T1=3	T2=3	T3=5	R1=2	R2=4	R3=-1
S3	P-650	T1=3	T2=5	T3=4	R1=1	R2=2	R3=1
S3	P-600	T1=1	T2=7	T3=4	R1=0	R2=1	R2=1
..	..	..	..	..	..	..	..

Table 6.1 : An example of the table format applied to define the compensation functions for the real-time software error compensation. For the X-axis an interval of 10 mm has been chosen; for the Y-axis 20 mm and for the Z-axis 50 mm. 'T' indicates the translation terms; 'R' indicates the rotation terms. Value are given in [μm] and [arcsec].

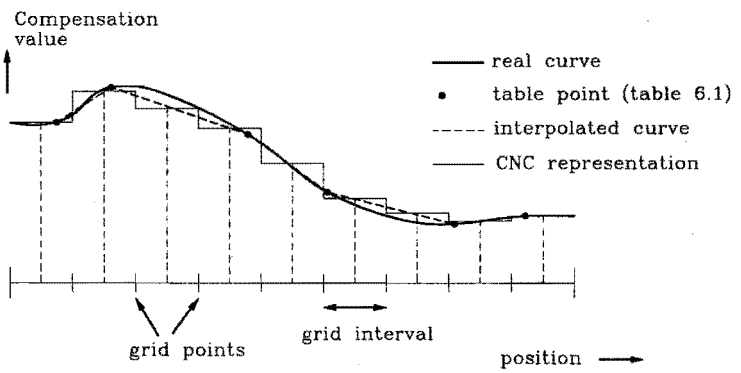

Figure 6.3 : Internal representation of the compensation functions.

Configuration of the different machine tools

In order to constitute the appropriate error propagation model the actual machine configuration must be defined in the NC-controller. As the kinematic model has been defined such that a minimum of parameters are necessary, the machine configuration can be defined rather simply. The following parameters have to be defined:

- Configuration of the machine axes

  For the description of the error propagation model the compensation module uses the machine axis naming conventions as defined in ISO 841 [39]. Therefore, the axis numbering in the NC-controller must be mapped on the ISO axis numbering. A total of six machine constants are available to relate the ISO and the NC axis numbers. Machine constants are user-accessible variables with which the NC can be made to fit the actual machine configuration. During normal operation the machine constants remain constant : only after a complete reset of the machine tool a new value defined in a machine constant memory will be considered. With the six machine constants all possible machine configurations can be defined (with a maximum of three translation and three rotation axes).

- The kinematic configuration

  The kinematic configuration of a machine is defined by the actual axis configuration. The information on this configuration is needed for the correct calculation of the contribution of a certain rotation error. For example, the rotation error yrx has to be multiplied with the Abbe-offset introduced by the Y- and Z-axis and the tool-vector when the machine has a kinematic configuration with first the X-axis, followed with respectively the Y- and the Z-axis. When the Y-axis is the last axis in the kinematic chain, only the Abbe-offset introduced by the Y-axis and the tool-vector has to be considered. The actual kinematic configuration is defined with the nine parameters b_{ii} (see Chapter 2, figure 2.4 and equations 2.5 to 2.8).

- Configurations of the tool holder

  The software error compensation system allows the implementation of different tool configurations caused by the implementation of a

swivelling head and/or a rotation axis. The investigated Maho 700S milling machine for example is equipped with both possibilities. As for normal milling operations it is sufficient to define the actual tool length and diameter, the different configurations have to be considered by the software error compensation system. Therefore, four different construction parameter sets are provided. In each of these sets the ISO number of the tool axis is entered, the ISO number of the axis that rotates the tool (when available) and the offsets in X, Y and Z of the centre point of the tool holder nose to the last machine axis.

For example, the Maho 700S is equipped with a swivelling head in combination with a C-axis. Two construction sets are needed to define the different tool configurations. The first construction set describes the machine as a vertical milling machine, with the Y-axis as the tool axis and the C-axis that rotates the tool head. Thus, the ISO tool axis is the Y-axis; the ISO axis that rotates the tool is the C-axis; the offsets in X and Z are zero; the offset in Y is the distance between the tool centre point and the location of the C-axis (measured in Y). The second construction set describes the machine as a horizontal milling machine, with the Z-axis as the tool axis. Thus, the ISO tool axis is the Z-axis; the ISO axis that rotates the tool is undefined (as the machine cannot use the rotation axis when it is used as a horizontal milling machine); the offset in X is zero; the offsets in Y and Z describe the distance between the tool centre point and the location of the C-axis.

Design of a stable compensation algorithm

In this paragraph the investigation on the stability of the compensation system will be described. Using the axis position the different compensation values will be searched in the compensation tables. The error propagation model, which has been configured by the machine constants, uses all these 18 compensation values and the actual tool-vector to calculate the compensation value for each axis (process 3 in figure 6.2). The compensation value is now sent to the motion controller (process 4 in figure 6.2).

The actual compensation value depends on the machine's position. This position can be read from the measuring system, attached to the machine's axes. This compensation method will be refered to as scale-compensation

(see figure 6.4). It is also possible to calculate the compensation values using the next set-point, generated by the controller. This compensation system will be refered to as 'Set-point compensation' (see figure 6.6).

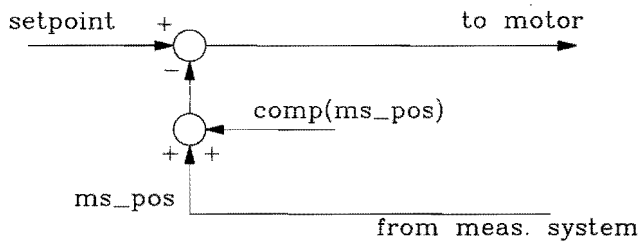

Figure 6.4 : Scale-compensation.

With a full implementation of the error propagation model a scale-compensation strategy can easily introduce instable or discontinuous behaviour of the axis position. When a change in the determined compensation value occurs which is larger than the resolution of the measuring system a limit cycle around a grid point appeared. Investigations on the Maho 700S showed that a compensation jump of 2 μm resulted in a limit cycle with an amplitude of 5 μm. A step of 1 μm, which equals the resolution of the measuring system, resulted in a stable system. For an opposite sign of the compensation value, a virtual hysteresis occurred together with a position jump. In figure 6.5 both the determined limit cycle and virtual hysteresis are graphically depicted.

A limit cycle is the most unwanted behaviour as it introduces an instable system which deteriorates the milled surface and even can destroy a machine. In order to avoid a possible limit cycle the compensation values are determined using the set-point of the motion controller. The set-point is the next point, generated by the interpolator of the machine tool controller, where the machine will move to. This point is generated every cycle-time of the controller (= 15 ms). In figure 6.6 the set-point compensation is presented. Note that the functional dependency of the compensations on the uncompensated set-point is the same as the dependency on the measuring system compensation. The value of the set-point position is the same as the measuring system position when the machine has reached the commanded position according to that set-point.

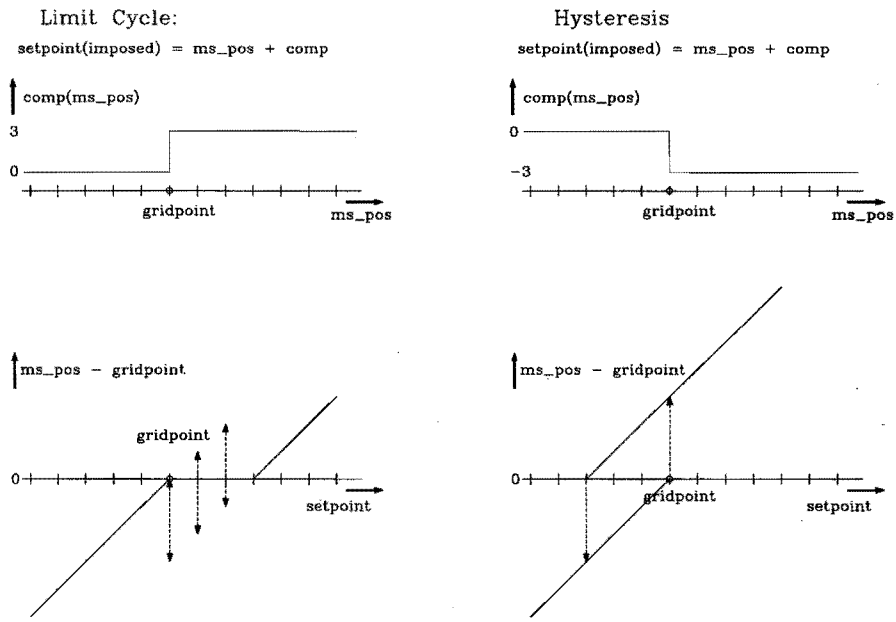

Figure 6.5 : Limit cycle and virtual hysteresis around a grid point which can occur with a scale-compensation.

The scheme presented in figure 6.6 shows that the stabilisation of the axis behaviour is in fact accomplished by calculating the compensation value from the imposed set-point and not by the measuring system position.

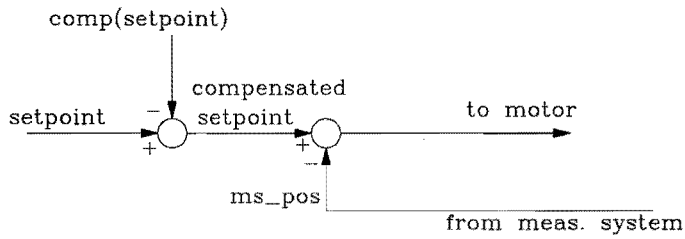

Figure 6.6 : Set-point compensation.

The effect of a set-point compensation around a grid-point is presented in figure 6.7. The limit cycle behaviour and the virtual hysteresis have disappeared. Both problems have been reduced to a position ambiguity and a forbidden zone, depending on the sign of the step.

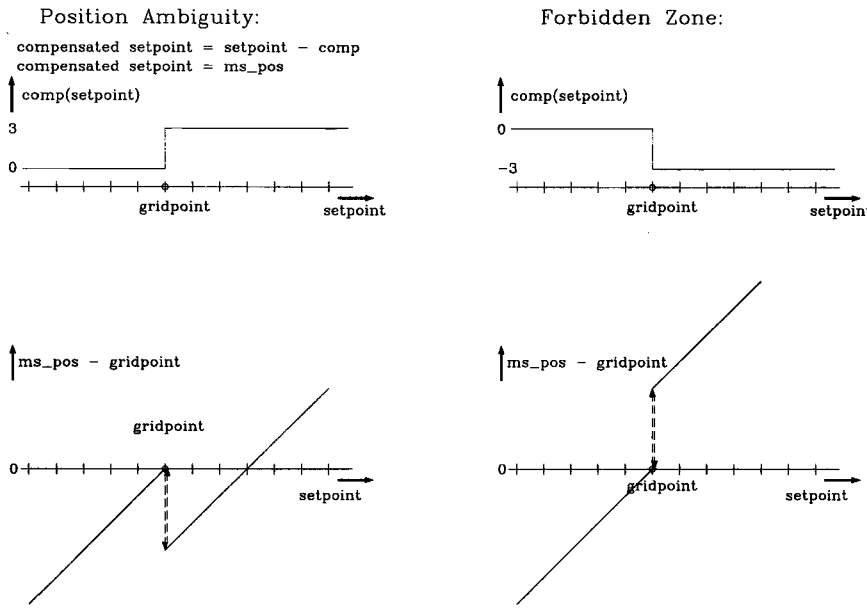

Figure 6.7 : Position ambiguity and forbidden zone with set-point compensation.

Considering the large number of internal grid-points, the continuity of the compensation functions and the found residual of about 7 μm of the geometric error model, the effect of both the position ambiguity and forbidden zones is not expected to significantly decrease the efficiency of the software error compensation system.

Compensation dosing system

Due to the fact that the compensation tables are time dependent the compensation values may exhibit sudden jumps. This effect should be reduced to avoid visible steps on the workpiece surface. Therefore, a compensation dosing system has been applied, which allows the compensation change in a gradual way (see figure 6.8). The change of the actual compensation is never more than a predefined number of increments per NC-controller cycle-time. This number is entered in a machine constant.

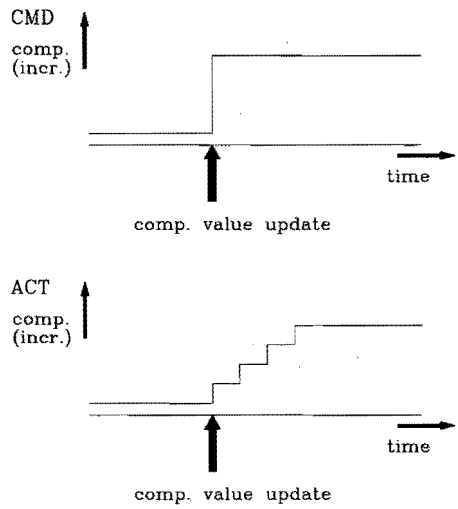

Figure 6.8 : Compensation dosing system.

The developed real-time software compensation system is implemented in the controller of the machine tool, enabling a full compensation of every movement of the machine. However, the main disadvantage of a real-time software error compensation is that it is only applicable with a new controller on a machine tool. It is not possible to utilise an existing controller for real-time software error compensation, as the software error compensation is embedded in the controller. To build a new controller to an existing machine tool is a costly job. Only very large and expensive machine tools could be taken into consideration for a new controller. Otherwise, a software error compensation which compensates the errors of a machine tool by changing the NC-program could be the solution. This compensation system will be discussed in the next chapter.

Chapter 7

NC-code Software Error Compensation

In this chapter a software error compensation system will be presented that operates directly on the NC-code of a part-program. When this NC-code is adapted to compensate the programmed trajectory for the modelled errors a software error compensation is realised. This compensation system will be implemented on a stand-alone computer system and therefore can be applied to any machine tool, without the need of a specially designed controller with a software error compensation mechanism inside. Two different compensation steps have been developed to compensate both the finite stiffness, the geometric errors and the thermally induced errors respectively. Both compensation steps will be described in this chapter. The NC-code compensation system could also be implemented in the 'post-processor' of a CAD-system. The NC-code generated by this 'post-processor' will then already be adapted for the errors involved during the actual milling process. This CAD/CAM compensation will not be described in this thesis.

The NC-code compensation system

Normally, NC-code part-programs are applied for automatic execution of the cutting process on the machine tool. The machine tool controller parses this NC-code and executes it command line by command line, resulting in the desired product. This NC-code contains all information of the cutting process (e.g. process parameters, tool, trajectory). When the NC-code is adapted to compensate the programmed trajectory for the modelled errors a software error compensation is realised. This, so called 'NC-code software error compensation' can be applied to any machine tool, without the need of a specially designed controller with a software error compensation mechanism inside.

With the NC-code language, the trajectory of the machine tool can be programmed in different coordinate systems. These coordinate systems are

stored inside the machine tool controller. This enables the programming of a part in workpiece coordinates, without noticeing the actual position of the workpiece inside the machine tool's range. A similar technique is used for the different tools applied during the cutting process. The data of all available tools are stored in the memory of the machine tool controller. Whenever a tool change occurs, the controller searches for the tool dimensions in this tool-table. The tool dimensions and the location of the workpiece coordinate system are used by the machine tool controller to calculate the actual trajectory of the machine tool.

As the compensation described by the derived model is a function of the position of the machine tool's axes, the NC-code software error compensation should carry out a similar task. Before a software compensation can be carried out, the programmed trajectory has to be translated from workpiece coordinates to machine coordinates. Therefore, a direct access to the workpiece coordinate system table and the tool table is needed by the NC-code software error compensation system.

An NC-code software error compensation should be carried out before the machine tool starts the cutting process. This means that, after the translation to machine coordinates, the NC-code has to be compensated for the errors from the various sources involved. Then, it can be sent to the machine tool controller, which parses the program and generates the desired trajectory. It is not possible to compensate an NC-program completely before the actual milling process is initiated. As the derived compensation functions depend on the actual load and temperature of of machine, which continuously varies during the actual milling process, large errors would remain. Therefore, the NC-code compensation system will be split into two parts. The first part compensates the error sources that remain constant during the milling of a workpiece. This compensation is carried out off-line before the milling process is initiated. The second part compensates for the errors that continuously vary during the actual milling process. This compensation system should be applied during the milling process.

In this thesis three different error sources are investigated. From these error sources, both the geometric and finite stiffness errors are found to remain constant during the milling process (see paragraph "NC-code compensation for geometric and finite stiffness errors"). Hence, these error sources will be compensated by the first step of the NC-code compensation system. The second step of the compensation system will compensate the

thermally induced errors, using the compensated NC-code received from the first step. This compensation will be carried out during the milling process. Just before the NC-code is sent to the controller of the machine tool where it is processed immediately the actual compensation values will be determined and added to the programmed coordinates.

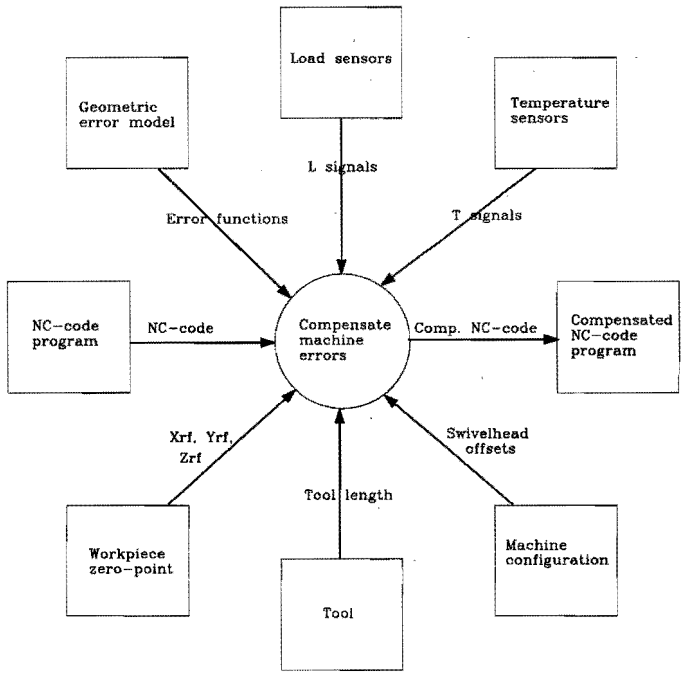

Figure 7.1 : Data context diagram of the NC-code compensation system.

In figure 7.1 the NC-code software error compensation system is depicted in relation to its environment, with the input and output data.

The inputs are:

- The NC-code (part-program);
- Location of the workpiece (workpiece zero-point);
- Actual tool and machine parameters;
- The geometric error functions;
- The workpiece load data to calculate the error terms;
- The actual temperature distribution.

The outputs are:

- The compensated part-program;

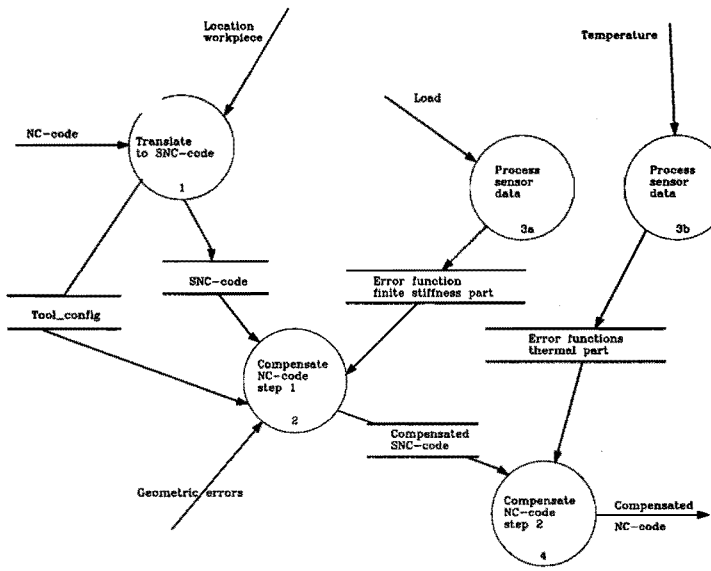

Figure 7.2 : Highest level data flow diagram of the NC-code compensation system.

Figure 7.2 shows the functionality of the NC-code software error compensation system. Process 1 in this diagram translates the NC-code to a subset of this NC-code, called SNC-code. The definition of this SNC-code and the translation-process will be described in the next paragraph. Process 2 compensates the SNC-code for the geometric and finite stiffness errors. The finite stiffness error model is received from process 3. Finally, process 4 compensates for the thermally induced errors. The generated SNC-code is now sent to the machine tool controller.

In the next paragraphs the different elements of the NC-code software error compensation system will be presented as depicted in figure 7.2.

Transformation of NC-code to SNC-code

With SNC-code every movement of a machine tool can be programmed like normal NC-code. However, SNC-code only consists of Cartesian coordinates with simple linear and circular movements. Furthermore, the coordinates are expressed as machine coordinates, i.e. relative to the machine origin. The translation of NC-code is necessary because the respective models are developed with respect to this origin.

The NC-code's syntax has been standardised in DIN 66025 [17, 18]. Unfortunately, this standard only defines the elementary commands and has left some space for controller manufacturers to add extra commands. This has resulted in a large amount of different NC-code languages. In this research project, the NC-code software error compensation has been developed for the Grundig (previously Philips) controller CNC5000/V200 [30]. This controller was attached to the machine tool and therefore available for a practical evaluation of the NC-code software error compensation technique.

To translate the NC-code to SNC-codes, an SNC-code generator has been developed, which will generate the SNC-codes. For a complete overview of this SNC-code generator, see the CAQ-project 'Automatic Geometric Correction of NC-Programs' [91].

The following requirements have been defined for the SNC-code generator :

- The SNC-code part program and the original NC-code part program must be 100% compatible, that is, the resulting product should be geometrically identical for both milling with NC-code and SNC-code;
- All coordinates appearing in the SNC-code part program must:
  - be Cartesian, not polar or mixed;
  - be relative to the machine origin;
  - relate to the Tool Centre Point.
- The transformation module must support all machine axes (A, B, C, X, Y, Z);
- All compound movements must be split up into elementary movements (G0, G1, G2 and G3, respectively linear and circular movements);
- Subprogram calls are not allowed in the SNC-code part program;
- Branch or repeating constructs are not allowed in the SNC-code part program;
- Radius correction commands are not allowed in the SNC-code part program;
- Point definitions and parameter definitions are not allowed in the SNC-code part program;
- Mirroring and scaling commands are not allowed in the SNC-code part program;
- Circle milling commands are to be translated to elementary movements;
- Chamber cycles must be transformed such that the edge of the chamber is milled with elementary movements.

The SNC-generator consists of several parts, which are contained in several submodules. In figure 7.3 these different modules are graphically depicted.

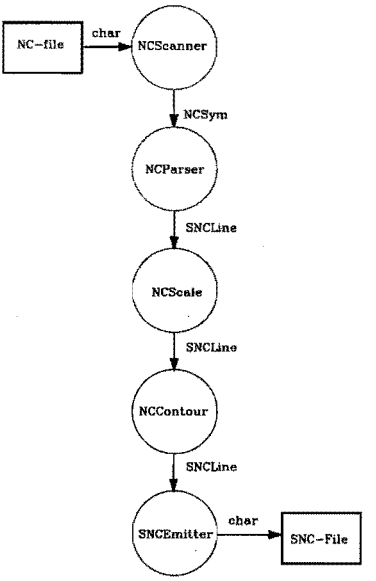

Figure 7.3 : Global design of the SNC-code generator.

The normal processing proceeds as follows:

1. The NCScanner unit reads characters from the NC-file and assembles them into symbols;

2. The NCParser unit combines NC-symbols to NC-lines and transforms these to a standard format [91]. These lines are called SNCLines;

3. The NCScale unit performs any scaling and mirroring of SNCLines it receives and eliminates the corresponding G72 and G73 codes;

4. The NCContour unit performs any contour correction of SNCLines and eliminates the corresponding G40..G44 codes;

5. The SNCEmitter unit transforms the SNCLines to ASCII format and writes them to a user-defined file or to the screen.

The described processing is a sequential process. However, since the NC-code can contain G14, G23 and G29 codes, which invocate a (conditional) branching in the program, the NCParser unit sometimes needs to skip backwards or forwards in the NC-file. This results in a instruction from the

NCParser to the NCScanner unit to go to the beginning of a line. The branching mechanism has been implemented as follows:

- *G14 and G29 codes (loop codes)*

  These codes involves one of two types of repetition conditions, a starting line, an ending line and a return line. G14 applies just a simple repeat counter, which indicates the number of times a loop is repeated. G29 is based on the value of an E-parameter (which is a parameter, stored in the memory of the NC-controller and accessible from the NC-program file). The NCParser unit supports three loops that are nested.

- *G22 (macro invocation)*

  This code requires a macro number. This code will set a global variable to this number so that the NCScanner unit looks for lines inside the macro. Since macro calls may be nested (upto eight macro calls may be active at one time), this requires some sort of stacking mechanism.

With this design it is possible to transform any NC-file programmed for the Grundig NC-controller, to a SNC-file. This SNC-file can be processed by the NC-code software error compensation system. Although the generator has been designed for the Grundig controller, it can easily be adapted to another NC-language as only the NCParser unit has to be changed for this purpose.

NC-code compensation for geometric and finite stiffness errors

The first step of the NC-code software error compensation is the compensation of the errors that remain constant during the milling of one workpiece. Both the geometric and finite stiffness errors can be classified to this group. The finite stiffness errors are induced by the weight of the workpiece placed on the table. As the weight of a workpiece will not vary much during the finishing of a workpiece, this error source can also be considered constant during the milling of one workpiece. The only restriction made is that all finishing operations have to be shifted to the end of the milling process.

Similar to the real-time software error compensation, the geometric error model is applied as the basis for software error compensation purposes. With this model all 18 degrees of freedom of a three-axes Cartesian machine can be described. Hence, the influence of the workpiece load placed on the table, has to be added to the matching error models of the geometric errors. The resulting model will compensate the errors as a function of the actual axes positions and the tool-vector applied during the milling process.

In the previous paragraph an SNC-code generator has been described. This SNC-code only consists of elementary linear and circular movement commands. The individual movements are described with respect to the machine zero-point, like the combined finite stiffness and geometric error model. A compensation of these errors has only to be carried out for the actual milling process: when material is removed from the workpiece. Thus all G0 commands (rapid movement to position the tool near a workpiece) can be skipped by the NC-code compensation system. All other movements will be compensated. The compensation is realised by adding the calculated compensation value to the defined machine coordinates (the respective X-, Y- and Z-coordinates in the SNC-code file). However, it is not sufficient to compensate the coordinates as they are defined in the SNC-file. NC-code commands can define a trajectory over a relatively long distance with a single command. Along this trajectory the actual error vector may significantly change. Hence, when only the start- and end-points are compensated a large residual error can still be found in the generated path (see figure 7.4).

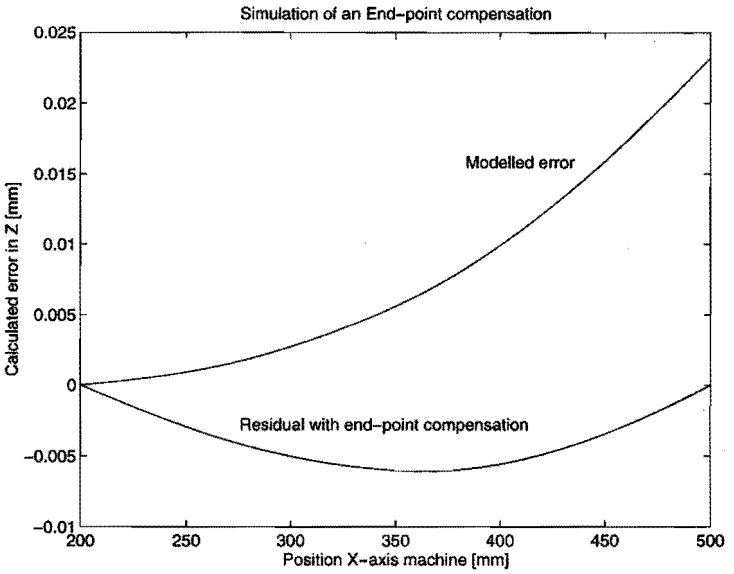

Figure 7.4 : Simulation of an End-point compensation carried out in the XZ-plane with a tool-length of 200 mm. The error presented is calculated perpendicular to the direction of movement of the machine.

The residual found on the intermediate points can be compensated by an interpolation of the trajectory defined in the SNC-code. The interpolation has to be carried out in three dimensions (X, Y and Z). The interpolation step-size can be chosen dynamically or fixed. A dynamically interpolation algorithm will maximise the step-size, considering a maximum allowed residual. The fixed-size interpolation algorithm will cut the trajectory into a number of equally distanced parts. The second method has been implemented in the NC-code compensation system. The first mentioned dynamical method will result in more optimised step-sizes and therefore in a minimum of compensated SNC-code lines. The fixed step-size algorithm is less efficient as interpolations may be carried out which are not really necessary. However, the number of lines is not a limiting factor, especially as the SNC-code will be sent to the machine tool controller where it is processed immediately. As the fixed-size algorithm can be implemented very easily and no accuracy loss is to be expected, this algorithm has been implemented in the NC-code compensation system.

The actual interpolation size is determined by a simulation carried out with the combined geometric and finite stiffness error model. To introduce the 'worst-case situation' the model simulation has been carried out with a relatively long tool-vector and a maximum load placed on the workpiece table. To determine the step-size the length of the calculated error vector is considered as it is not known how the actual cutting process will take place. For the investigated Maho 700S milling machine this resulted in a step-size of 20 mm, allowing a maximum residual of 5 μm [6].

The interpolation of the trajectory has been described for linear movements. The step-size is defined along one axis. This implies that when the machine is moved from X=10, Y=10 towards X=110, Y=60, the X-axis movement is interpolated 4 times and the corresponding Y-axis position is calculated for each X-position.

For the circular movements which can be defined with the SNC-code commands G2 and G3 a similar technique has been applied. Considering the programmed radius and the start- and end-point of the circular movement, the travelled distance is calculated for each axis. When the interpolation size is exceeded, the circular movement is split up into circle segments with an arc length of the interpolation size. Like the linear movements, the end-point of a circular movement is always compensated.

As the SNC-code only consists of elementary movements, the described compensation mechanism is sufficient to compensate the whole trajectory for the geometric and finite stiffness errors during the actual cutting process of a workpiece. The resulting compensated SNC-code is now sent to the second step in the compensation system to be compensated for the thermally induced errors.

Compensation methodology for thermally induced errors

The thermal error compensation will be based on the actually measured temperature distribution. This temperature continuously varies due to environmental influences and different operating conditions. As it is not possible to predict the temperature distribution from the operating conditions the thermally induced errors can only be compensated when the actual measured temperatures are used. This implies that the compensation has to be carried out just before the SNC-code is processed by the controller of the machine tool. As the milling of a workpiece can take from 5 minutes to more than 8 hours, a thermal error compensation acting on the NC-code is only possible when the controller can process and read the same NC-program at a time.

Most controllers already support this option as it is necessary for processing large NC-programs, which canot be stored completely in the memory of the controller. Such large NC-programs are generated by CAD-stations (e.g. with complex surfaces, the programmed trajectory is split up into a large number of very small steps). As the importance of a direct connection between the CAD-station and a machine tool is increasing, the option of reading and processing the same NC-program has become a standard option for most machine tool controllers.

During the first step the SNC-code has already been interpolated to avoid large steps in the trajectory. A further interpolation is not needed as the applied thermal models yield compensation functions which are linear with respect to the axis positions.

Similarly to the real-time software error compensation system, the temperatures are measured every 60 seconds. The thermal error models are also evaluated immediately after the temperature measurement resulting in the following compensation functions:

Analytical model

- Zero point drift (ntx, nty and ntz);

  The zero point drift results in an offset independent on the actual axes position and will be added to every coordinate in SNC-code file.

- Scale and workpiece expansion (xtx, yty and ztz):

  The scale and workpiece expansion are combined resulting in three error functions which are a linear function dependent on the axis position. The compensation values are determined using the position of the axes extracted from the SNC-code file and added to the respective coordinates.

- Squareness errors (xsy, xsz and ysz).

  The squareness errors will be added to the matching rotation compensation functions. The actual compensation strategy depends on the kinematic configuration of the machine tool. E.g. the squareness error xsy will be considered by the rotation compensation function yrz, when the machine has the following kinematic configuration X-Y-Z.

Statistical model

- Zero point drift as a function of Z (ntx, nty and ntz);

  The zero point drift is modeled as a function dependent on the Z-axis position. For every Z-position extracted from the SNC-code file, the error functions are evaluated resulting in three compensation values which are added to the respective coordinates.

- Scale and workpiece expansion (xtx, yty and ztz):

  The scale and workpiece expansion are combined resulting in three error functions which are linear functions dependent on the axis position. The compensation values are determined using the position of the axes, extracted from the SNC-code file, and added to the respective coordinates.

When the SNC-code lines are compensated for the thermally induced errors they are sent to the NC-controller where they are processed immediately. In order to avoid that the NC-controller has to wait for the next line from the NC-code compensation system, which would result in visible edges on the workpiece, a buffer is present in the NC-controller. This buffer will contain a maximum number of 5 lines to avoid that too many lines are present in the NC-controller's memory, which would take a relatively long period of time to be processed. To synchronise the process the amount of lines present in the buffer is monitored by the NC-code compensation system.

Chapter 8

Validation

In this chapter a complete validation will be presented of the developed software error compensation systems including the different error models. The validation has been carried out separately for every error source. Firstly, a software error compensation system with the geometric error model has been verified using hole plate and ball bar experiments. Secondly, a validation of the software error compensation system with the finite stiffness error model will be presented. This validation has been carried out with hole plate measurements and an additional load placed on the workpiece table. Thirdly, the compensation of the thermally induced errors has been validated using the measurement set-up as introduced in Chapter 5. Finally, at the end of this chapter, a total validation of the software error compensation system will be presented, which has been carried out by milling test-workpieces with and without the developed software error compensation system.

Validation of the geometric error compensation

In this paragraph the validation of the geometric error compensation will be presented for both software error compensation systems; the real-time software error compensation and the NC-code software error compensation. Two different verification experiments have been carried out. The real-time software compensation has been validated with hole plate measurements. The NC-code software error compensation has been verified with ball bar experiments. Both verification experiments use the geometric error model using the direct measurement technique.

Real-time software error compensation

The validation of the geometric part of the real-time software error compensation has been carried out by measuring a hole plate on the machine tool with and without compensation. A total of five different locations of the hole plate have been applied:

- Two hole plate measurements in the XZ-plane;
- Two measurements in the YZ-plane;
- One measurement in the XY-plane.

For the experiments in the XZ-plane the vertical milling head is applied with two different tool-vectors. In the XY-plane the hole plate is measured with the probe in the horizontal spindle. In the YZ-plane the vertical milling head is applied but with the C-axis rotated respectively 60° and -60°. Thus, these hole plate experiments implicitly check the developed real-time software error compensation including the compensation for different machine configurations and tool-vectors. During these experiments also the linear expansion of the scales and the workpiece (hole plate) has been compensated.

In figure 8.1 the measurement results of the hole plate applied in the XY-plane is depicted; figure 8.2 depicts the results of the hole plate measurements in the YZ-plane.

The validation experiments show an impressive accuracy improvement of the machine tool with the developed real-time software error compensation for the geometric errors. An overview including all hole plate experiments is given in the next table (table 8.1). In this table the achieved compensation efficiency is presented together with the maximum remaining error. The presented maximum remaining error is the length of the maximum error vector found during the experiment. The efficiency is calculated as the ratio of the remaining error with compensation to the error without compensation (see Chapter 2 and 3). The efficiency is calculated over the entire experiment. Thus, the measurement results of all holes are included in this ratio.

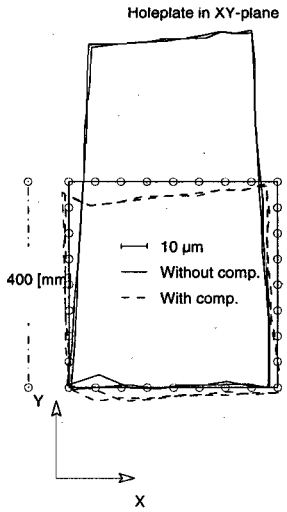

Figure 8.1 : Validation of the geometric part of the real-time software error compensation with a hole plate measurement carried out in the XY-plane.

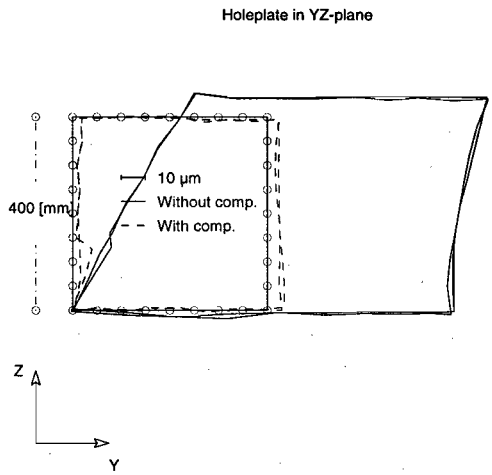

Figure 8.2 : Validation of the geometric part of the real-time software error compensation with a hole plate measurement carried out in the YZ-plane.

Hole plate experiment	Measured [µm]	Residual [µm]	Efficiency [%]
XY-plane	80	11	87
XZ-plane	53	11	73
YZ-plane	109	11	93

Table 8.1 : An overview of the efficiency of the real-time software error compensation: experiments carried out with hole plate measurements to validate the geometric error compensation.

In table 8.1 the performance of the real-time software error compensation is clearly shown: an averaged efficiency of 84% is achieved. For each plane a maximum residual error of 11 µm is found, which is very small. The lubrication pulses previously found with the simulations of the different geometric error models (see Chapter 3) are not present here, as the lubrication-pump has been switched off during the experiment.

NC-code software error compensation

The NC-code software error compensation system is based on the same model as the real-time software error compensation. Also the implementation of the NC-code compensation is equivalent to the real-time compensation. The only difference between the two compensation systems is the interpolation interval of 10 mm for the real-time compensation system and 20 mm for the NC-code compensation system respectively.

Unfortunately, it is not possible to compensate a hole plate measurement with NC-code compensation. The investigated Maho 700S cannot evaluate the difference between the programmed and the actually measured coordinates. It is only possible to store the measured coordinates which are directly read from the scales. A software error compensation on the measurement can only be carried out afterwards, like coordinate measuring machines. In fact, this has already been carried out by the simulations of the hole plate measurements (presented in Chapter 3), where the measured coordinates are compensated afterwards for the errors involved during the actual measurement.

Therefore, to validate the implementation of the NC-code software error compensation a different method has been applied : ball bar measurements. The compensation is realised by adapting the NC-code part program applied to position the tool with respect to the centre-point of the sphere. On every position the length of the ball bar is measured. As the

absolute length of the ball bar is known, the residuals found in the individual measurements directly represent the residuals of the NC-code software error compensation.

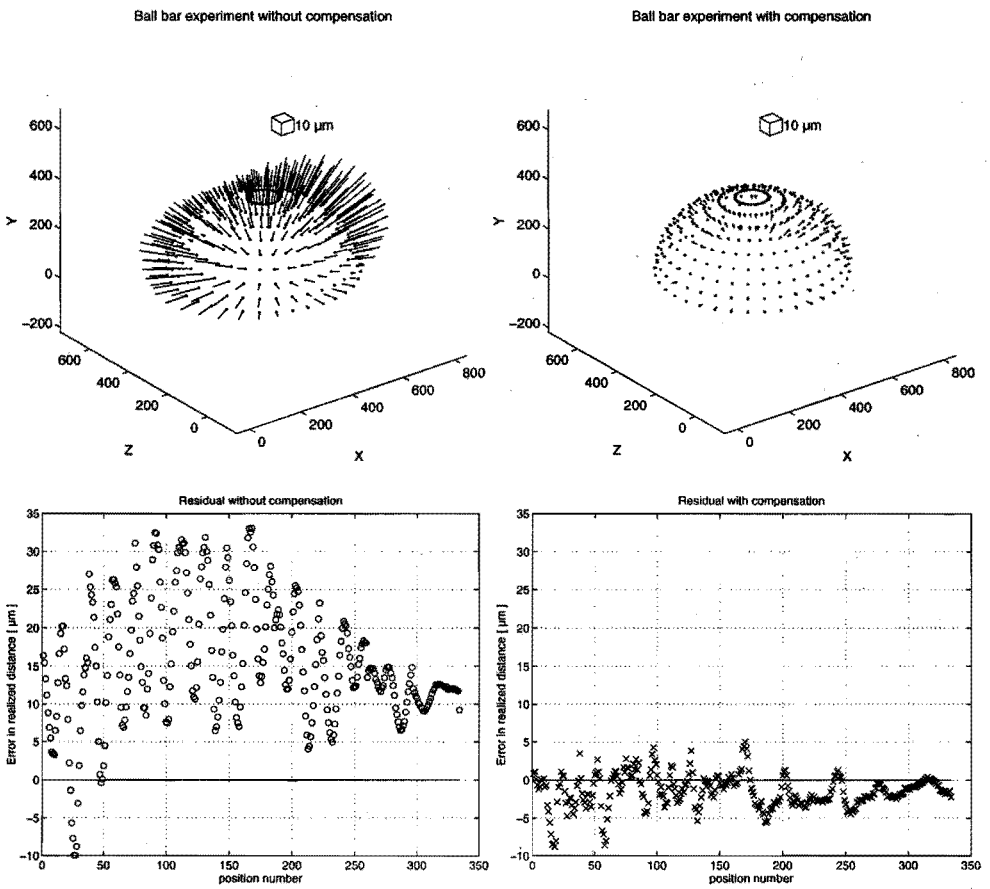

Figure 8.3 : Validation of the NC-code software error compensation, carried out with a ball bar experiment. The two left graphs represent the measured error without compensation; the two right graphs represent the residual measured with the compensated NC-code.

In figure 8.3 the results of two ball bar experiments carried out in the XZ-plane are depicted. Firstly, the ball bar has been measured without compensation. Secondly, the ball bar has been measured using the compensated NC-codes. Similar to the hole plate experiments a maximum

residual of about 10 μm is found with software error compensation. As the model underlying both compensation mechanisms is equivalent this residual was to be expected.

Validation of the compensation for the workpiece load

In the compensation system the errors due to the weight of a workpiece are modelled in addition to the geometric errors. The software compensation mechanism sec has already been tested by the hole plate and ball bar experiments for compensation of the geometric errors presented in the previous paragraph. Therefore, to validate the developed finite stiffness error model it is sufficient to determine the modelling efficiency of the load-induced error terms. This verification will only be carried out for the real-time software error compensation as the implementation of the NC-code software error compensation is equivalent.

In Chapter 4 a relation between the measured strain in the X-axis carriage and the actual load placed on the table has been presented. Also the relation between this load and the additional geometric errors has been determined. To verify both models a hole plate has been measured in the YZ-plane with a workpiece load positioned on the table.

The hole plate measurement has been carried out for two different cases, with a load of 1700 N placed on the front end of the table (Z= -280) and on the back end of table, near the column (Z=280). Each measurement has been carried out three times. Firstly, the hole plate is measured without compensation. Secondly, the hole plate is measured with the compensation enabled. The actual load and its position on the workpiece table have been used as inputs for the finite stiffness error model. The relation between the load and the load induced errors has been verified with this experiment. Thirdly, the hole plate is measured again with the compensation enabled. Now the load is estimated using the strain-gauges. The geometric errors have been subtracted from the measurement results to obtain the pure load induced errors.

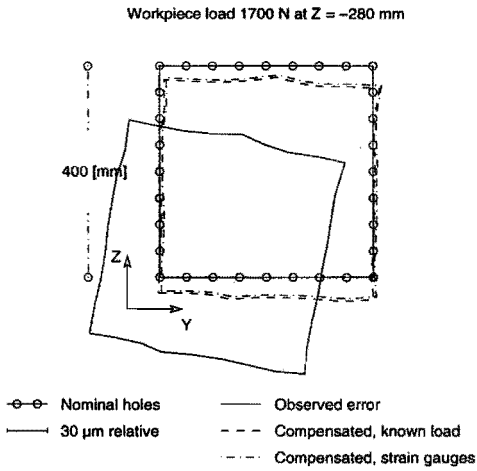

Figure 8.4 : Verification of the finite stiffness error compensation with a workpiece load of 1700 N placed on the front end of the table.

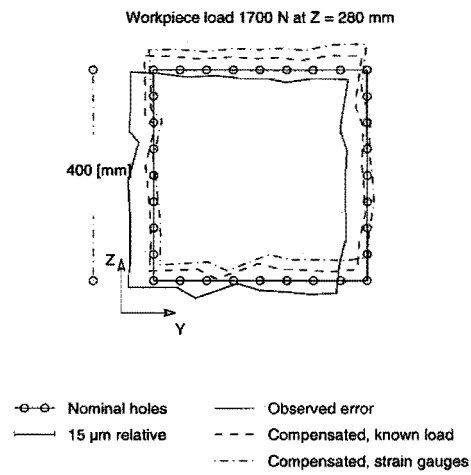

Figure 8.5: Verification of the finite stiffness error compensation with a workpiece load of 1700 N placed on the back end of the table.

In figures 8.4 and 8.5 the results of these experiments are depicted graphically. One can clearly observe a significant improvement of the

machine accuracy, especially when the workpiece is placed on the front end of the table. The observed error without a compensation is the combined effect of the additional xrx error and the rotation of the workpiece table around X. A small difference is found in the residuals of the software compensation with the load or the strain gauges applied as input data. The maximum found error without load compensation is 78 μm when the load is positioned on the front end of the table. With software error compensation this maximum residual is reduced to 14 μm. An averaged efficiency of 75% for the experiment presented in figure 8.4 is determined. For the experiment presented in figure 8.5 this efficiency is much lower. However, the maximum error found without compensation is also very small in this situation: a maximum residual of 11 μm is found with load compensation, which is equal to the geometric part of the software error compensation system.

Validation of the compensation for the thermally induced errors

The thermally induced errors are the third error source which is compensated by the software error compensation system. Two different models are developed to describe these errors. The statistical model will be applied for the verification of the compensation mechanism. Two verification experiments will be described, which are carried out for both the real-time software compensation system and the NC-code software compensation system.

Real-time software error compensation

In order to verify the thermal part of the real-time software error compensation system the drift measurement set-up is applied as presented in Chapter 5. The machine tool is loaded with a constant spindle speed of 6000 rpm and spindle stop after 360 minutes. The experiment is carried out twice. Firstly, the zero-point drift of the machine is measured without any compensation. Secondly, the zero-point drift of the machine is measured with the real-time software error compensation enabled. In figures 8.6 and 8.7, the respective measurement results are depicted graphically.

The measurement results clearly show a significant improvement of the accuracy of the machine tool. Without a compensation, a zero-point drift has been measured up to 118 μm (drift in Y-direction). With compensation this drift has been reduced to a maximum of 23 μm.

NC-code software error compensation

To verify the NC-code software error compensation the same measurement set-up is applied. Now, the machine is loaded with the varying spindle speed spectrum defined in DIN 8602. As the machine is held on one position a special NC-code program has been applied. With this program the machine is ordered to go to the present position using the 'G1'-command followed by a 'G4'-command to program a dwell-time. For this application a dwell-time has been programmed of 1 s. The NC-code program is presented to the second step of the NC-code compensation system, which compensates the 'G1'-commands for the thermally induced errors. Together with the 'G4'-commands the compensated 'G1'-commands are sent to the controller line by line, where they are processed.

In figures 8.8 and 8.9 the measurement results are presented. Similar to the real-time software error compensation system a significant improvement of the accuracy of the machine tool is achieved. Without compensation, a zero-point drift has been measured up to 58 μm (drift in Y-direction). With compensation this drift has been reduced to a maximum of 12 μm (in X-direction) and -12 μm (in Y-direction).

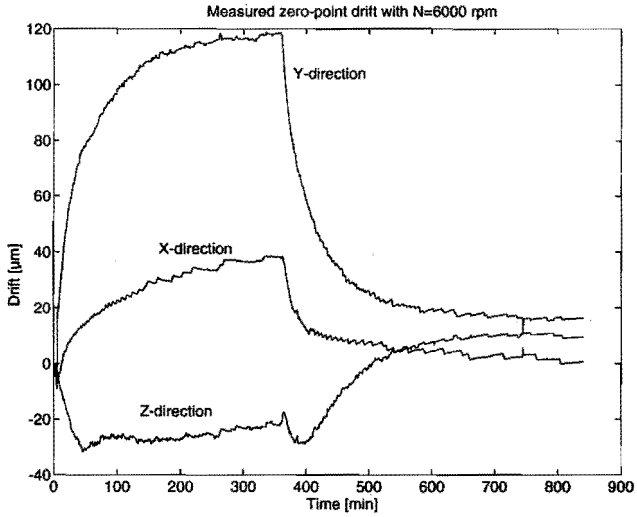

Figure 8.6 : A zero-point drift measurement carried out in the XZ-plane without compensation with N=6000 rpm.

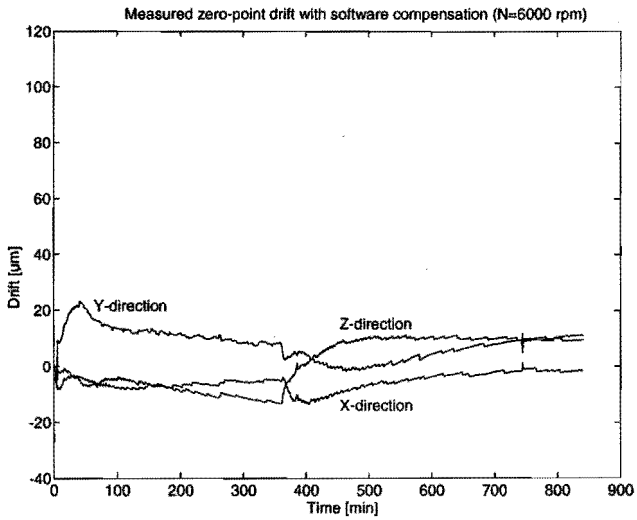

Figure 8.7 : A zero-point drift measurement carried out in the XZ-plane with N=6000 rpm with the real-time software error compensation.

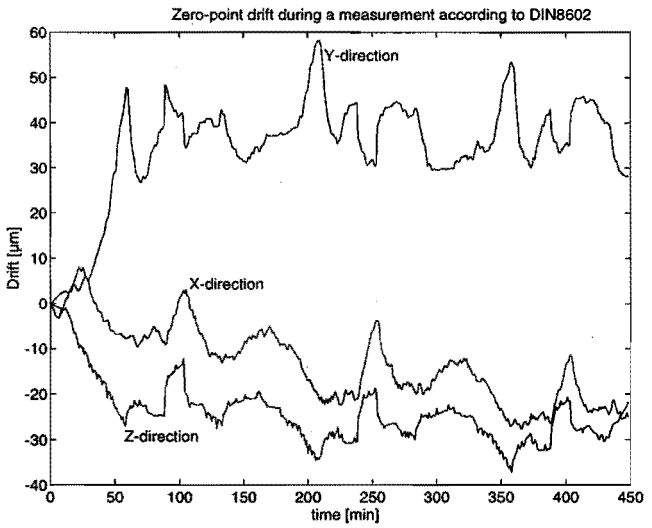

Figure 8.8 : A zero-point drift measurement in the XZ-plane without compensation, DIN8602 spectrum.

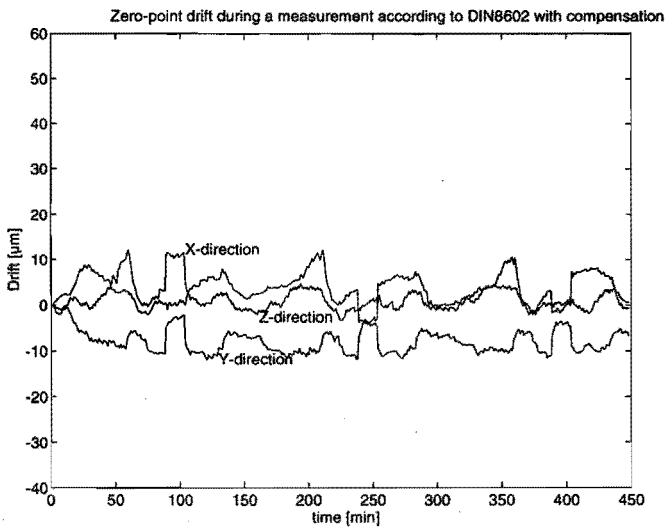

Figure 8.9 : A zero-point drift measurement with the NC-code software error compensation, DIN8602 spectrum.

Validation of the real-time software error compensation system with test-workpieces

Finally, a complete validation of the software error compensation system has been carried out by milling test-workpieces (see Chapter 5, figures 10, 11 and 12). This validation has been carried out for the real-time software error compensation system. In the paragraphs presented above, the performance of the NC-code software error compensation has already been demonstrated. These experiments clearly show that a similar performance can be expected from the NC-code software error compensation as from the real-time software error compensation. This was to be expected as both compensation systems are based on the same principle. A verification of the NC-code software error compensation with test-workpieces would result in a comprehensive amount of work. Considering the equivalent implementation of both methods and the limited amount of time and resources, it was decided not to verify the NC-code compensation with test-workpieces.

A total of nine workpieces have been milled on the machine tool. Three workpieces without compensation; three workpieces with a compensation based on the analytical thermal model; and three workpieces with a compensation based on the statistical thermal model. The geometric and finite stiffness model have also been included in the software error compensation system for the latter two groups of experiments.

After the milling process the geometry of a test-workpiece is measured on a coordinate measuring machine. The measurement results are compared with the programmed geometry of a workpiece to obtain the errors during the milling process. In the next two subsections the results of the validation experiments will be presented.

Analytical model

Three test-workpieces have been milled on the machine tool with software error compensation. The software compensation system was provided with the analytical thermal error model, the finite stiffness model and the geometric error model using the direct measurement techniques. The errors in the geometry of the workpieces are compared to the errors found in the workpieces milled without compensation. In the next section the results of the zero-point drift extracted from the workpieces are presented and the results of an evaluation of the complete workpiece geometry. The

complete package of verification experiments can be found in the report : 'Development of methods for the numerical error compensation of machine tools' [78].

Firstly, the zero-point drift components are extracted from the workpieces milled with and without compensation. In figure 8.10, 8.11 and 8.12 respectively the drifts in X-, in Y- and in Z-direction are presented. Both the results from the compensated and the uncompensated workpiece are presented in one figure. The geometric error compensation has no effect on the efficiency of the drift compensation, as the drift is determined relative to the beginning of the experiment. In the next table (table 8.2) the performance of the analytical thermal error compensation is presented for the zero-point drift.

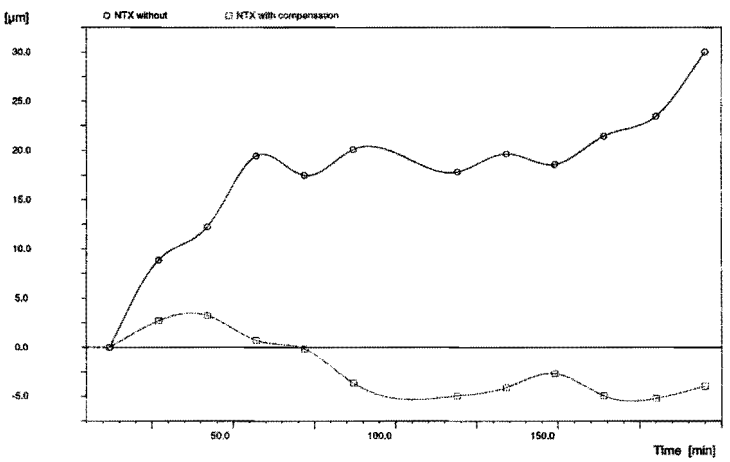

Figure 8.10 : Zero-point drift in X-direction extracted from two workpieces milled with and without compensation. The workpieces have been milled in the XY-plane with the Pseudo-DIN8602 spectrum.

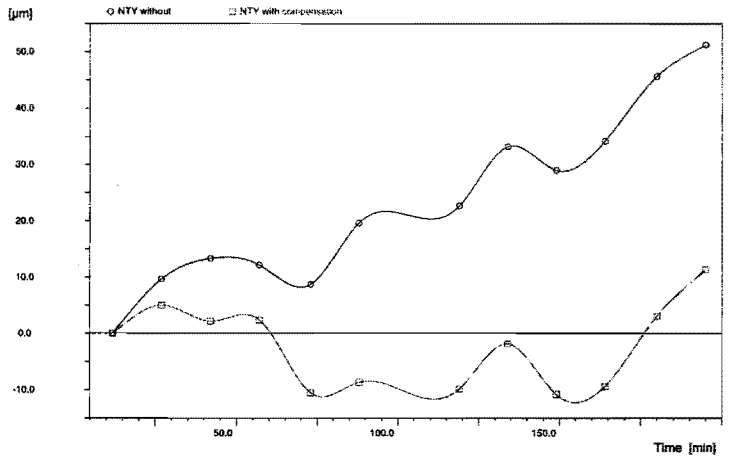

Figure 8.11 : Zero-point drift in Y-direction extracted from two workpieces milled with and without compensation. The workpieces have been milled in the XZ-plane with the Pseudo-DIN8602 spectrum.

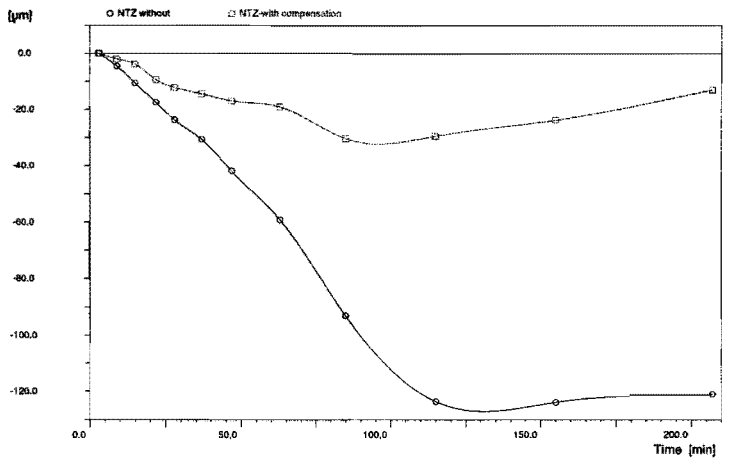

Figure 8.12 : Zero-point drift in Z-direction extracted from two workpieces milled with and without compensation. The workpieces have been milled in the XZ-plane with N= 6000 rpm.

Zero-point drift	Measured [µm]	Residual [µm]	Efficiency [%]
ntx	37	12	69
nty	95	24	72
ntz	124	30	59

Table 8.2 : An overview of the efficiency of the analytical thermal error compensation: validation of the zero-point drift compensation.

In figures 8.13 and 8.14 the errors found in the test-workpiece geometry are presented. In figure 8.13 the errors measured in Y-direction are presented. In figure 8.14 the errors in X- and Z-direction are presented for each location of the holes. In both figures the errors found in the workpiece milled with and without compensation are presented. In table 8.3 an overview is given of the efficiency of the complete real-time software error compensation, using the analytical model.

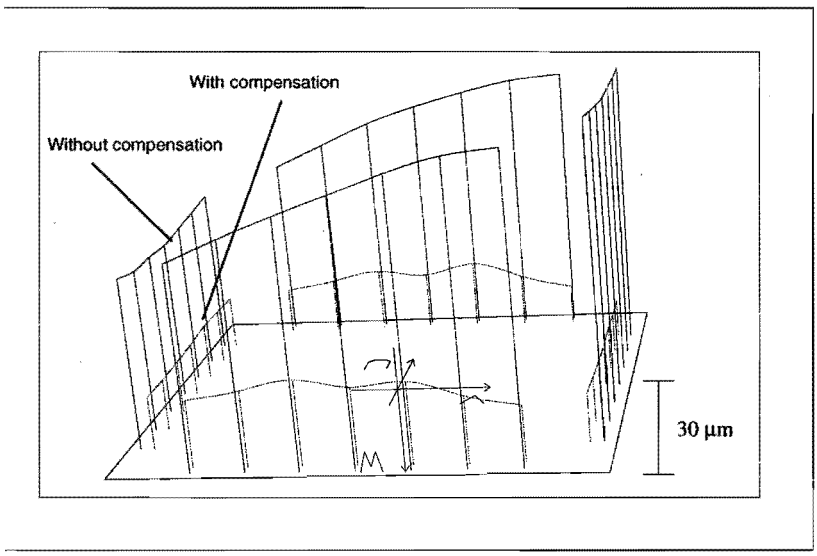

Figure 8.13 : Residuals in Y-direction extracted from the twelfth plane from a workpiece milled with and one without compensation. The workpieces have been milled in the XZ-plane with N=6000 rpm.

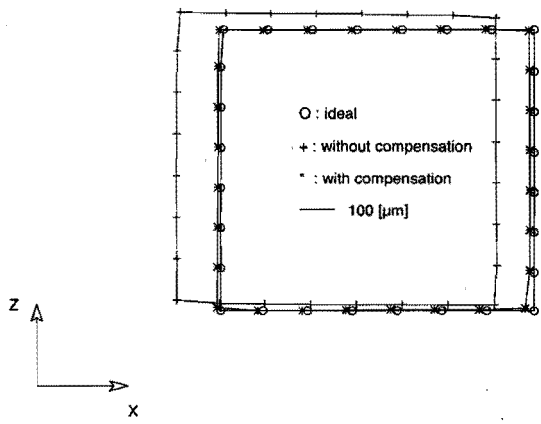

Figure 8.14 : Residuals in X- and Z-direction extracted from the twelfth plane from a workpiece milled with and one without compensation. The workpieces have been milled in the XZ-plane with N=6000 rpm.

Workpiece geometry	Measured [µm]	Residual [µm]	Efficiency [%]
XY-plane, DIN8602	117	29	68
XZ-plane, N=6000 rpm	131	39	73
XZ-plane, DIN8602	61	29	71

Table 8.3 : An overview of the efficiency of the software error compensation system with the analytical thermal error model: validation of the errors in the workpiece geometry.

The results show that the accuracy of the machine tool can be improved significantly with the real-time software error compensation combined with the analytical thermal error model. The zero-point drift extracted from the test-workpieces can be reduced with an averaged efficiency of 67%. The errors present in the geometry of the test-workpieces can be reduced with 71%. The maximum error found in the workpieces is reduced from 131 µm to 39 µm.

Statistical model

A similar validation as for the analytical model has been carried out for statistical thermal error model. The analytical model has been replaced by the statistical model. Again three test-workpieces have been machined. The errors found in the workpieces with compensation are compared to the

errors found in the workpieces without compensation. In the next section the measurement results are presented.

In figures 8.15, 8.16 and 8.17 the zero-point drift extracted from the test-workpieces are presented for the different workpieces milled with and without compensation. In figure 8.15 the drift in X-direction is presented, in figure 8.16 the drift in Y-direction and in figure 8.17 the drift in Z-direction. The geometric error compensation has no effect on the efficiency of the drift compensation, as the drift is determined relative to the beginning of the experiment. In the next table (table 8.4) the performance of the statistical thermal error compensation is presented for the zero point drift.

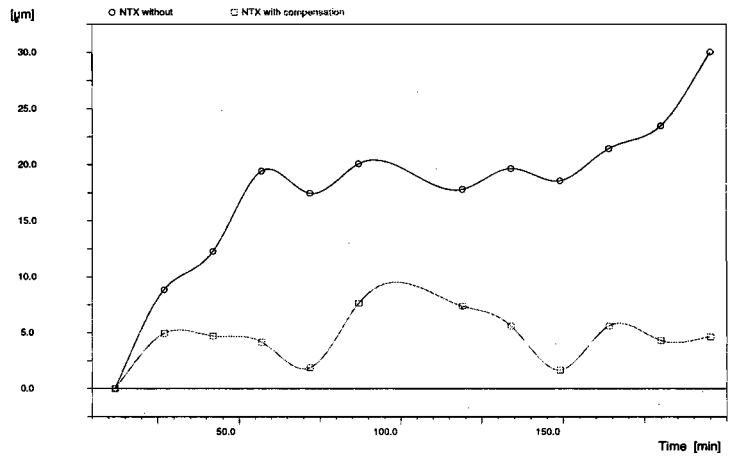

Figure 8.15 : Zero-point drift in X-direction extracted from two workpieces milled with and without compensation. The workpieces have been milled in the XY-plane with the Pseudo-DIN8602 spectrum.

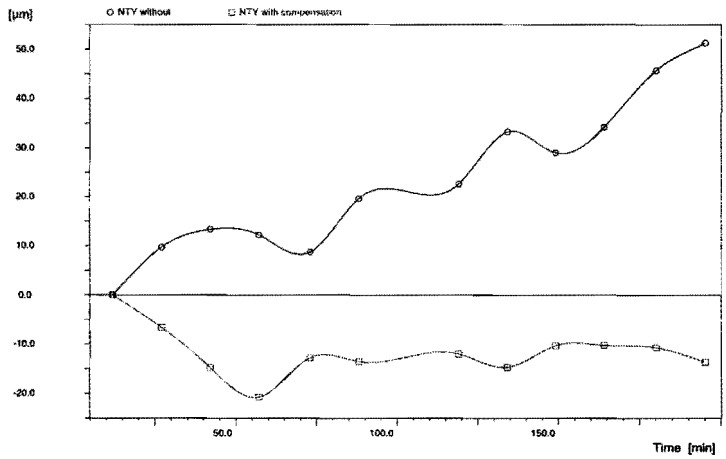

Figure 8.16 : Zero-point drift in Y-direction extracted from two workpieces milled with and without compensation. The workpieces have been milled in the XZ-plane with the Pseudo-DIN8602 spectrum.

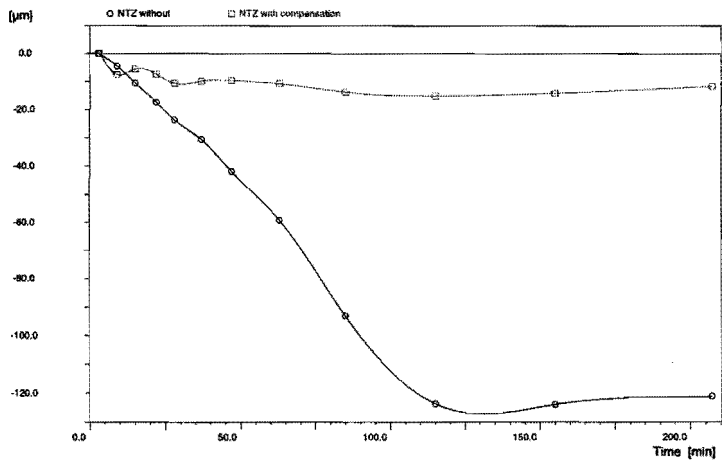

Figure 8.16 : Zero-point drift in Z-direction extracted from two workpieces milled with and without compensation. The workpieces have been milled in the XZ-plane with N= 6000 rpm.

Zero-point drift	Measured [µm]	Residual [µm]	Efficiency [%]
ntx	37	8	78
nty	95	24	61
ntz	124	16	72

Table 8.4 : An overview of the efficiency of the statistical thermal error compensation: validation of the zero-point drift compensation.

In figures 8.17 and 8.18 the errors found in the test-workpiece geometry are presented. In figure 8.17 the errors measured in Y-direction are presented. In figure 8.18 the errors in X- and Z-direction are presented for each location of the holes. In both figures the errors found in the workpiece milled with and without compensation are presented together.

In table 8.5 an overview is given of the efficiency of the complete real-time software error compensation, using the statistical model.

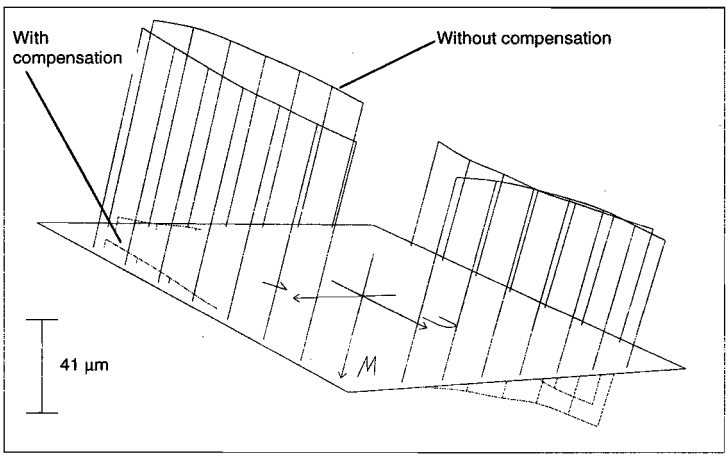

Figure 8.17 : Residuals in Y-direction extracted from the twelfth plane from a workpiece milled with and one without compensation. The workpieces have been milled in the XZ-plane with N=6000 rpm.

Workpiece geometry	Measured [µm]	Residual [µm]	Efficiency [%]
XY-plane, DIN8602	117	24	80
XZ-plane, N=6000 rpm	131	32	88
XZ-plane, DIN8602	61	22	70

Table 8.5 : An overview of the efficiency of the software error compensation system with the statistical thermal error model: validation of the errors in the workpiece geometry.

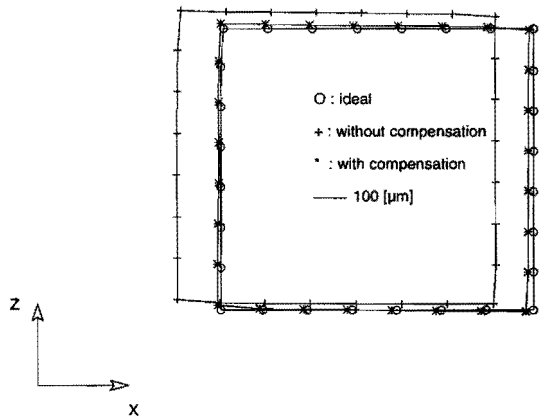

Figure 8.18 : Residuals in X- and Z-direction extracted from the twelfth plane from a workpiece milled with and one without compensation. The workpieces have been milled in the XZ-plane with N=6000 rpm.

The experiments with the statistical model show slightly better results than the performance of the real-time software error compensation with the analytical model. The zero-point drift extracted from the test-workpieces can be reduced with an averaged efficiency of 70%. Milling the test-workpieces with and without compensation showed an average accuracy improvement of 80%. The maximum remaining error of 131 µm present in the workpiece milled without compensation is reduced to 32 µm for the workpiece milled with compensation.

Chapter 9

Conclusions and Recommendations

In this thesis the development of a software error compensation system for machine tools is described. This software error compensation compensates the reproducible geometric, finite stiffness and thermally induced errors involved during the production process.

Conclusions

The software error compensation system

The compensation system is based on a kinematic modelling procedure. This model relates the errors in the location of the tool with respect to the workpiece to the errors in the relative location of coordinate frames attached to the successive elements of the structural loop (parametric errors). The individual coordinate frames coincide with the machine zero-point when all axes are positioned on this machine zero-point. This results in a machine type dependent model with one chain and no construction parameters. Only the actual kinematic configuration (e.g. X-Z-Y) has to be defined.

The parametric errors are described with error functions which are obtained by superposition of individual error models. The individual models describe the effects of the different error sources independently. This design enables direct implementation of the different models in the software error compensation system without affecting the compensation mechanism itself. This so called 'Open Architecture Design' allows the investigation of different error models during the actual operating conditions.

The error models

Firstly, a model is developed for the geometric errors of a machine tool. The models for the geometric parametric errors are based on least squares fitted piecewise polynomials. To determine the model parameters for these geometric errors, three different methods have been applied. Firstly, a direct measurement technique has been investigated. With this technique the individual parametric errors are measured directly. Secondly, a two-dimensional artefact has been applied: a hole plate. A total of six hole plate measurements have been used to estimate all parametric geometric errors. The third method presented in this thesis uses a ball bar. With this ball bar it is possible to carry out a 3-dimensional test-sequence, by moving one end of the ball bar to discrete positions located on a sphere and keeping the other end on one fixed position on the table. The ball bar measurement is a very robust and cheap method to determine the geometric errors of a machine tool. A total of eight experiments is needed to estimate the parametric geometric errors.

A comparison of the three different methods has been carried out. The direct measurement technique turned out to be the most flexible method, as both the ball bar and the hole plate are limited with respect to their working range. Within two days the investigated machine can be measured completely with the direct measurement technique. For these measurements expensive equipment and a skilled operator are needed. The ball bar and hole plate are less expensive than the measurement equipment used for the direct measurement technique. The ball bar and hole plate can be applied by a local operator and take 2-4 hours. Both the direct measurement technique and the hole plate method showed a very high modelling efficiency. The ball bar method showed the smallest modelling efficiency, but can be optimised further with respect to the measuring device and the experimental set-up.

The second error source investigated is the finite stiffness error of the structural loop. These errors are induced by the weight of moving machine components and/or the weight of a workpiece load. The finite stiffness errors due to the weight of moving machine components are already included in the geometric error model. The errors due to the workpiece weight have been described separately with empirical models. Strain gauges are applied to determine the actual load and its position on the table.

Thirdly, for the thermally induced errors two different models have been described: the statistical and the analytical model. The statistical model is based on a direct relationship between temperature sensors attached to the machine tool and the measured drift. In order to determine this relationship the drift has been measured on several locations within the range of the machine tool. This drift turned out to be dependent on the Z-axis position. During these measurements the machine is loaded with different spindle speeds. Besides the spectrum defined in DIN8602, two new spectra have been applied: a randomly distributed spindle speed spectrum and a constant spindle speed over a long period of time. The statistical model has been developed using the data measured with both newly developed spectra.

A method has been developed to determine which temperature sensors are relevant for the description of the displacement. Given a fixed number of sensors the best regression model is determined using the value of C_p. Using this set of sensors the coefficients of the predictors are determined. The efficiency of each individual model is calculated using a verification data set which has been created by independent measurements. With this technique the number of sensors can be chosen given the desired efficiency. For the investigated machine an optimal model has been realised with 16 sensors.

The applied analytical model is based on the physical relationship between the temperature distribution of a body and its deformation. The structure of the machine tool is divided into large segments. The deformation of each segment is calculated. The displacement of the tool is calculated by superposition of the deformation of each element.

A comparison of both models has shown that a large amount of sensors is needed for the analytical model. It is also difficult to realise an analytical model. On the other hand, the analytical model could be developed further to realise a type dependent model, which is valid for every machine of the same type. The statistical model is more robust against faulty readings, but has to be estimated for every individual machine.

Both thermal models show very good results for stationary states; the zero point drift can be described very accurately. For transient states, both models show a smaller efficiency. This is mainly caused by the quick temperature changes in the machine with transient states.

The compensation methods

Two different compensation strategies have been developed: a real-time software error compensation system, which is embedded in the controller of the machine tool and an NC-code software error compensation, which directly acts on the NC-code part program.

The real-time software error compensation has been implemented in a controller. The real-time compensation system compensates the whole trajectory of the machine tool. Therefore, the compensation model is evaluated every cycle time of the interpolation task (= 15 ms). On every position the actual compensation value is determined for each axis. This compensation value is calculated with the error propagation model considering the machine tool configuration (e.g. the position of the C-axis, or the position of a swivelling head which enables both horizontal and vertical milling). The error propagation model uses 18 individual compensation functions which are received from the accumulator. In the accumulator these compensation functions are created using the parametric error functions received from the different error models.

Two different methods have been described how the NC-controller can handle the compensation values: a scale-compensation and a set-point compensation. With a scale-compensation the compensation values are determined as functions of the position information read from the measuring systems. With an implementation of the total error propagation model this can easily introduce instable or discontinuous behaviour of the axis position. Therefore the set-point generated by the interpolation task is applied to calculate the actual compensation values. This results in a stable compensation mechanism. In order to avoid visible edges on a workpiece due to a sudden change in the compensation value, a time dosing system is implemented which makes the compensation change in a gradual way.

The NC-code software error compensation adapts the NC-code of a part-program to compensate the programmed trajectory for the modelled errors. Before the compensation can be carried out the NC-code has to be translated to SNC-code. This SNC-code contains only simple linear and circular movements, programmed in Cartesian machine coordinates with respect to the machine zero-point. The SNC-code can be handled by the software compensation module. The generated SNC-code contains rapid movement commands to locate the tool near a workpiece and cutting feed commands to actually remove the material from the workpiece. All rapid

movement commands will not be compensated as these movements are not applied to remove material from the workpiece. All other commands will be compensated by adding the calculated compensation values to the programmed machine coordinates. As an end-point compensation is not sufficient, the programmed trajectory is interpolated with a fixed step-size. For every grid-point a compensation value is determined and added to its coordinates.

The NC-code compensation is split into two parts. The first part compensates off-line for the geometric and finite stiffness errors. The second part compensates for the thermally induced errors which vary continuously during the actual milling process. To compensate for these thermally induced errors the NC-code is adapted and sent to the controller line by line where they are processed immediately.

Validation

A validation has been carried out for the developed software error compensation systems including the different error models. The validation has been carried out separately for every error source. Firstly, the software error compensation has been verified with the geometric error model. The verification has been carried out with ball bar and hole plate experiments. The maximum error found during these experiments has been reduced from 109 μm without compensation to 11 μm with compensation, resulting in an averaged modelling efficiency of 84%.

The finite stiffness error model has been verified with hole plate measurements. Without compensation a maximum error is found of 78 μm; with software error compensation a maximum residual is found of 14 μm. An averaged efficiency for the finite stiffness error model has been determined of 75%.

The implementation of the thermal error compensation has been verified with zero-point drift measurements. The measurement results showed a significant improvement of the accuracy of the machine tool with an efficiency of 80%.

Finally, a validation of the total software error compensation system has been carried out by milling test-workpieces. A total of nine workpieces have been milled on the machine tool. Three workpieces without compensation; three workpieces with a compensation based on the analytical thermal model; and three workpieces with a compensation based on the statistical

thermal model. To determine the real performance of the compensation system the geometric and finite stiffness error models have also been enabled.

The results show that the accuracy of the machine tool can be improved significantly with the real-time software error compensation combined with the analytical thermal error model. The zero-point drift extracted from the test-workpieces can be reduced with an averaged efficiency of 67%. The errors present in the geometry of the test-workpieces can be reduced with 71%. The maximum error found is reduced from 131 μm to 39 μm.

The experiments with the statistical model show slightly better results than the experiments with the analytical model. The zero-point drift extracted from the test-workpieces can be reduced with an averaged efficiency of 70%. Milling the test-workpieces with and without compensation showed an averaged accuracy improvement of 80%. The maximum remaining error of 131 μm present in the workpiece milled without compensation is reduced to 32 μm for the workpiece milled with compensation.

Recommendations

The realised software error compensation system can improve the accuracy of machine tools significantly. Different error models have been developed to accomplish this task. Also different methods of software error compensation have been developed. Although the results can be considered as very good, the following recommendations can still be made for future research:

- The direct measurement techniques can only be applied by a skilled operator. Especially the definition of the signs of the measured errors appears to be very difficult for an inexperienced operator and likely to introduce mistakes. A protocol should be developed for the direct measurement techniques to reduce these problems.

- The application of different extension rods for the ball bar introduced systematic errors up to 3 μm. A better construction will eliminate these errors, resulting a in better modelling efficiency. The measuring method can be improved further when the ball bar would have a longer range. The application of the different extension rods would not be needed anymore and the measurement sequence could be carried out faster. The modelling efficiency can also be improved with an optimisation of the experimental set-up.

- The possibilities of the diagonal laser measurement developed by Soons [86, 87] to determine the geometric errors should be investigated. For machines with moving tables (like the investigated Maho 700S) the application of this technique is very difficult due to the limited space between the table and the ram of the machine with the Y-axis positioned on Y=0.

- The position and actual load of a workpiece placed on the table are estimated with strain gauges. The measurement has to be carried out by moving the X-axis to different positions, due to a significant influence of temperature variations on the applied strain gauge. When the strain gauge would be replaced by another sensor this measurement sequence could be simplified significantly.

- The thermal error models showed a smaller efficiency in modelling the transient states. In order to achieve a more accurate model for these transient states a further investigation is necessary. The statistical

model can be extended by including history in the model; the analytical model can be extended with an empirical part (hybrid model). Also the dynamic model introduced by Soons [87] is a very promising technique and should be investigated on its modelling capacity for these transient states.

- Several compensation systems have been developed and described in this thesis. Hereby a strict separation has been made between the real-time software error compensation and the NC-code software error compensation. However, a combination of both methods is also possible or an implementation which cannot be classified within both methods. For example, the thermally induced zero-point drift can be compensated very efficiently by an adaptation of the programmed workpiece zero-point stored in the controller. This method can not be classified within both mentioned methods but has proven to give very good results.

- All investigations have been carried out on an existing machine. However, during the design-phase of such a machine the possibilities of software error compensation should be considered. Normally, special attention is paid to the construction of the machine to achieve a high accuracy. Instead of focusing on the high accuracy more attention should be paid to the reproducibility of the machine. Then, with the aid of software error compensation a machine can be developed with very high accuracy. This machine will also be less expensive as the application of a software error compensation system is much cheaper than the purchase and manufacturing of expensive high accuracy construction parts.

Bibliography

[1] Asao, Y. Mizugaki, M. Sakamoto, H. Sato, Precision Turning by Means of a Simplified Predictive Function of Machining Error, Annals of the CIRP (41:1), pages 447-450, 1992.

[2] M.H. Attia, L. Kops, Calculation of Thermal Deformation of Machine Tools, in Transient State, with the Effect of Structural Joints taken into Account, Annals of the CIRP (28:1), pages 247-251, 1979.

[3] ASME B5 TC52 Committee, Methods for Performance Evaluation of Computer Numerically Controlled Machining Centers and Work Centers (draft standard version 3.0), The American Society of Mechanical Engineers, New York, USA 1989.

[4] A. Balsamo, D. Marques, S. Sartori, A Method for Thermal Deformation Corrections of Coordinate Measuring Machines, Annals of the CIRP (39:1), pages 557-560, 1990.

[5] G. Belforte et al., Coordinate Measuring Machines and Machine Tools Selfcalibration and Error Correction, Annals of the CIRP (36:1), pages 359-364, 1987.

[6] H. Bratatjandra, Software Correctie voor Lineaire en Circulaire Beweging van de Freesmachine Maho 700S, WPA 1395, Eindhoven University of Technology, 1992.

[7] J. B. Bryan, A Simple Method for Testing Measuring Machines and Machine Tools. Part 1: Principles and Applications, Precision Engineering, Volume 4, No. 2, pages 61-69, 1982.

[8] J. B. Bryan, A Simple Method for Testing Measuring Machines and Machine Tools. Part 2: Construction Details, Precision Engineering, volume 4, No. 3, pages 125-129, 1982.

[9] J. B. Bryan, International Status of Thermal Error Research (1990), Annals of the CIRP (39:2), pages 645-656, 1990.

[10] K. Busch, H. Kunzmann, F. Wäldele, Calibration of Coordinate Measuring Machines, Precision Engineering, pages 139-144, 1985.

[11] M. Burdekin, C. Voutsadopoulos, Computer Aided Accuracy Improvement in Large NC machine tools, Proceedings Institution of Mechanical Engineers, Volume 195, pages 231-239, 1981.

[12] J.S. Chen, J.X. Yuan, J. Ni, S.M. Wu, Real-time Compensation for Time-variant Volumetric Errors on a Machining Center, Journal of Engineering for Industry, Volume 115, pages 472-479, November 1993.

[13] DIN 8601, Abnahmebedingungen für Werkzeugmaschinen für die spanende Bearbeitung von Metallen, Allgemeine Regeln, 1986.

[14] DIN 8602, Verhalten von Werkzeugmaschinen unter statischer und thermischer Beanspruchung, Allgemeine Regeln für die Prüfung von Fräsmaschinen, 1985.

[15] DIN 8615, Fräsmaschinen, Abnahmebedingungen, 1979.

[16] DIN 8620, Werkzeugmaschinen, Abnahmebedingungen, 1978.

[17] DIN 66025, Programmaufbau für numerisch gesteuerte Arbeitsmaschinen, Allgemeine Regeln, 1983.

[18] DIN 66025, Programmaufbau für numerisch gesteuerte Arbeitsmaschinen, Wegbedingungen und Zusatzfunktionen, 1988.

[19] M. A. Donmez, A General Methodology for Machine Tool Accuracy: Theory, Application and Implementation, Ph.D. Thesis, Purdue University, 1985.

[20] M. A. Donmez, D. S. Blomquist, R. J. Hocken, C. R. Liu, M. M. Barash, A general Methodology for Machine Tool Accuracy Enhancement by Error Compensation, Precision Engineering, pages 187-196, 1986.

[21] M. A. Donmez, Quality in Automation, Progress Report, National Institute of Standards and Technology, NISTIR 4536, 1991.

[22] N. A. Duffie, S. J. Malmberg, Error Diagnosis and Compensation using Kinematic Models and Positions Error Data, Annals of the CIRP (36:1), pages 355-358, 1987.

[23] N. A. Duffie, S. M. Yang, Generation of Parametric Kinematic Error Correction Function from Volumetric error Measurements, Annals of the CIRP (34:1), pages 435-438, 1985.

[24] P. Dufour, R Groppetti, Computer aided Accuracy Improvement in large NC Machine Tools, MTDR Conference Proceedings, pages 611-617, 1980.

[25] H.J.M. Eijsermans, Een Softwarematige Compensatiemethode voor Afwijkingen van Produktiemachines als gevolg van een Onbekende Werkstukbelasting, WPA 1570, Eindhoven University of Technology, 1993.

[26] P. M. Ferreira, C. R. Liu, A Contribution to the Analysis and Compensation of the Geometric Error of a Machine Center, Annals of the CIRP (35:1), pages 259-262, 1986.

[27] P. M. Ferreira, C. R. Liu, An Analytical Quadratic Model for the Geometric Error of a Machine Tool, Journal of Manufacturing Systems, pages 51-63, 1986.

[28] P. M. Ferreira, C. R. Liu, A Method for Estimating and Compensating quasistatic errors of Machine Tools, The winter annual meeting of the American Society of Mechanical Engineers, PED volume 27,pages 205-229, 1987.

[29] D. French, S. H. Humphries, Compensation for the Backlash and Alignment Errors in a Numerically Controlled Machine Tool by a Digital Computer Programme, MTDR Conference Proceedings, pages 707-726, 1967.

[30] Grundig Numeric BV, Programming Manual CNC5000 Series Milling V200, 1993.

[31] Grundig Numeric BV, Operating Manual CNC5000 Series Milling V200, 1993.

[32] Y. Hatamura, T. Nagao, M. Mitsuishi, A Fundamental Structure for Intelligent Manufacturing, Precision Engineering Journal, Volume 15, No 4, pages 266-273, 1993.

[33] R.P. van Helvoirt, De Bovengrens-Methode als Complement van Kalibratie-Procedures voor Meerassige Freesmachines, WPA 1337, Eindhoven University of Technology, 1992.

[34] C. Hemingray, Some Aspects of the Accuracy Evaluation of Machine Tools, Proceedings of the 14th MTDR Conference, pages 281-284, 1973.

[35] R. J. Hocken and the Machine Tool Task Force, Technology of Machine Tools, Vol 5. : Machine Tool Accuracy, Lawrence Livermore Laboratory, University of California.

[36] R. J. Hocken et al., Three Dimensional Metrology, Annals of the CIRP (26:2), pages 403-408, 1977.

[37] ISO 230/1, Acceptance Code for Machine Tools, Part 1 : Geometric Accuracy of Machine Tools under Noload or Finishing Conditions 1986.

[38] ISO 840, Numerical Control of Machines - 7-Bit Coded Character set, ISO International Standard, 1973.

[39] ISO 841, Numerical Control of Machines - Axis and Motion Nomenclature, ISO International Standard, 1974.

[40] ISO 1056, Numerical Control of Machines - Punched Tape Block Formats - Coding of Preparatory Functions G and Miscellaneous Functions M, ISO International Standard, 1975.

[41] ISO 1701, Test Conditions for Milling Machines with Table of Variable Height, with Horizontal or Vertical Spindle - Testing the Accuracy, ISO International Standard, 1974.

[42] ISO 2539, Numerical Control of Machines - Punched Tape Block Format for Contouring and Contouring/Positioning, ISO International Standard, 1974.

[43] H. Jam, Meetopstelling voor Ruimtelijke Metingen op de Maho 700S, WPA 1615, Eindhoven University of Technology, 1993.

[44] J. Jedrzejewski, J. Kaczmarek, Z. Kowal, Z. Winiarski, Numerical Optimization of Thermal Behaviour of Machine Tools, Annals of the CIRP (39:1), pages 379-382, 1990.

[45] F. Jouy, Theoretical Modelisation and Experimental Identification of the Geometrical Parameters of Coordinate Measuring Machines by Measuring a Multi-directed Bar, Annals of the CIRP (35:1), pages 393-396, 1986.

[46] J. Kaczmarek, Principles of Machining by Cutting, Abrasion and Erosion, Peregrinus, 1976.

[47] V. Kiridena, P.M. Ferreira, Mapping the Effects of Positioning Errors on the Volumetric Accuracy of Five-axis CNC Machine Tools, International Journal of Machine Tools & Manufacturing, Volume 33, No 3, pages 417-437, 1993.

[48] V. Kiridena, P.M. Ferreira, Kinematic Modeling of Quasistatic Errors of Three-axis Machining Centers, International Journal of Machine Tools & Manufacturing, Volume 34, No 4, pages 85-100, 1994.

[49] V. Kiridena, P.M. Ferreira, Parameter Estimation and Model Verification of First Oder Quasistatic Error Model for Three-axis Machining Center, International Journal of Machine Tools & Manufacturing, Volume 34, No 4, pages 101-125, 1994.

[50] V. Kiridena, P.M. Ferreira, Computational Approaches to Compensating Quasistatic Errors of Three-axis Machining Centers, International Journal of Machine Tools & Manufacturing, Volume 34, No 1, pages 127-145, 1994.

[51] W. Knapp, Test of the Three-Dimensional Uncertainty of Machine Tools and Measuring Machines and its Relation to the Machine Errors, Annals of the CIRP (32:1), pages 459-464, 1983.

[52] W. Knapp, Circular Test for Three Coordinate Measuring Machines and Machine Tools, Precision Engineering Journal, Volume 5, No. 3, pages 115-124, 1983.

[53] W. Knapp, S. Hrovat, The Circular Test for Testing NC-Machine Tools, S. Hrovat, Zürich, Switzerland, 1987.

[54] W. Knapp, A. Wirtz, Testing Rotary Axes on NC Machine Tools, Annals of the Cirp (39:2), 1990.

[55] J. P. Kruth, P. Vanherck, L. de Jonge, A Self-calibration Method and a Software Error Correction for Three Dimensional Coordinate Measuring Machines, Proceedings of the International Symposium on Metrology and Quality Control in Production, pages 100-115, 1992.

[56] J. P. Kruth, L. de Jonge, Self-calibration Method for Three Dimensional Coordinate Measuring Machines Usign a Ball Plate, Proceedings of the 7th International Precision Engineering Seminar, pages 402-413, 1993.

[57] A. Kurtoglu, The accuracy improvement of machine tools, Annals of the CIRP (39:1), pages 417-419, 1990.

[58] H. Kunzmann, E. Trapet, F. Wäldele, A Uniform Concept for Calibration, Acceptance Test, and Periodic Inspection of Coordinate Measuring Machines Using Reference Objects, Annals of the CIRP (39:1), pages 561-564, 1990.

[59] H. Kunzmann, E. Trapet, F. Wäldele, Concept for the Traceability of Measurements with Coordinate Measuring Machines, Proceedings of the 7th International Precision Engineering Seminar, pages 40-52, 1993.

[60] D. L. Leete, Automatic Compensation of Alignment Errors in Machine Tools, International Journal of Machine Tool Design and Research, pages 293-324, 1961.

[61] W. J. Love, A. J. Scarr, The Determination of the Volumetric Accuracy of Multi Axis Machines, MTDR Conference Proceedings, pages 307-315, 1973.

[62] E. R. McClure, Manufacturing accuracy through the Control of Thermal Effects, PhD Thesis, Lawrence Livermore National Laboratory, 1969.

[63] D.C. Montgomery, E.A. Peck, Introduction to Linear Regression Analysis, John Wiley & Sons, New York, 1982.

[64] NAS 979, Uniform Cutting Tests - NAS Series, Metal Cutting Equipment Specifications, Aerospace Industries of America Inc., 1969.

[65] J. Ni, S.M. Wu, An On-line Measurement Technique for Machine Volumetric Error Compensation, Journal of Engineering for Industry, Volume 115, pages 85-92, February 1993.

[66] R.P. Paul, Robot Manipulators: Mathematics, Programming and Control, MIT press, Cambridge, MA 1981.

[67] J. Peters, Metrology in Design and Manufacturing - Facts and Trends, Annals of the Cirp (26:2), pages 415-421, 1977.

[68] V. T. Portman, Error Summation in the Analytical Calculation of Lathe Accuracy, Machines & Tooling 51, pages 7-10, 1977.

[69] H.M. de Ruiter, URS Improved Error Compensation BCR, DER6-32.1-5158, Philips Machine Tool Controls, 1992.

[70] H.M. de Ruiter, EPS Improved Error Compensation BCR, DER6-32.1-5159, Philips Machine Tool Controls, 1992.

[71] H.M. de Ruiter, The Compensation System : Interface Description, Grundig Numeric BV, 1994.

[72] SAS STAT, Release 6.03, SAS Institute Inc., Cary USA, 1988.

[73] T. Sata, Y. Takeuchi, N. Okubo, Improvement of working accuracy of a Machining Center by Computer Control Compensation, MTDR Conference Proceedings, pages 93-99, 1976.

[74] T. Sata, Y. Takeuchi, N. Sato, N. Okubo, Analysis of Thermal Deformation of Machine Tool Structure and its Application, MTDR Conference Proceedings, pages 275-280, 1973.

[75] T. Sata et al., Development of Machine Tool Structural Analysis Program (MASAP), Annals of the CIRP (25:1), pages 287-290, 1976.

[76] P. H. Schellekens, H.A.M. Spaan et al., Geometric Error Modelling of Machine Tools, BCR-project : Development of Methods for the Numerical Error Correction of Machine Tools, milestone report, Bureau Communautaire de Reference, 3320/1/0/160/89/8-BCR-NL, Brussels,1991.

[77] P. H. Schellekens, H.A.M. Spaan et al., Modelling the Thermal Behaviour of Machine Tools, BCR-project : Development of Methods

for the Numerical Error Correction of Machine Tools, milestone report, Bureau Communautaire de Reference, 3320/1/0/160/89/8-BCR-NL, Brussels, 1992.

[78] P. H. Schellekens, H.A.M. Spaan et al., Development of Methods for the Numerical Error Correction of Machine Tools, BCR-project : Development of Methods for the Numerical Error Correction of Machine Tools, Final report, Bureau Communautaire de Reference, 3320/1/0/160/89/8-BCR-NL, Brussels, 1993.

[79] P. H. Schellekens. H.A.M. Spaan et al., Development of Methods for the Numerical Error Correction of Machine Tools, Proceedings of the 7th International Precision Engineering Seminar (IPES-1993), 1993.

[80] G. Schlesinger, Inspection Tests on Machine Tools, Machinery Publishing Co. London, 1932.

[81] R. Schultschik, Geometrische Fehler in Werkzeugmaschinen-strukturen, Annals of the CIRP (24:1), pages 361-366, 1975.

[82] R. Schultschik, The Components of the Volumetric Accuracy, Annals of the CIRP (26:1), pages 223-228, 1977.

[83] R. Schultschik, The Accuracy of Machine Tools under Load Conditions, Annals of the CIRP (28:1), pages 339-344, 1979.

[84] R. Schultschik, Das volumetrische Fehlerverhalten von Mehrkoordinaten-Werkzeugmaschinen, Zusammensetzung und Darstellung der Fehler, Werkstatt und Betrieb (122:4), pages 231-235, 1979.

[85] J.A. Soons, F.C.C.J.M. Theuws, P.H.J. Schellekens, Modelling the Errors of Multi-Axis Machines: A General Methodology, Precision Engineering, Volume 14, No. 1, pages 5-19, 1992.

[86] J.A. Soons, P.H. Schellekens, On the Calibration of Multi-axis Machines using Distance Measurements, Proceedings of the International Symposium on Metrology and Quality Control in Production, pages 321-340, 1992.

[87] J.A. Soons, Accuracy Analysis of Multi-Axis Machines, PhD Thesis, Eindhoven University of Technology, 1993.

[88] J.A. Soons, H.A.M. Spaan, H.J. Eijsermans, P.H. Schellekens, Software Compensation of Machine Tool Errors due to the Weight of Machine Components and Workpiece, Proceedings of the 3rd International Conference on Ultraprecision in Manufacturing Engineering, pages 122-127, 1994.

[89] H.A.M. Spaan, H.M. de Ruiter, J.A. Soons, Real-time Parametrische Software Compensatie, Draft of International Patent Application, Internal Philips Report No. GK 76226, 1993.

[90] H.A.M. Spaan, F.C.C.J.M. Theuws, Classification of Multi-axes Machine Tools, WPA 1007, BCR-90/012, Eindhoven University of Technology, 1991.

[91] H.A.M. Spaan, E. van den Broek, R. Lukassen, M. van Nieuwenhoven, S. Pauws, R. Schieffer, E. Suijs, CAQ-project : Automatic Geometric correction of NC-programs, Final project report, Eindhoven University of Technology, 1994.

[92] Y. Takeuchi, M. Sakamoto, T. Sata, Precision Engineering Volume 4, pages 19 - 24, 1982.

[93] J. Tlusty, Comments on the Article by A. Kurtoglu, Annals of the CIRP (39:2), page 772, 1990.

[94] J. Tlusty, F. Koenigsberger, Specifications and Tests of Metal Cutting Machine Tools, Technical Report UMIST, Manchester, 1970.

[95] F.C.C.J.M. Theuws, Enhancement of Machine Tool Accuracy, Theory and Implementation, PhD Thesis, Eindhoven University of Technology, 1991.

[96] E. Trapet, F. Wäldele, Koordinatenmeβgeräte in der Fertigung - Temperatureinfüsse und erreichbare Meβunsicherheit, VDI Berichte 751, pages 209-227, 1989.

[97] M. Tsutsumi, K. Sakai, New Measuring Method of Circular Movement of NC Machine Tools, JSME International Journal, Vol 36, No. 4, pages 463-469, 1993.

[98] VDI/VDE 2617, Characteristic Parameters and their Checking, Components of Measurement Deviation of the Machine, Volume 3, VDI-Verlag, 1991.

[99] VDI-DGQ 3441, Statische Prüfung des Arbeits- und Positionsgenauigkeit von Werkzeugmaschinen, VDI-verlag, 1977.

[100]VDI-DGQ 3442, Statische Prüfung des Arbeits- und Positionsgenauigkeit von Drehmaschinen, VDI-Verlag, 1978.

[101]VDI-DGQ 3443, Statische Prüfung des Arbeits- und Positionsgenauigkeit von Fräsmaschinen, VDI-Verlag, 1978.

[102]VDI-DGQ 3444, Statische Prüfung des Arbeits- und Positionsgenauigkeit von KoordinatenBohrmaschinen und Bearbeitungszentren, VDI-Verlag, 1978.

[103]VDI-DGQ 3445, Statische Prüfung des Arbeits- und Positionsgenauigkeit von Schleifmaschinen, VDI-Verlag, 1978.

[104]R. Venugopal, Thermal Effects on the Accuracy of Numerically Controlled Machine Tools, Annals of the CIRP (35:1), pages 255-258, 1986.

[105]R. Venugopal, Thermal Effects of the Accuracy of Numerically controlled Machine Tools, PhD Thesis, Purdue University, 1985.

[106]M. Weck, L. Zangs, Computing the Thermal Behaviour of Machine Tools using the Finite Element Method - Possibilities and Limitations, MTDR Conference Proceedings, pages 261 - 273, 1975.

[107]M. Weck, Werkzeugmaschinen Band 2, VDI-verlag, 1981.

[108]M. Weck, Geometrisches Maschinenverhalten unter Statischer und Thermischer Belastung, Fertigungstechnik, Volume 104, No. 1, pages 25-28, 1982.

[109]M. Weck, R. Eckstein, Meβtechniken zur Beurteilung von Werkzeugmaschinen, Industrie Anzeiger, Volume 107, No. 72, pages 154-157, 1985.

[110]M. Weck, H-B Schröder, E. Trapet, Thermal Effects on High Precision Machine Tools and Coordinate Measuring Machines, Tutorial during

the 3rd International Conference on Ultraprecision in Manufacturing Engineering, 1994.

[111]West European Calibration Cooperation, Guidelines for the Expression of the Uncertainty of Measurement in Calibration, Technical Report, WECC-Document 19-1990, 1990.

[112]C.S. Wilson, Precision Contouring Error Analysis, Proceedings of Mechanisms and Controls for Ultraprecision Motion, ASPE Spring Topical Meeting, pages 37-42, 1994.

[113]G. S. Wong, F. Koenigsberger, Automatic Correction of Alignment Errors in Machine Tools, International Journal of Machine Tool Design and Research, pages 171-197, 1966.

[114]Y. Yosida, F. Honda, Thermal Deformation of a Vertical Milling Machine, MTDR Conference Proceedings, pages 83-96, 1967.

[115]G. Zhang et al., Error Compensation of Coordinate Measuring Machines, Annals of the CIRP (34:1), pages 445-448, 1985.

[116]G. Zhang et al., A Displacement Method for Machine Geometry Calibration, Annals of the CIRP (37:1), pages 515-518, 1988.

[117]Controle van de Geometrie van Gereedschapmachines: De Kogelstangtest voor een Snelle Diagnose, MB-produktie-techniek, jaargang 60, No. 3, pages 53-59, 1994.

Acknowledgements

The research described in this thesis has been performed at the Precision Engineering group of the Eindhoven University of Technology. This study was performed partly in the context of the European research project : "Development of Methods for the Numerical Error Correction of Machine Tools" and partly in the context of the PBTS-project "Software compensatie van thermische afwijking in bewerkingsmachines". I would like to thank for the opportunity of realising this project.

Special thanks go to the copromotor dr.ir. H.M. de Ruiter and both the promotors prof.dr.ir. P.H.J. Schellekens and prof.dr.ir. A.C.H. van der Wolf for their patience, support and perception during this study. In particular I would like to thank my copromotor dr.ir. Helmi de Ruiter for the thoroughness by which she read each first version of a chapter, for her valuable ideas and advises and for the very pleasant cooperation. Furthermore I am much obliged to the other members of the main promotion committee, prof.dr.ir. A.J.A. Vandenput and prof.dr.ir. J.P. Kruth for the time spent reviewing this document.

I would like to express my thanks to the staff members and students of the Precision Engineering group for their cooperation and the pleasant work climate. In particular I would like to thank Hans Soons and Frank Theuws, whose many-sided talent and insights greatly contributed to this study. Furthermore, the permanent staff members Fred Beer, Adriaan de Gilde, Harry Sonnemans, Klaas Struik and Frits Theuws should be mentioned for their practical support and interest in this study.

A special word of thanks goes to Huub Eijsermans, who executed many of the often exotic experiments on the milling machine.

Finally, I would like to thank Marian for her patience and encouragement that were always a stimulus to complete this study.

Stellingen

behorende bij het proefschrift

Software Error Compensation of Machine Tools

1. De dimensionele nauwkeurigheid van een produkt wordt mede bepaald door de oppervlakte kwaliteit. Het verspanen van produkten met een hoge nauwkeurigheid dient dan ook zodanig te gebeuren dat de oppervlakte kwaliteit slechts een klein deel van de produkt-tolerantie bestrijkt.

2. Een thermische software compensatie behoeft een opspanning met een voorspelbaar thermo-mechanisch gedrag van het werkstuk.

3. Gezien het toenemende belang van informatie (zeker in een onderzoek) en de hoeveelheid waarin deze wordt vergaard, dient elke opleiding aandacht te besteden aan het beheren van informatie.

4. Een algehele toepassing van software compensatie is commercieel pas interessant indien de afwijkingen in een machine snel en betrouwbaar kunnen worden vastgesteld.

5. NC-code compensatie opent de mogelijkheid om elke machine te voorzien van een software compensatie.

6. Om realistische aannames te kunnen maken, zou elke wetenschapper ten minste 1 maand per jaar dienen te besteden in een relevante praktijk-omgeving.

7. Het resultaat van een verkiezingscampagne wordt door de media direct gemeten aan de opiniepeilingen. Het beleid van een politieke partij lijkt dan ook meer door deze opiniepeilingen bepaald te worden dan door een visie.

8. De toename in detachering en uitzendkrachten geeft aan dat de huidige positie van de werknemer veel te veel wordt beschermd. Arbeid moet flexibeler gemaakt worden.

9. Vaak kun je kwaliteit beter ongedefinieerd laten. Kwaliteit moet je in de eerste plaats aanvoelen. Je puur richten naar de normen is voor degenen die dat gevoel niet hebben.
(Robert Pirsig, Zen en de kunst van het motoronderhoud)

10. Het adagium "De klant is koning" geldt nog steeds. Maar men dient zich hierbij wel te realiseren dat een koning ook maar een mens is.

11. Een bedrijf excelleert via haar deskundigheid en niet via haar kennis.

12. Het verbieden van nachtvluchten getuigt niet bepaald van een wereldvisie.

Eindhoven, november 1995 H.A.M. Spaan